3-1-2016 12:00 AM

GLUCAN SYNTHASE-LIKE 8: A Key Player in Early Seedling Development in Arabidopsis

Behnaz Saatian
The University of Western Ontario

Supervisor
Dr. Yuhai Cui
The University of Western Ontario Joint Supervisor
Dr. Susanne Kohalmi
The University of Western Ontario

Graduate Program in Biology
A thesis submitted in partial fulfillment of the requirements for the degree in Doctor of Philosophy

ABSTRACT

Plants' cell walls have unique chemical composition and features which enable them to play essential roles during plant development as shaping the cells and providing intercellular communication between adjacent cells. Polysaccharides, including callose, and glycoproteins are known as the main constituents of the cell wall. Callose, a linear β-1,3-glucan polymer, is accumulated at the cell plate during cytokinesis, in plasmodesmata, where it regulates cell-to-cell communication, in dormant phloem, where it seals sieve plates after mechanical injury and pathogen attack, and in male and female gametophytes. *GLUCAN SYNTHASE-LIKE* (*GSL*) genes in Arabidopsis comprise a family of 12 members. A new allele of *GSL8*, *essp8*, was identified as having seedling-lethal phenotype through a genetic screen for Arabidopsis mutants showing ectopic expression of seed storage proteins (*essp*). The gene responsible for the observed mutant phenotype was detected using a combination of bulked-segregant analysis, rough-mapping, and next-generation mapping. An EMS-induced point mutation was identified at an intron splice site of *GSL8*, predicted to introduce a premature STOP-codon. *essp8* seedlings exhibit pleiotropic phenotypic defects, including disruption of root tissue patterning, dwarfism and seedling lethality. Histochemical detection of callose and cell-to-cell diffusion assays showed reduction of callose deposition at the cell plates and plasmodesmata, cytokinesis defects and significant increase in size exclusion limit of plasmodesmata in *essp8* seedlings. Further investigation showed that the increase in size exclusion limit leads to an alteration in symplastic trafficking in primary roots of *essp8* seedlings. Plasmodesmata defects in *essp8* induce ectopic movement of two non-cell-autonomous factors, SHORT ROOT and microRNA165/6, both required for root radial patterning during embryonic root development. Attempts to identify the components of a hypothetical callose synthase complex revealed the interaction of GSL8 with two plasmodesmata-associated proteins, PLASMODESMATA-LOCALIZED PROTEIN 5 and β-1,3-GLUCANASE, as well as SUCROSE SYNTHASE 1, suggesting that they all might be parts of a single complex. The proposed putative complex might regulate callose deposition at the plasmodesmata and thereby determines the size exclusion limit. In summary, my findings suggest that GSL8 is required for cell wall integrity, maintaining the basic ploidy level and regulation of symplastic movement during early seedling development in Arabidopsis.

KEYWORDS

Arabidopsis thaliana, callose, GLUCAN SYNTHASE-LIKE 8, cytokinesis, plasmodesmata, β-1,3-GLUCANASE, PLASMODESMATA-LOCALIZED PROTEIN 5, intercellular signaling, symplastic trafficking, callose synthase complex

ACKNOWLEDGMENTS

Firstly, I would like to express my sincere gratitude to my supervisor and mentor Dr. Yuhai Cui for his immense knowledge and continuous support of my research. His guidance and patience helped me during my Ph.D. and writing of this thesis. I genuinely appreciate all the support and valuable advice from my co-supervisor Dr. Susanne Kohalmi, thanks for helping me to get through the hard times and frustrations.

Beside my supervisors, I would like to thank the rest of my thesis committee Dr. Abdelali Hannoufa and Dr. Sashko Damjanovski for their insightful comments and encouragement which led me to widen my research from various perspectives. I also would like to thank Dr. Ryan Austin in Agriculture and Agri-Food Canada (AAFC) for assisting with the next-generation sequencing data analysis.

I thank all my fellow labmates in Dr. Cui's lab, Dr. Gang (Gary) Tian, Dr. Chenlong Li, Chen (Alex) Chen, Jie Shu, Dr. Shaomin Bian, Vi Nguyen, Md Jakir Hossan and Raj Thapa, for all their stimulating discussions and help.

My sincere thanks go to Dr. Reza Saberianfar for all his helpful advice and comments on confocal microscopy, and his friendship.

I am grateful to Ms. Dorothy Drew for proofreading this thesis.

I also thank all my friends in AAFC and department of biology at Western, with special mention of Mandana Miri, Dr. Mehran Dastmalchi, Arun Angurajvadivel, Dr. Preetam Janakirama and Sara Abolhassani Rad, for all the joyful conversations during the last five years. In particular, I thank Dr. Nadia P. Morales for all her support and wonderful friendship.

I specifically would like to thank Amir Beygi for all his endless support, encouragement and incredible patience. I could not have completed this project without him. Thanks for making my life shinier.

Lastly, but definitely not the least, I thank my parents, Mohammad Hossein and Farzaneh, and my sister, Bita, for supporting me throughout my whole life and this journey. I am really grateful for everything that you have done for me.

TABLE OF CONTENTS

LIST OF TABLES

LIST OF FIGURES

LIST OF APPENDICES

LIST OF ABBREVIATIONS

ABRC	Arabidopsis Biological Resource Center
amiRNA	Artificial microRNA
AP2	APETALA 2
ARF7	AUXIN RESPONSE FACTOR 7
BAC	Bacterial Artificial Chromosome
BC	Back Cross
BG	Endo-1,3-β-GLUCOSIDASE
bHLH	Basic Helix-Loop-Helix
BSA	Bulked-Segregant Analysis
CALS	Callose Synthase
CaMV	Cauliflower Mosaic Virus
cDNA	Complementary DNA
CDS	Coding Sequence
CEI	Cortex/Endodermis Initial
CEID	Cortex/Endodermis Initial Daughter Cell
CENH3	Centromeric Histone H3
CESA	Cellulose Synthase Complex
CFP	Cyan Fluorescent Protein
CLV	CLAVATA

cM	Centimorgan
Col-0	Columbia Accession
CZ	Central Zone
DMSO	Dimethyl Sulfoxide
DNA	Deoxyribonucleic Acid
dsRNAi	Double-Stranded RNA Interference
EDTA	Ethylene Diamine Tetraacetic Acid
EMS	Ethyl Methanesulfonate
ER	Endoplasmic Reticulum
essp	Ectopic Expression of the Seeds Storage Protein
et2	Enlarged Tetrad2
FRET	Förster Resonance Energy Transfer
FT	FLOWERING LOCUS T
GAPDH	GLYCERALDEHYDE-3-PHOSPHATE DEHYDROGENASE
GAT	GFP ARRESTED TRAFFICKING
gDNA	Genomic DNA
GFLV	Grapevine Fan Leaf Virus
GFP	Green Fluorescent Protein
GPI-AP	Glycosylphosphatidylinositol-Anchored Protein

GSL	Glucan Synthase-Like
GTP	Guanosine-5'-Triphosphate
HD-ZIP III	Class III Homeodomain Leucine Zipper
HG	Homogalacturonan
KN1	KNOTTED1
KNOX	KNOTTED 1-Like Homeobox
KOB1	KOBITO 1
LB	Luria-Bertani Broth
LCR	LEAF CURLING RESPONSIVENESS
L*er*	Landsberg *erecta*
LFY	LEAFY
MADS	MCM1, AGAMOUS, DEFICIENS and SRF
MC	Middle Cortex
miR165/6	MicroRNA165/6
miRNA	MicroRNA
MP	Movement Protein
MS	Murashige and Skoog
NCATF	Non-Cell-Autonomous Transcription Factor
NGS	Next-Generation Sequencing

OE	Overexpression
PCR	Polymerase Chain Reaction
PD	Plasmodesmata
PDLP	PLASMODESMTA-LOCALIZED PROTEIN
PHB	PHABULOSA
PI	Propidium Iodide
PLT2	PLETHORA 2
PM	Plasma Membrane
PME	Pectin Methylesterase
PVX	Potato Virus X
QC	Quiescent Center
qRT-PCR	Quantitative Reverse Transcription-PCR
RAM	Root Apical Meristem
RGP	Reversibly Glycosylated Polypeptide
RLP	Receptor-Like Protein
RNA	Ribonucleic Acid
RNAi	RNA Interference
ROP	RHO-LIKE GTPase
ROS	Reactive Oxygen Species

SA	Salicylic Acid
SAM	Shoot Apical Meristem
SCD1	STOMATAL CYTOKINESIS-DEFECTIVE 1
SCR	SCARECROW
SCW	Secondary Cell Wall
SDS	Sodium Dodecyl Sulfate
SEL	Size Exclusion Limit
SHR	SHORT ROOT
SIEL	SHR-INTERACTING EMBRYONIC LETHAL
siRNA	Small Interfering RNA
SNP	Single Nucleotide Polymorphism
SPCH	SPEECHLESS
SSLP	Simple Sequence Length Polymorphism
SSP	Seed Storage Protein
SuSy	Sucrose Synthase
tasiRNA	Trans-acting siRNA
TMD	Transmembrane Domain
TMV	Tobacco Mosaic Virus
TRX-m3	Type m Thioredoxin

TVCV	Turnip Vein Clearing Virus
UDP-Glc	Uracil-Diphosphate Glucose
UGT1	UDP Glucose Transferase 1
UTR	Untranslated Region
VRC	Viral Replication Complex
WT	Wild Type
WUS	WUSCHEL
YFP	Yellow Fluorescent Protein

All numerical units included in this thesis are standard SI units

CHAPTER 1

1 INTRODUCTION

1.1 Plant cell wall: more than a physical barrier

Proper development of multicellular organisms is achieved through coordination of cell proliferation and differentiation. Different from animal systems, plant cells have rigid cell walls and, therefore, remain still after cell division. Plat cell walls have a unique chemical composition that enables them to perform several essential functions during plant development, such as shaping different types of cells, providing intercellular communication between adjacent cells and serving as a source of signaling molecules (Burton et al., 2010). Specialized cell walls in plants are responsible for shaping the cells Plant cell walls are mainly composed of polysaccharides such as cellulose and callose, and glycoproteins (Lerouxel et al., 2006). During the past two decades, due to the emergence of new cellular, molecular and genomics tools, an impressive progress has been made towards identification of callose structure and its important roles in plant development.

1.1.1 Callose

The chemical structure of callose was characterized for the first time in 1957 by Aspinall and Kessler (1957). Callose is formed by β-glucan polysaccharides and known as a component of cell walls in yeasts, plants, fungi, and lichens. β-glucans usually form local depositions at the cell wall and can also act as an energy reservoir in living organisms (Piršelová and Matušíková, 2013).

1.1.2 Structure of callose

Callose is a linear β-1,3-glucan with some 1,6 branches formed by hundreds of glucose residues bound by β-1,3-glycosidic bridges (Fig. 1.1). The structure and chemical composition of callose, such as the number of branches, can differ slightly depending on the cell wall type. The callose structure is not well characterized compared to cellulose, which is a linear long (>1,000 glucose units) chain of unbranched β-1,4-glucan with a crystal-like structure. Callose seems to form more of a helical structure (Piršelová and Matušíková, 2013).

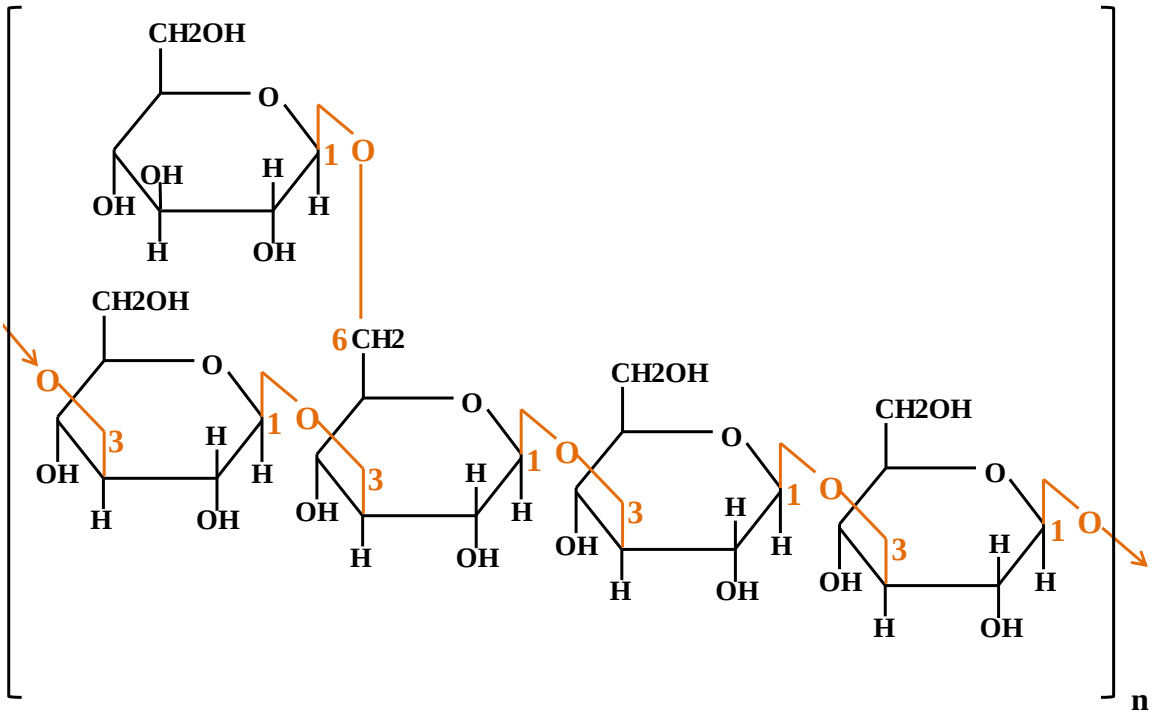

Figure 1.1 Chemical structure of callose.

Callose is a polymer of glucose formed by hundreds of glucose residues bound via β-1,3-glycosidic bridges. A Few 1,6 branches can also be found in callose structure. Figure modified from Chen and Kim (2009).

1.1.3 Callose in fungi

Glucan is known as the major structural polysaccharide in the cell wall of fungi which constitutes approximately 50-60% of its dry weight (Kapteyn et al., 1999). Glucan polymers are formed through assembly of repeating glucose residues into chains using different types of chemical linkages. Around 65-90% of the fungi cell wall glucan is β-1,3-glucan, with a lower ratio of other glucans, such as β-1,6-, mixed β-1,3- and α-1,4-, α-1,3-, and -1,4-linked glucans (Bernard and Latgé, 2001; Klis et al., 2001; Grün et al., 2005). β-1,3-glucan has been characterized as the most important component of fungi cell walls which forms a platform for the other components to attach covalently. Therefore, β-1,3-glucan synthesis is required for cell wall formation and normal development of fungi (Bowman and Free, 2006). Polymers of β-1,3-glucan are synthesized by β-1,3-glucan synthase complexes, which are associated with the plasma membrane. β-1,3-glucan polymers are expelled into the extracellular space after synthesis (Shematek et al., 1980; Douglas, 2001). Glucan chains are integrated within the cell wall at points of active cell wall synthesis.

Glucan synthase complexes are mainly localized to areas of cell growth, budding, or branching (Qadota et al., 1996; Beauvais et al., 2001). Long linear chains of glucan have approximately 1,500 glucose residues which are connected via β-1,3-linkages. In every 40-50 glucose residues, the carbon-6 positions become sites for attachment of additional β-1,3-glucans to generate a branched structure (Manners et al., 1973; Fontaine et al., 2000). Branched glucans provide mechanical strength and integrity to the cell wall by cross-linking with each other, as well as with mannoproteins (Kollár et al., 1997).

1.1.4 Callose in plants

In contrast to extensive studies on cellulose, a similar linear polysaccharide that accounts for 15-30% of the dry mass of all primary cell walls, research on callose and the molecular mechanism of its synthesis in plants has begun relatively recently (Verma and Hong, 2001; Dong et al., 2005; 2008; Dhugga, 2012). Callose is synthesized in the cell walls of specialized cells during specific stages of development.

Even though callose is accumulated in the cell wall at a lower level compared to cellulose, it is biologically significant as it plays crucial roles in various biological processes during plant growth, development, and also plant defense in response to adverse environmental stimuli (Chen and Kim, 2009). Callose is required for cell plate formation during cell division and cytokinesis, and is an important part of vascular bundles, pollen wall exine, and trichomes (Piršelová and Matušíková, 2013). Callose deposition at plasmodesmata (PD) and its subsequent degradation are critical for the regulation of symplastic movement of various substances. It is also important for formation and closing of sieve plate pores. Thus, callose plays an important role in cell-to-cell communication, and is required for proper development at different stages (Levy et al., 2006; Lucas et al., 2009; Xu and Jackson, 2010; Maule et al., 2011; Zavaliev et al., 2011; Xie et al., 2012). Most of the recent knowledge regarding the function of callose in plant development has been generated through studying *Arabidopsis thaliana* knockout lines for genes encoding callose synthases (Piršelová and Matušíková, 2013).

1.1.5 Role of callose in cytokinesis and cell plate formation

Cytokinesis in plants is different from that in animals because of some unique properties which can be considered as a type of polarized secretion (Assaad, 2001). At the end of anaphase of cell division, the components required for cell wall formation are carried to the equator of the dividing cell by secretory vesicles that are derived from Golgi. Later, these vesicles will fuse to form a membrane-attached structure, called the tubulovesicular network, which will give rise to the cell plate (Söllner et al., 2002). The cell plate will keep expanding until it binds to the mother cell wall at the division site. Callose deposition at the tubulovesicular network enforces widening and consolidation of tubules leading to conversion of the network into a fenestrated sheet (Samuels et al., 1995) to prevent the swelling of this structure (Verma, 2001). Cell plate maturation will proceed by callose replacement with cellulose and pectin that will eventually form the cell wall (Kakimoto and Shibaoka, 1992; Samuels et al., 1995). Therefore, a delay or absence of callose biosynthesis, as well as its overproduction can cause alteration of the cell plate composition and generate daughter cells with different ploidy levels (Verma, 2001) (Fig. 1.2).

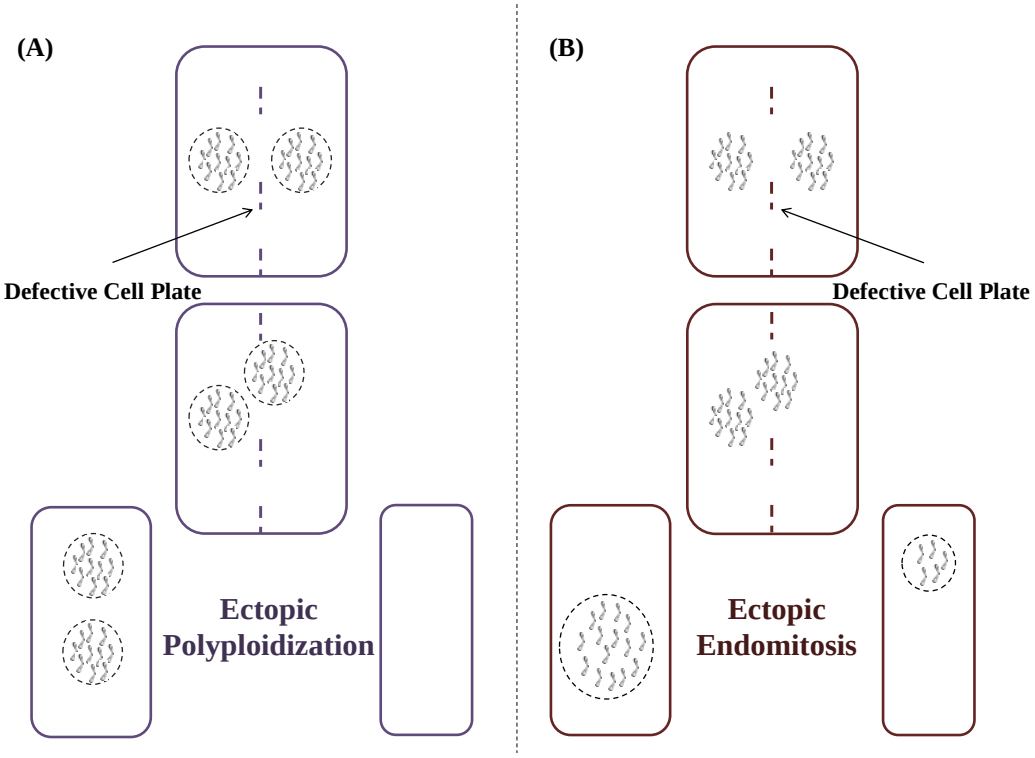

Figure 1.2 Formation of defective cell plate can lead to abnormal mitosis.
(A) Abortion of cell division after formation of nuclear envelope causes packaging of two newly formed nuclei into one cell and generation of binucleated cell and, therefore, ectopic polyploidization. (B) If the cell division abortion occurs before nuclear envelope formation, even though the sister chromatids have already been separated, they will be encapsulated into the same nucleus and, therefore, cells with different ploidy levels, which is known as ectopic endomitosis, will be generated.

Defects in cytokinesis can induce ectopic endopolyploidy which has been reported for several organisms and cell types (Hatzfeld and Buttin, 1975; Thompson and Lindl, 1976; Karess et al., 1991; Castrillon and Wasserman, 1994; Neufeld and Rubin, 1994; Liu et al., 1997; Spielman et al., 1997; Lordier et al., 2008; Pampalona et al., 2012; Serres et al., 2012). Cell plate-destructive conditions can also mimic ectopic endopolyploidization (Röper and Röper, 1977; De Storme et al., 2012). The cytological mechanism responsible for nuclear fusion in cell-plate defective mutants, resulting in enlarged cells with either multi-nucleated or polyploid nuclei, is not yet clear.

1.1.6 Role of callose in plasmodesmata regulation

Unlike animal cells, plant cells have stiff cell walls and do not move after cell division. Therefore, determination of a plant cell identity is highly dependent on positional cues. Accordingly, exchange of information between cells is required. Intercellular signaling processes occur through either apoplastic signaling using ligands and transmembrane-localized receptors, or symplastic movement of molecules (Stahl and Simon, 2013). Plant cells are interconnected via narrow channels of PD that facilitate symplastic movement of nutrients and signaling molecules (Rinne and van der Schoot, 1998) (Figure 1.3).

The PD pores that are formed between cells, allowing macromolecular trafficking through the cell wall barrier, are more than fixed passive channels. Instead, they dynamically allow passing of molecules of different sizes and are regulated by the production and/or degradation of callose (Vatén et al., 2011; Zavaliev et al., 2011). It has been proposed that callose is accumulated in the apoplastic neck of the PD to regulate its connectivity (Kitagawa et al., 2015).

Reversible deposition of callose seems to be an important mechanism to control PD permeability and regulates the PD's size exclusion limit (SEL) (Yadav et al., 2014). SEL determines the size of the PD pores and is typically defined based on the size of the largest molecule that can pass through PD aperture. The PD SEL is mostly shown by kDa as its unit (Kempers and van Bel, 1997; Oparka and Cruz, 2000). For example, in poplar and birch, PD in shoot apical meristems (SAMs) are closed during the dormancy

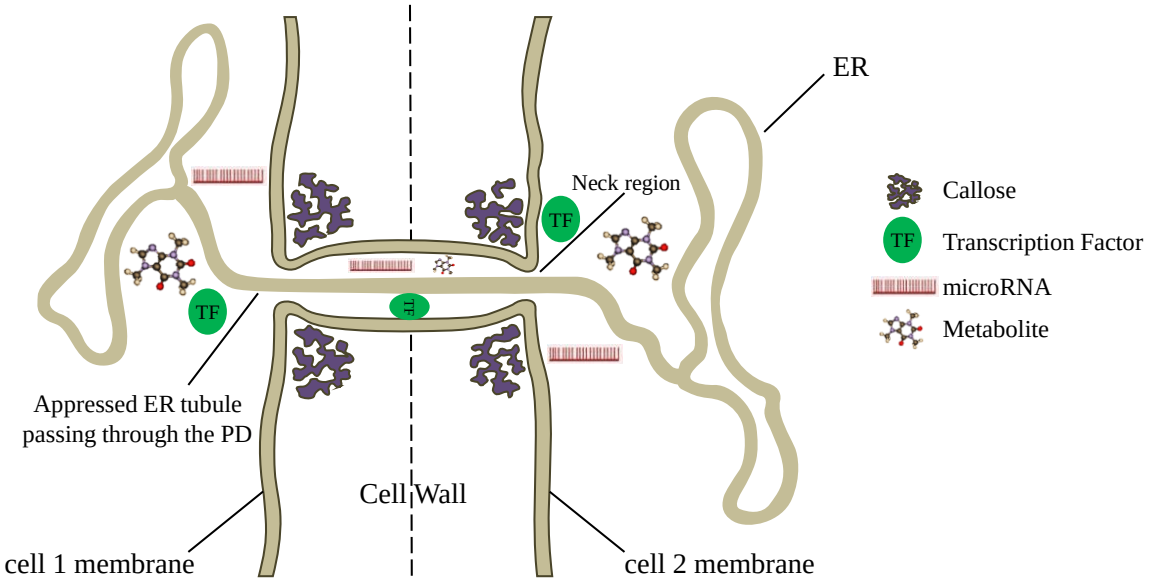

Figure 1.3 Diagram of a simple primary PD.

Primary PD consist of a narrow cytoplasmic channel which extends across the cell wall with an appressed endoplasmic reticulum (ER) tubule passing through its middle connecting two neighboring cells. It has been suggested that callose deposition at the neck of the PD modulates the SEL of PD and its permeability. PD facilitate symplastic movement of nutrients and different signaling molecules including mobile transcription factors and miRNAs. Figure modified from Morgan et al. (2010).

dormancy period via the deposition of callose. However, after induction of dormancy release by chilling, open PD are restored through degradation of callose by activity of β-1,3-glucanases (Rinne et al., 2001; 2011a). Although genetic, molecular, and biochemical studies during the last decades have implicated the important role of callose equilibration at the PD in regulation of PD SEL and symplastic movement, the molecular mechanism(s), which can clearly link the identified players for endogenous signaling to callose homeostasis, is not well-known yet (De Storme and Geelen, 2014).

1.2 Callose biosynthesis

Uracil-diphosphate glucose (UDP-glucose) is the precursor for callose biosynthesis (Chen and Kim, 2009). Biochemical and molecular studies in several plant species have shown that callose is synthesized by a class of enzymes, termed callose/ glucan synthases (Verma and Hong, 2001; Brownfield et al., 2007; Brownfield et al., 2008).

1.2.1 Glucan synthase in fungi

Synthesis of (1,3)-D-glucan polymer in fungi is catalyzed by UDP-glucose β(1,3)-D-glucan β(3)-D-glucosyltransferases (Douglas, 2001). These enzymes are known to form membrane-associated complexes that use UDP-glucose as a substrate and produce a linear polysaccharide. Several lines of evidence have suggested that the reaction is progressive. Chains of polysaccharide with increasing length are produced by adding one mole of glucose for hydrolyzing each mole of UDP-glucose (Shematek et al., 1980). Even though more than a hundred β-1,3-glucan synthase genes in fungi are available in public databases (Yang et al., 2014), only a few fungal genes encoding a β-1,3-glucan synthase have been characterized (Park et al., 2014). In *Saccharomyces cerevisiae*, three homologues of FKSs, which encode the enzymes forming a complex with β-1,3-glucan synthase activity, have been identified. FKS1 is active in the cell during the vegetative growth phase of yeast. β-1,3-glucan required during sporulation is synthesized by FKS2 (Douglas et al., 1994; Mazur et al., 1995), while FKS3 is needed for spore wall formation (Ishihara et al., 2007). In contrast to *S. cerevisiae*, only one homologous gene for *FKS1* (*fksA*) has been identified and isolated from *Aspergillus nidulans* (Kelly et al., 1996). The

subcellular localization of the β-1,3-glucan synthases and their regulatory interactors in filamentous fungi remain to be investigated.

1.2.2 Glucan synthase-like proteins in plants

Glucan synthases in Arabidopsis were first identified through their sequence similarity with the β-1,3-glucan synthase catalytic subunit FKS1 of yeast (Hong et al., 2001a). The homologs of glucan synthase in yeast, FKS1 and FKS2, are regulated by Rho1 GTPase that modifies their phosphorylation status. In plants, however, the activity of glucan synthases is usually dependent on Ca^{+2} (Qadota et al., 1996; Calonge et al., 2003).

The Arabidopsis genome has 12 genes encoding GLUCAN SYNTHASE-LIKE (GSL) (Richmond and Somerville, 2001), also called CALLOSE SYNTHASE (CALS) (Verma and Hong, 2001). *GSL* genes mostly have 40-50 exons except for *GSL1* and *GSL5* that only have two and three exons, respectively (Enns et al., 2005). *GSLs* code for large integral membrane proteins with multiple predicted transmembrane helices. The transmembrane domains are clustered into two regions (N-terminal and C-terminal), leaving a large hydrophilic cytoplasmic loop in between (Töller et al., 2008). The hydrophilic loop region possesses several glycosylation and phosphorylation sites. Therefore, it might act as an interaction and catalytic site for several regulatory proteins and substrates such as UDP-glucose (Verma and Hong, 2001). However, no specific domain containing a binding site for UDP-glucose has been identified yet (Brownfield et al., 2009; Zavaliev et al., 2011).

GSLs are known as enzymes synthesizing callose in response to different developmental, physiological, and environmental signals and in various tissues in plants (Verma and Hong, 2001). GSL isoforms play various roles during plant development. The actual organization of these enzymes, their stoichiometry and regulation are not well understood. Several studies have shown that a series of intracellular and extracellular factors and signals might be required to regulate GSLs' enzyme activity (Hayashi et al., 1987; Andrawis et al., 1993; Li et al., 1997, 1999a; Cui et al., 2001).

In Arabidopsis, *GSL1* and *GSL5*, differ from the other 10 genes of the family with having fewer and shorter introns. *GSL1* and *GSL5* are both located on chromosome 4, being about 8 centimorgan (cM) apart from each other. They also show similar expression patterns in roots, rosette leaves, stems, and flowers (Enns et al., 2005). Both genes have been shown to be involved in sporophytic development in Arabidopsis, where *GSL5* plays a more substantial role. Studies indicate that GSL1 and GSL5 are required for callose formation in the cell wall that separates the tetraspores, but are not needed for callose deposition at the wall surrounding the pollen mother cells. Since *GSL2* is highly expressed in the pollen, it might be the one that is involved in callose biosynthesis in the wall of pollen tubes (Doblin et al., 2001; Becker et al., 2003).

GSL2 was shown to be localized to the plasma membrane and Golgi-associated endomembrane structures (Xie et al., 2012) (Doblin et al., 2001; Becker et al., 2003). However, callose deposition was detected only in the cell wall and not in the Golgi vesicles. It is predicted that the plasma-membrane localized GSL2 might be the 'active' form of the enzyme whereas the endomembrane-associated GSL2 may be the 'inactive' form. It is still not clear what function the inactive form of the enzyme contributes in this intracellular compartment (Xie et al., 2012).

There are no studies available on GSL3 and its role in plant development. According to microarray data (Schmid et al., 2005), *GSL3* is highly expressed during embryo development. At the amino acid sequence level, GSL3 shows the highest similarity to GSL6.

GSL4 mutations were shown to have no substantial impact on the plant phenotype or deposition of callose, indicating that GSL4 enzyme activity does not play a major role during plant development (Maeda et al., 2014).

GSL5 is the best characterized member of the GSLs family in Arabidopsis and is known as a callose synthase that is required for formation of callose in response to fungal pathogens (Wawrzynska et al., 2010; Ellinger et al., 2013; Kopischke et al., 2013; Ellinger et al., 2014). A *GSL5* knockdown line, generated by a double-stranded RNA interference (dsRNAi) approach, showed absence of papillary callose deposition after inoculation of leaves with the fungal pathogens. Although the typical round wall

appositions, which is formed beneath fungal appressoria, was indistinguishable from wild type, the cell walls lacked callose in the *gsl5* knockdown lines (Jacobs et al., 2003). It has been suggested that GSL5 plays a role in stimulating the activity of pre-existing callose synthase enzyme, as well as specifically targeting the newly synthesized enzyme to the cellular "stress site" (Jacobs et al., 2003). It has been recently suggested that tocopherols, a family of vitamin E compounds, might be required for post-translational activation of GSL5 through a mechanism which is unlikely to be dependent on the wound-signaling pathway (Maeda et al., 2014).

GSL6 is a cell plate-specific callose synthase localized at the cell plate of cells during cytokinesis and has been suggested to form a complex with a UDP-glucose transferase (Hong et al., 2001a; Hong et al., 2001b). *GSL6* expression is up-regulated in response to salicylic acid (SA), indicating that, similar to GSL5, it might be involved in callose deposition after pathogen attack. *gsl6* mutant plants do not show any detectable phenotypic defects under regular growth conditions (Dong et al., 2008).

GSL7 is only expressed in the vascular system and more specifically in the phloem sieve elements and companion cells, indicating that GSL7-mediated callose synthesis is highly tissue-specific (Xie et al., 2011). In support of this, *gsl7* mutants do not display any obvious macroscopic phenotypic defects, suggesting that GSL7 has no biological function other than phloem-specific PD callose synthesis (Huang et al., 2009). *GSL7* is highly and specifically expressed in phloem during root development, when a large number of symplastic connections are required (Vatén et al., 2011).

According to a promoter analysis (Dong et al., 2008) and microarray data (Schmid et al., 2005), *GSL9* is poorly expressed in most of the tissues and organs compared to the other *GSLs*. At the amino acid sequence level, GSL9 is most closely related to GSL12, but there is no evidence available yet to show their functional redundancy.

Although among all members of the GSL family, GSL10 is most closely related to GSL8, with 63.7% DNA and 63.4% protein sequence identity, respectively, it acts independently from GSL8 in different sporophytic tissues and organs, and during plant growth (Zimmermann et al., 2004; Töller et al., 2008). It has been shown that GSL8 and GSL10

are independently required during pollen development. In *gsl10* mutants, entry of microspores into mitosis is prevented (Töller et al., 2008), therefore, efforts to obtain homozygous knockouts have not been successful.

Similar to *gsl4, gsl6* and *gsl7, gsl11* mutant plants do not show any noticeable growth defects compared to wild-type plants. Loss of enzyme activity does not reduce callose deposition (Maeda et al., 2014), suggesting that GSL11 does not play a major role and probably is not required for plant development. The possibility of having a more specialized role cannot be ruled out.

GSL12 synthesizes callose at certain sites in the cell walls surrounding the PD and, therefore, can determine PD size and control molecular trafficking through PD. During plant development, *GSL12* is highly expressed in the phloem, stele and root meristem (Vatén et al., 2011). Expression of *GSL12* in a *gsl7* background can complement the mutant phenotype (Xie et al., 2011). GSL7 is responsible and required for callose biosynthesis in the phloem and during phloem development (Barratt et al., 2011). These observations led to the proposal that these two proteins are, at least partially, if not completely, redundant regarding their function during sieve elements development, (Vatén et al., 2011).

1.2.3 GLUCAN SYTHASE-LIKE 8

GLUCAN SYNTHASE-LIKE 8 (*GSL8*) is known as one of the few members of the GSL family with ubiquitous expression in most of the tissues and organs during plant development with the highest expression in vasculature (Schmid et al., 2005). Since most of the callose in the vasculature is deposited at the PD to reduce SEL of PD, GSL8 has been suggested to be associated with PD regulation. According to genomic and amino acid sequence, GSL8 is most closely related to GSL10, and is also required during pollen development with an important role in sporophyte (Töller et al., 2008).

GSL8 callose biosynthesis activity is required for proper cell plate formation during cytokinesis. *massue*, a mutant allele of *GSL8*, showed significant delay in cell plate formation, similar to that reported for cytokinesis defective mutants such as *knolle* and

keule (Thiele et al., 2009). Although a direct link between callose deposition at the cell plate and cytokinesis defects was not confirmed, the incomplete cell walls and multi-nucleated cells in *massue* were explained as downstream effects of defects in callose deposition (Thiele et al., 2009). A substantial role of GSL8 in proper cell plate constitution during cytokinesis was further confirmed using an inducible RNA interference (RNAi) line of *GSL8* (Chen et al., 2009). *gsl8* mutant seedlings showed stubs in their cell walls, two nuclei in one cell, excessive cell proliferation at the epidermis, and clusters of stomata (Chen et al., 2009). A weak mutant allele of *GSL8*, called *enlarged tetrad2* (*et2*), showed induction of endomitotic polyploidization in different tissues due to defects in cytokinesis and cell wall establishment, indicating that callose is required for retaining the ploidy level. Different from other *gsl8* mutant alleles, in *et2* plants cytokinesis impairments do not induce serious damage on the plant's vegetative growth and its normal development, therefore, *et2* plants appear similar to the wild type (De Storme et al., 2013). Even though several indirect lines of evidence have already confirmed callose requirement for cell plate growth and cytokinesis, no direct functional evidence is yet available.

Guseman et al. (2010) showed that *CHORUS*, another allele of *GSL8*, is required for formation of normal stomatal patterns and organizing stomatal cell lineage initiation. The numbersof stomatal-lineage cells were significantly increased in *chorus* mutant plants, and this increase was mediated by SPEECHLESS (SPCH) (Guseman et al., 2010), a basic helix-loop-helix (bHLH) protein that specifically initiates stomatal lineage (Lampard et al., 2008). In *chorus*, there was also an increase in symplastic movement of macromolecules between epidermal cells, and larger molecules which would normally not pass through the PD could diffuse to the neighboring cells, suggesting that in addition to cytokinesis defects, *gsl8* mutants exhibit PD defects as well (Guseman et al., 2010). The *gsl8* mutant's pleiotropic phenotype suggests that GSL8 might have important regulatory roles during plant development, rather than just being an enzyme responsible for callose biosynthesis at the cell plate to complete cytokinesis and at the PD to regulate their SEL.

1.2.4 Callose synthase complex

Highly regulated synthesis and deposition of callose indicates that an extremely-specialized protein complex is involved in this process (De Storme and Geelen, 2014). It is predicted that GSLs might be integrated into a complex, hypothetically named the CalS complex. Based on the genetic evidence obtained from studying *de novo* cell plate formation, pollen tube tip growth and cotton fiber elongation, there are at least four proteins which can potentially comprise the CalS complex, including at least one of the GSLs, UDP glucose transferase1 (UGT1), Rho-like GTPase (ROP), and sucrose synthase (SuSy) (Andrawis et al., 1993; Amor et al., 1995; Shin and Brown, 1999; Hong et al., 2001a; 2001b; Verma and Hong, 2001). Degradation of sucrose is catalyzed by UDP-glucose:D-fructose 2-alpha-D-glucosyltransferase (SuSy), a sugar metabolic enzyme which has been characterized as a critical part of cellulose synthase complexes to provide UDP-Glc. Since GSLs also use UDP-Glc as the precursor for β-1,3-glucan polymer synthesis, it is tempting to speculate that SuSy might provide the supply of UDP-Glc to GSLs as well. Supporting this hypothesis, UDP-Glc transfer from SuSy to GSLs occurs in presence of UGT1 activity (Hong et al., 2001a; 2001b). UGT1 interacts with Rho-like GTPase 1 (ROP1) and this interaction only takes place in GTP-bound state of UGT1, indicating that UGT1-dependent activity of ROP1 might regulate GSLs by restricting their substrate supply (Li et al., 1999b; Verma and Hong, 2001). UGT1, ROP1 and SuSy lack transmembrane domains. Therefore, if there is any sort of interactions between these proteins and GSLs, it should be through their association with the hydrophilic loop of GSLs (De Storme and Geelen, 2014).

Although the significance of a CalS complex and its components required for callose deposition at the cell plate during cytokinesis has been well studied and characterized, it is not clear if all of these subunits are needed for synthesizing callose at the PD. It has been suggested that CalS complex composition likely differs depending on the tissue and process that it is involved in (Verma and Hong, 2001). Hence further research is required to reveal if the CalS complex at the PD is closely-related to the one at the cell plate.

1.3 Regulatory role of plasmodesmata in development

During plant development and in response to biotic and abiotic stresses, cell walls undergo structural modifications that are predicted to introduce changes in PD structure (Knox and Benitez-Alfonso, 2014). Genetic screening to identify mutants defective in intercellular communications has confirmed that PD components are required for viability as functional or structural PD mutants are mostly lethal (Wu et al., 2002). The number and SEL of PD vary depending on the tissue and developmental state (Wu et al., 2002). SEL restricts passage of those molecules with sizes larger than SEL through PD (Crawford and Zambryski, 2000).

Cell wall PD can be primary or secondary. Primary PD are formed during cell division when the cell plate is forming, while secondary PD are formed in localized breaks in the established cell walls. Both primary and secondary PD contain a membranous channel and a desmotubule that is connected to the ER of both cells (Fig. 1.3) (Burch-Smith and Zambryski, 2012). PD plasma membrane has a distinct lipid composition compared to the other regions. It consists of complex sphingolipids, sterols and glycerolipids, suggesting that they may have a role in signaling for a variety of receptor proteins, some of which have shown specialized localization and/or activity at either PD or plasma membrane (Kitagawa et al., 2015).

While PD were previously considered to be channels used for passive movement of water, nutrients, and ions based on their concentration gradients, newer research has shown PD's function is not restricted to passive diffusion. It is now well known that movement of larger molecules is also facilitated by PD and is more selective than a gradient-based movement (Burch-Smith and Zambryski, 2012). Transcription factors, metabolites, and small RNAs, which are responsible for cell-to-cell communication during plant development and for plant defense upon virus infection, are transported through PD (Stahl and Simon, 2013).

PD are required for symplastically restricted movement of plant virus pathogens and their invasion to neighboring cells (Lucas, 2006). Virus transport upon infection is affected by formation of complex PD and callose biosynthesis at the PD which are regulated by SA

(Wang et al., 2013). A range of molecular interactions between host and pathogen are required by viruses to access PD. Two models have been suggested to describe the movement of viruses via PD. In the first model, viral replication complexes (VRCs) can be translocated, i.e. *Tobacco mosaic virus* (TMV), in which VRCs are formed intracellularly via its interaction with ER-microtubule junctions at PD (Heinlein, 2015). In the second model, encapsulated viral RNA movement plays an important role. *Potato virus X* (PVX) cap proteins have been detected on both sides of PD, suggesting that viral replication occurs at PD and this seems to be required for intercellular movement of PVX (Tilsner et al., 2014). Biotrophic fungi invasion into plant tissues has also been suggested to be facilitated by PD (Kankanala et al., 2007). All of these macromolecules and organisms have sizes above the normal SEL of PD, indicating the importance of PD regulation to recognize and transport highly specific molecules between cells (Thomas et al., 2008).

1.4 Protein constituents of plasmodesmata

Secondary PD are formed *de novo* (Faulkner et al., 2008). Twined, Y- and H-shaped (branched) PD are probably the intermediates during the process of PD *de novo* formation (Maule, 2008). PD are known as complex structures. Attempts to purify PD have not been successful. Therefore, their molecular composition and the mechanisms that regulate them are not well understood. Since cell-to-cell communication is required for survival, PD mutants exhibit severe developmental defects as early as embryogenesis (Burch-Smith and Zambryski, 2012). In recent years, by taking advantage of improved methods, attempts towards isolating cell wall fractions harboring PD have become more successful. More than a thousand PD-associated candidate proteins have been identified using nano-liquid chromatography and an Orbitrap ion-trap tandem mass spectrometer in combination with using Arabidopsis cell cultures as plant material (Fernandez-Calvino et al., 2011).

Distinguishing PD proteins from other plasma membrane proteins has remained a challenge due to lack of a specific motif/domain. PD proteome analyses revealed association of several cell wall remodeling enzymes, as expected (Table 1.1). This set of enzymes is involved in cell wall modification and remodeling primarily with a role in

Table 1.1 List of a subset of proteins previously identified in the PD proteome.
The identified proteins have putative functions important for cell wall modifications and remodeling (Brecknock et al., 2011; Fernandez-Calvino et al., 2011).

Gene name	Gene ID	Function
GLUCAN SYNTHASE-LIKE 3	AT2G31960	Callose metabolism
GLUCAN SYNTHASE-LIKE 5	AT4G03550	Callose metabolism
GLUCAN SYNTHASE-LIKE 6	AT1G05570	Callose metabolism
GLUCAN SYNTHASE-LIKE 8	AT2G36850	Callose metabolism
GLUCAN SYNTHASE-LIKE 10	AT3G07160	Callose metabolism
GLUCAN SYNTHASE-LIKE 12	AT5G13000	Callose metabolism
β-1,3-GLUCANASE	AT1G64760	Callose metabolism
β-1,3-GLUCANASE	AT3G07320	Callose metabolism
β-1,3-GLUCANASE	AT3g55430	Callose metabolism
β-1,3-GLUCANASE	AT4G31140	Callose metabolism
β-1,3-GLUCANASE (ATBG_PPAP)	AT5G42100	Callose metabolism
β-1,3-GLUCANASE	AT5G58090	Callose metabolism
PECTIN METHYLESTERASE 1	AT1G53840	Pectin modification
PECTIN METHYLESTERASE 26	AT3G14300	Pectin modification
PECTIN METHYLESTERASE INHIBITOR 1	AT4G12390	Pectin modification
POLYGALACTURONASE/PECTINASE	AT1G65570	Pectin modification
GLYCOSYL TRANSFERASE ACTIVITY	AT1G02730	Biosynthesis of cell wall
UDP-GLYCOSYL TRANSFERASE	AT3G46650	Biosynthesis of cell wall
PLASMODESMATA-LOCATED PROTEIN 1	AT5G43980	Plasmodesmal structural protein
PLASMODESMATA-LOCATED PROTEIN 6	AT2G01660	Plasmodesmal structural protein
ACTIN 1	AT2G37620	Structural constituent of cytoskeleton
ACTIN 7	AT5G09810	Structural constituent of cytoskeleton
ACTIN 8	AT1G49240	Structural constituent of cytoskeleton
MYOSIN VIII A	AT1G50360	Glucuronoxylan metabolism
MYOSIN XI K	AT5G20490	Actin filament-based movement

callose biogenesis and homeostasis, including glucan synthase-likes (GSLs) and β-1,3-glucanases (BGs) (Gaudioso-Pedraza and Benitez-Alfonso, 2014). Even though pectin metabolism-related proteins have been detected in PD proteome, there is not enough information on how these enzymes might be involved in regulating symplastic intercellular communication. Pectin seems to be important for stabilizing PD anchorage to cell walls. Therefore, lack of pectin can presumably destabilize PD channel structure (Yu et al., 2004).

PD proteome revealed other enzymes involved in general cell wall biosynthesis and assembly, including glycosyl transferases and reversibly glycosylated polypeptides (RGPs). It is not known yet how expression of these proteins can modify PD structure and function (Pagant et al., 2002; Kong et al., 2012). An independent study revealed binding of RGPs class 1 family members to PD (Sagi et al., 2005). Reversible glycosylation of these proteins with UDP-sugars makes them a potential substrate for the enzymes involved in the biosynthesis of cell wall components. Overexpression of these proteins can increase callose accumulation which consequently restricts virus spreading and photoassimilates transport to sink tissues (Zavaliev et al., 2010; Burch-Smith et al., 2012). A novel regulator of symplastic trafficking was identified during a genetic screen for stomata differentiation mutants and was named KOBITO 1 (KOB1) (Kong et al., 2012). *KOB1* encodes a glycosyl transferase-like protein and is involved in cellulose biosynthesis (Pagant et al., 2002). However, it is not clear how cellulose biosynthesis and PD permeability might be linked (Kong et al., 2012). It has been hypothesized that KOB1 might regulate cell-to-cell connectivity at the PD by providing carbohydrates supply for the CalS complex. To address this hypothesis, subcellular localization of KOB1 and its interaction with other protein constituents of PD should be further investigated (De Storme and Geelen, 2014).

The identity of the proteins detected in the PD proteome analyses, mostly with roles in biosynthesis and modification of cell wall components, needs to be further studied. Independent modification of these cell wall microdomains can potentially provide more detailed information on their specific role in regulating PD aperture and its SEL (Knox and Benitez-Alfonso, 2014).

1.4.1 Plasmodesmata-localized proteins

PLASMODESMATA-LOCALIZED PROTEIN 1 (PDLP1) to PDLP8 belong to a small subfamily of the RECEPTOR-LIKE PROTEINs (RLPs) family with two conserved Cys-rich repeats and two extracellular DUF26 domains. PDLPs have a distinct N-terminal domain that is exposed to the apoplast and can act as a receptor for extracellular signals (Thomas et al., 2008). Since PDLPs have extremely short cytoplasmic domains (less than 20 amino acids) with no known signaling capacity, it has been proposed that the extracellular domains of PDLPs are their interacting domains with other proteins. PDLPs' interaction with other modifying enzymes, which are localized at the PD, can theoretically initiate signal transduction (Thomas et al., 2008). *PDLP1*-overexpression lines exhibit a reduction in GFP cell-to-cell diffusion, suggesting that PDLP1 is a negative regulator of trafficking through PD (Thomas et al., 2008). None of the PDLPs single knockouts show either phenotypic defects or changes in symplastic movement, which suggests that members of the PDLP family are highly redundant (De Storme and Geelen, 2014). Thomas et al. (2008) demonstrated that PDLPs' transmembrane domain (TMD) is required and sufficient for their localization to the PD, while the C-terminal cytoplasmic domain is less likely to be required for their intercellular targeting. The receptor-like targeting of PDLPs and their localization at the PD suggest that extracellular signaling can also have a role in controlling symplastic trafficking (De Storme and Geelen, 2014). Therefore, PDLPs might play a role during plant development, and in response to both internal and external signals (Lee et al., 2011).

PDLPs might negatively regulate PD SEL by inducing callose deposition at the PD, which might be mediated through their interaction with callose homeostasis proteins such as GSLs (De Storme and Geelen, 2014). Key evidence supporting this hypothesis was obtained from *PDLP5*-overexpression plants, in which an increase in callose deposition at the PD and concomitant reduction in cell-to-cell movement of viral genome movement proteins (MPs) was observed. This finding suggested that PDLP5 controls PD size exclusion limit through modification of callose accumulation at the PD in response to pathogen invasion, also confirmed by strong up-regulation of *PDLP5* upon bacterial infection (Lee et al., 2008; 2011). A recent study has shown that callose accumulation at

PD is mediated by PDLP5 and is dependent on both the presence and an increase in SA. This finding suggested that both PDLP5 and SA are required and are likely to act interdependently to reduce cell-to-cell permeability and symplastic movement (Wang et al., 2013).

Interestingly, contrary to PDLPs' negative regulation of PD, under specific conditions PDLPs can also positively regulate cell-to-cell communication through PD. It has been recently reported that the MPs from tubule-forming *Grapevine fan leaf virus* (GFLV) can physically interact with all PDLPs isoforms (Amari et al., 2010). Additionally, MPs targeting to the PD, MP tubule assembly and GFLV PD-mediated movement require this interaction with PDLPs (Amari et al., 2010). Hence, further research is required to identify the molecular mechanisms and factors underlying these two different functions of PDLPs: induction of callose deposition in response to pathogens, and facilitation of the viral genome spreading.

1.4.2 β-1,3-Glucanases

β-1,3-glucanases or glucan endo-1,3-β-glucosidases (BGs) are enzymes that hydrolyze the linkages in 1,3-β-D-glucosidic polymers and generate single β-1,3-glucan subunits. These enzymes are not restricted to plant species and can also be found in bacteria, fungi, metazoa and viruses (Bachman and McClay, 1996; Sun et al., 2000).

BGs were first identified due to their role in protecting plants against pathogens (Kauffmann et al., 1987; Bowles, 1990; Sela-Buurlage et al., 1993; Stintzi et al., 1993; Jach et al., 1995; Douglas, 2001). BGs in Arabidopsis are a family with 50 members (Levy et al., 2007), and belong to glycosylphosphatidylinositol-anchored proteins (GPI-APs) (Elortza et al., 2003). GPI-APs have a specific plasma membrane localization pattern known for the absence of TMDs. BGs bear a cleavable hydrophobic N-terminal secretion signal peptide for translocation into the ER, and a hydrophobic C-terminal tail, which most likely forms a transient TMD, for targeting them to PM (Elortza et al., 2003). Three members of the BG family, ATBG_PPAP, PdBG1, and PdBG2, were shown to have a role in callose degradation at the PD (Benitez-Alfonso et al., 2013).

Genetic characterization of PD-localized enzymes which degrade callose suggests their requirement for balancing callose level at the PD. In support of this hypothesis, *atbg_ppap* mutants show an increase in callose accumulation at the PD as well as decrease in the systematic spread of the TMV and *Turnip vein clearing virus* (TVCV) (Levy et al., 2007; Zavaliev et al., 2013).

PdBG1 and PdBG2 localization at the PD was confirmed by their punctate distribution pattern at the cell periphery (Benitez-Alfonso et al., 2013). Although single mutants do not exhibit any phenotypic defects, most likely due to functional redundancy, double mutants (*pdbg1 pdbg2*), show an increase in callose accumulation at the PD as well as restricted cell-to-cell transport of macromolecules. *PdBG1*-overexpression plants show the opposite effect. Therefore, it can be concluded that callose accumulation at the PD and symplastic movement in the developing roots are negatively regulated by two redundant β-1,3-glucanases (PdBG1 and PdBG2) (Benitez-Alfonso et al., 2013).

Involvement of β-1,3-glucanases in PD regulation has also been observed in other plants. For example, in Populus, two closely-related genes encoding PD-located BGs were identified with roles in mediating FLOWERING LOCUS T (FT) movement into the bud during the dormancy release period (Rinne et al., 2011b). BGs' involvement in intercellular trafficking regulation has been identified mostly in permanent processes, suggesting that callose turnover mechanisms are used by plants for longer-lasting closure of PD (Levy et al., 2007). It needs to be further investigated whether plants employ other mechanisms for short-term changes in the PD channels.

1.5 Symplastic movement of mobile factors through plasmodesmata

PD connect almost all plant cells providing selective passage of macromolecules (Crawford and Zambryski, 2000; Lucas and Lee, 2004). There are a number of transcription factors, in shoot and root apical meristems (SAMs and RAMs, respectively), which are expressed in different cells from where they are localized and have functions, known as non-cell-autonomous transcription factors (Kurata et al., 2005a; Lee et al., 2006). Transcription factors that are involved in development, particularly KNOTTED 1-LIKE HOMEOBOX (KNOX) and MCM1, AGAMOUS, DEFICIENS and SRF (MADS)

family members, exhibit intercellular movement, potentially through PD (Xu and Jackson, 2010; Burch-Smith et al., 2011). Similar to transcription factors, some small RNAs, particularly those playing roles in RNA silencing pathways, also show non-cell-autonomous activity (Dunoyer et al., 2005).

1.5.1 Mobile transcription factors

Plants, similar to animals, use signal peptides, hormones, and microRNAs (miRNAs) for intercellular signaling. They are, however, additionally equipped with a collection of mobile transcription factors to deliver intercellular signals (Han et al., 2014a). Since plant cells are surrounded by rigid cell walls, the movement of most of the mobile proteins is facilitated via PD, which provides a direct route for protein movement between cells (Oparka, 2004).

Co-operation and co-ordination of individual cells is required for the development of multicellular organisms. Intercellular communication between cells is mandatory to co-ordinate proliferation, differentiation, and programmed cell death during tissue formation. Precise control of intercellular signaling during development is the key to generate a multicellular organism (Long et al., 2015). Movement of molecular signals plays important roles in many highly regulated cell proliferation and specification phenomena. However, the molecular context of all these signals is not yet entirely known. Regulation of trichome and root-hair patterning (Bouyer et al., 2008; Digiuni et al., 2008; Pesch and Hülskamp, 2009; Wester et al., 2009), RAM and SAM development (Lucas et al., 1995; Kim et al., 2003; Schlereth et al., 2010; Xu et al., 2011), and the patterning and development of the mature root (Nakajima et al., 2001; Gallagher et al., 2004; Kurata et al., 2005b; Cui et al., 2007) are all mediated by mobile transcription factors.

Root tissue patterning is determined by a group of pluripotent cells in the meristematic tissue surrounding the quiescent center (QC) cells (Dolan et al., 1993; Van den Berg et al., 1997). Communication between these cells and those around them is achieved by different mobile signals, including the phytohormone auxin and mobile proteins or peptides (Sabatini et al., 1999; Stahl et al., 2009; Matsuzaki et al., 2010; Schlereth et al.,

2010). Although the concept of mobile transcription factor signaling seems to be simple, several pieces of evidence have revealed an astonishing complexity of this process.

Since KNOTTED 1 (KN1), a homeodomain protein from *Zea mays*, was characterized as the first mobile transcription factor (Hake and Freeling, 1986; Lucas et al., 1995), the list of mobile transcription factors, also called non-cell-autonomous transcription factors (NCATFs), has been growing continuously. Some of the proteins with confirmed regulatory roles in plant development include LEAFY (LFY), a regulator of flower development (Sessions et al., 2000); SHORT-ROOT (SHR), a GRAS-domain transcription factor regulating stem cell activity and radial patterning of the Arabidopsis root (Nakajima et al., 2001); FT, a long-distance signal inducing floral transition (Corbesier et al., 2007); WUSCHEL (WUS), a homeodomain transcription factor maintaining stem cell homeostasis in the SAM (Yadav et al., 2011); PLETHORA 2 (PLT2), an APETALA 2 (AP2) transcription factor driving auxin-dependent root zonation (Mähönen et al., 2014); and many more (Han et al., 2014a).

Depending on the type of NCATF, the movement pattern can be different. If the protein size is smaller than the SEL of plasmodesmata, like LFY, the movement takes place via diffusion between plant cells similar to what happens with free green fluorescent protein (GFP) (Wu et al., 2003). However, cell-to-cell movement of most NCATFs is highly controlled, and is tightly linked to their activities and role in development.

1.5.2 SHORT ROOT

Intercellular movement of endogenously encoded SHR is essential for a plant's normal growth and development (Nakajima et al., 2001; Gallagher and Benfey, 2009; Yadav et al., 2011). SHR is required for cell division, endodermis specification (Benfey et al., 1993; Helariutta et al., 2000) and turning on microRNA165/6 (miR165/6) in the endodermis (Carlsbecker et al., 2010). *shr* mutants show reduced root length, loss of a ground tissue layer and endodermal cell fate (Benfey et al., 1993; Scheres et al., 1995; Helariutta et al., 2000).

SHR protein is a transcription factor which has the ability to move from the stele cells, its domain of transcription, to a single layer of adjacent cells including QC, the cortex/endodermis initial (CEI) and daughter cells (CEIDs), as well as to all endodermis cells (Fig. 1.4) (Nakajima et al., 2001; Wu and Gallagher, 2013). SHR movement acts both as a signal from the stele and an activator of endodermal cell identity determination and cell division through the transcriptional activation of *SCARECROW* (*SCR*) (Nakajima et al., 2001). Ectopic expression of *SHR* in adjacent layers induces an increased number of cell layers and cell identity change (Cui et al., 2007). The protein's subcellular localization differs depending on the tissue. In the stele cells, SHR is localized in both the nucleus and cytoplasm, while in the neighboring cell layer, including the QC, CEI, and endodermis, it specifically resides in the nucleus (Nakajima et al., 2001). SHR movement needs to be carefully regulated to guarantee both up- and down-regulation of asymmetric cell divisions in the endodermis (Vatén et al., 2011).

SHR moves through PD (Vatén et al., 2011). This movement is mediated through SHR interaction with the SHR binding protein, SHR-INTERACTING EMBRYONIC LETHAL (SIEL) (Gallagher et al., 2004; Gallagher and Benfey, 2009; Koizumi et al., 2011). Recent study showed that the movement of SHR is facilitated by endosomes (Wu and Gallagher, 2014). SHR can be localized to early and late endosomes. However, it is not clear how this localization can promote SHR movement. Two models have been proposed to explain endosome-mediated movement of SHR. In the first model, endosomes can interact with SIEL to facilitate SHR movement towards the plasma membrane and then diffuses to PD. In the second model, endosomes act as a platform where SHR can associate with SIEL as well as other proteins that can directly or indirectly facilitate its movement between cells (Wu and Gallagher, 2014).

1.5.3 WUSCHEL

Intercellular communication between different cell types within plants' stem cell niches is required for both stem cells maintenance and their differentiation (Spradling et al., 2008; Rieu and Laux, 2009). Several studies have shown that WUSCHEL (WUS), a homeodomain transcription factor produced in the organizing center cells of SAM, is required and sufficient for stem cell specification (Laux et al., 1996). *WUS* transcription

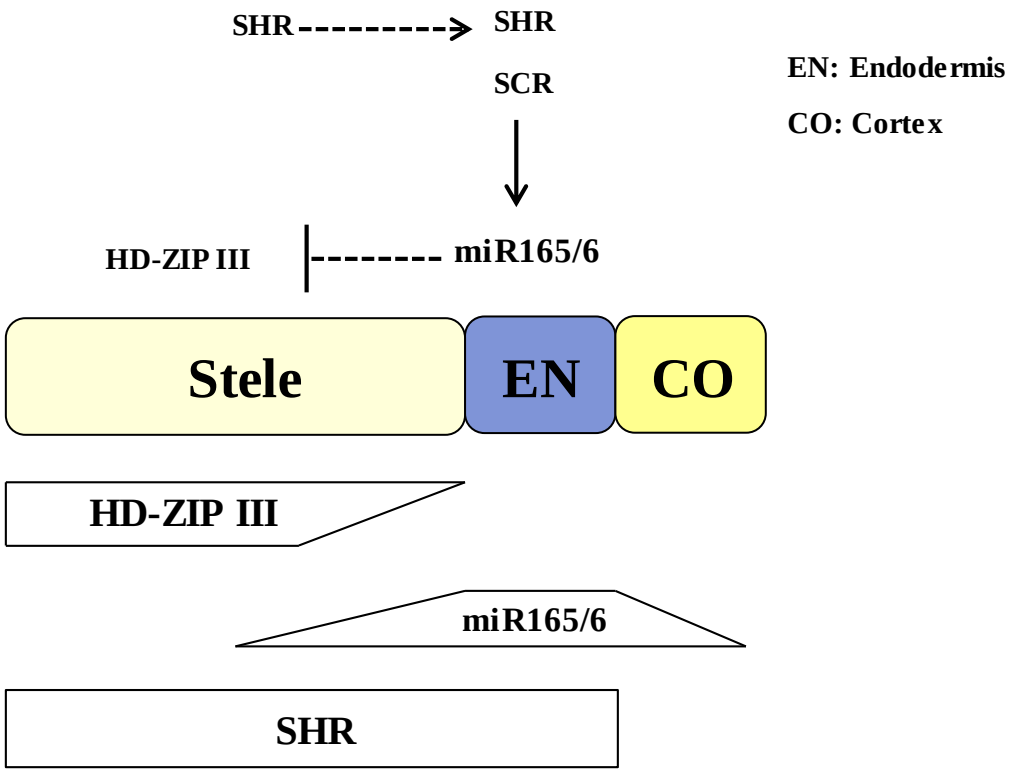

Figure 1.4 Diagram of SHR and miR165/6 intercellular movement in Arabidopsis root. After expression in the stele cells, SHR moves from stele into the neighboring cells including endodermis where it transcriptionally activates *SCR*. SHR-SCR complex activates miR165/6 in the endodermis. After activation, the mature miR165/6 move from endodermis to stele as well as from endodermis to cortex. miR165/6 suppress the family of *HD-ZIP III* genes in stele by targeting their transcripts.

is restricted to cells of the SAM organizing center, which is known to be critical for keeping the number of stem cells constant (Yadav et al., 2011). The CLAVATA (CLV) signaling pathway mediates this process (Fletcher et al., 1999; Brand et al., 2002). WUS can move laterally in the SAM for at least two cell layers (Yadav et al., 2011).

WUS is synthesized in the organizing center cells of the SAM from which it can then move to adjacent cell layers. Studies have shown that interference with WUS movement does not hinder its biological activity, but inhibits SAM regular function (Yadav et al., 2011). WUS protein directly activates *CLV3* transcription through binding to its promoter after migrating to surrounding cells of SAM central zone. Misexpression of *WUS* in adjacent cells of SAM central zone (CZ) causes expansion of the stem cells and meristem proliferation (Brand et al., 2002; Yadav et al., 2010). Cell-to-cell communication via PD in the CZ of the SAM is required for stem cell activity. Analysis of endogenous WUS has shown that WUS trafficking through PD is more possible than via either secretion or endocytosis. Since WUS degradation in SAM stem cells causes meristem termination, it can be concluded that WUS might be one of the critical signals derived from the stem cell niche (Daum et al., 2014). However, more studies are required to characterize WUS function and its molecular mechanisms in regulating cell division and differentiation of stem cells, which are crucial for stem cell maintenance.

1.5.4 Movement of small RNAs through plasmodesmata

It has been shown that in plants and animals small RNAs, including miRNAs, small interfering RNAs (siRNAs) and trans-acting siRNAs (tasiRNAs) have the potential to move between cells and mediate cell-to-cell communication. Although several pieces of evidence have indicated the movement of siRNAs, tasiRNAs and miRNAs, the mechanism(s) of this movement remains to be uncovered (Juarez et al., 2004; Dunoyer et al., 2007; Lin et al., 2008; Tretter et al., 2008; Chitwood et al., 2009; Nogueira et al., 2009).

miR165/6, two very closely related miRNAs that differ by only one single nucleotide in their sequence, regulate plant development by targeting the family of class III homeodomain leucine zipper (*HD-ZIP III*) genes including *PHABULOSA* (*PHB*) (Jung and Park, 2007; Zhou et al., 2007; Liu et al., 2009). It has been reported that the

transcription of *HD-ZIP III* family genes is mostly restricted to the vascular cylinder (Lee et al., 2006) whereas miR165/6 is produced in the endodermis and targets *HD-ZIP III* mRNA in the stele (Fig. 1.4) (McConnell et al., 2001; Emery et al., 2003; Prigge et al., 2005). Hence, a mobile signal should exist to assist miR165/6 to accomplish its goal. Several studies have shown that miR165/6 movement plays critical roles in both shoot apical meristem and in root patterning (Juarez et al., 2004; Chitwood et al., 2009; Nogueira et al., 2009; Carlsbecker et al., 2010).

miR394 was identified as another mobile miRNA (Knauer et al., 2013). miR394 is produced in the protoderm and represses the transcript encoding the F box protein LEAF CURLING RESPONSIVENESS (LCR) by moving to the distal meristem. This repression is critical for maintaining stem cell pluripotency by synergistically increasing the signaling from beneath the stem cell generated by WUS. miR394, similar to WUS, can move for a distance of about three cell layers (L1-L3) in the SAM (Knauer et al., 2013).

1.6 Regulation of plasmodesmata size exclusion limit

Although the detailed process of SEL regulation is still under debate, several lines of evidence support callose turnover as an important mechanism for regulation of PD and symplastic trafficking through it (Levy et al., 2007; Vatén et al., 2011; Sevilem et al., 2013). Deposition of callose at the PD can physically constrict the channel. Therefore, reducing the SEL or even blocking the PD results in blockage of symplastic trafficking (Sevilem et al., 2013; Kitagawa et al., 2015). The SEL of the PD cytosolic space is decreased through callose deposition in the neck of the PD channel. On the other hand, callose removal from the PD increases PD SEL and hence, allows larger molecules to either passively or actively traffic via PD. It has been suggested that the amount of callose accumulated at the PD is regulated by a balance between the activity of enzymes synthesizing callose (GSLs) and those degrading the β-1,3-glucan polymer (BGs) (Fig. 1.5) (Benitez-Alfonso et al., 2009; Chen and Kim, 2009; Vatén et al., 2011; Zavaliev et al., 2011).

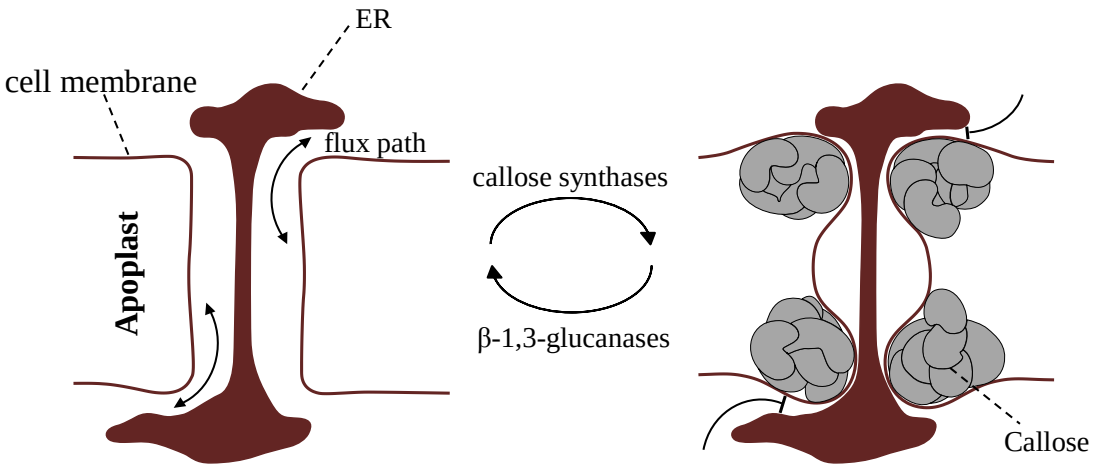

Figure 1.5 Callose deposition at the neck region regulates PD permeability.

Proper regulation of PD is achieved through a balance between the activity of the enzymes synthesizing callose and the ones degrading it, called β-1,3-glucanases. Callose turnover at the PD determines the status of the PD to be open (left) or closed (right), resulting in free or blocked symplastic movement between cells, respectively. Figure modified from Maule et al. (2012).

1.7 Dynamic modulation of plasmodesmata connectivity

Given that PDs are membranous structures facing the cytoplasm, cell wall, and apoplast, their function and development can be modified under the effect of any cytoplasmic and/or apoplastic change (Knox and Benitez-Alfonso, 2014). Studies on protein composition of PD have shown that these membrane-embedded structures are enriched in receptor and receptor-like proteins with roles in signaling pathways that are important for regulation of cell-to-cell communication (Jo et al., 2011; Faulkner, 2013; Faulkner et al., 2013; Stahl et al., 2013). These receptors, such as PDLP5 (see section 1.4.1), receive the signals from environmental changes or cell wall composition at the PD, and will respond to them by adjusting PD SEL.

Recent studies have shown that reactive oxygen species (ROS) can modulate plasmodesmal structure through affecting callose accumulation at PD (Benitez-Alfonso et al., 2009; Zavaliev et al., 2011). An earlier study had also proposed that the apoplastic ROS may act as an agent for loosening cell walls, which can then physically affect PD formation and function (Gapper and Dolan, 2006). The dependence of PD structure on ROS was further confirmed in *gfp arrested trafficking* (*gat*) mutant. The *gat* mutants exhibit reduced transport of GFP from the phloem to surrounding tissues and hyperaccumulation of ROS in their root meristems with approximately doubled level of callose at PD (Benitez-Alfonso et al., 2009). *GAT1* encodes a type *m* thioredoxin (TRX-m3) expressed in plastids of meristems and organ primordia.

Another molecule that has been shown to regulate PD formation and callose biosynthesis through interaction with redox signaling pathway is SA (Wang et al., 2013). Studies indicate that SA regulates PD indirectly via induction of *PDLP5* expression. This induction will positively affect callose metabolic enzyme activity and, therefore, can regulate symplastic movement and response to pathogens (Fitzgibbon et al., 2013; Wang et al., 2013).

Interestingly, several reports in recent years have implicated phytohormones as another factor influencing symplastic communication. For example, auxin has been shown to be related to cell wall and PD changes. During the phototropic response, callose plays a role

in auxin gradient formation. Auxin can positively regulate *GSL8* expression through a pathway in which the auxin response factor 7 (ARF7) is involved (Han et al., 2014b). Symplastic transport can be regulated by auxin through targeting several other callose metabolic genes. The expression of *PLASMODESMATA CALLOSE-BINDING PROTEIN 1* (*PDCB1*) is up-regulated in lateral root after auxin treatment (Maule et al., 2013). PDCB1 is also involved in callose deposition at the PD (Simpson et al., 2009). During later stages of lateral root emergence, PDCB1 function is required for callose deposition around the primordium to isolate it from the overlying tissue (Maule et al., 2013). It has been proposed that auxin-imposed modification of the PD might be through changes in pectin structure or distribution. An early study reported that auxin can induce pectin methylesterase (PME) activity (Bryan and Newcomb, 1954). PME, which was previously identified in the PD proteome (Table 1.1), is known as an enzyme that demethylesterifies homogalacturonan (HG) in the cell wall (Mohnen, 2008). Therefore, it is plausible that auxin affects cell wall-related mechanisms by interfering with pectin esterification, and ultimately causes alterations in PD transport (Knox and Benitez-Alfonso, 2014).

Further evidence supports the potential role of other small molecules, such as the amino acid tryptophan and phytohormone gibberellin in PD regulation (Rinne et al., 2011a; Rutschow et al., 2011). However it is still not clear how these molecules can modify PD, which pathway(s) are involved, and how specific they are compared to the other PD regulators.

1.8 Identification of the *essp8* mutant

The *essp8* mutant was isolated in an unrelated genetic screen developed to identify the gene(s) repressing the expression of seed storage protein (SSP) genes in vegetative tissues (Tang et al., 2008; Lu et al., 2010; Tang et al., 2012a; 2012b; Li et al., 2015). Transgenic Arabidopsis plants, expressing the *β-GLUCURONIDASE* (*GUS*) reporter gene under the control of a seed-specific gene (coding for the β-CONGLYCININ β-subunit) promoter from soybean, were generated (*pβCG:GUS*) (Tang et al., 2008). It was previously reported that the promoter can direct seed-specific gene expression in tobacco (Lessard et al., 1993) and Arabidopsis (Hirai et al., 1994). Analysis of the *pβCG:GUS*

transgenic line confirmed specific expression of the *GUS* reporter gene only in the embryo with no detectable activity in the vegetative tissues (Tang et al., 2008).

Ethyl methanesulfonate (EMS) was used for mutagenizing seeds from the homozygous *pβCG:GUS* plants. These seeds represented the M_1 generation. M_2 plants were screened for mutations causing the ectopic expression of *GUS* in the leaves as an indication of the ectopic expression of the seed storage proteins (*essp*) (Tang et al., 2008). Several mutant lines were isolated in this screen and were characterized (Tang et al., 2008; Lu et al., 2010; Tang et al., 2012a; 2012b). *essp8* is one of the mutants isolated and was used in this study. The major goal of this thesis was the molecular characterization of *essp8* mutant.

1.9 Thesis objectives

Considering the severe developmental defects and cell identity changes observed in the *essp8* mutant seedlings, it was hypothesized that GSL8 plays critical role(s) in cytokinesis and plasmodesmata regulation and is required during early seedling development in Arabidopsis. To test this hypothesis, the following specific objectives were proposed. Please note that some of these goals were developed during the course of this study, as the role of GSL8 became more apparent:

1. To confirm that the *GSL8* mutation is indeed the cause of developmental defects and cell identity changes observed in *essp8* seedlings.
2. To confirm GSL8 involvement and requirement for cytokinesis and plasmodesmata regulation and to demystify how these functions are linked to the *essp8* mutant phenotype.
3. To partially/completely rescue the *essp8* mutant phenotype through restoring the callose balance at plasmodesmata using two candidate genes, *PDLP5* and *AtBG_PPAP*.
4. To generate an interactome network for GSL8 by identifying proteins which physically interact with GSL8 *in vivo*.

CHAPTER 2

2 MATERIAL AND METHODS

2.1 Plant materials and growth conditions

Arabidopsis thaliana lines were either in Columbia (Col-0) or Landsberg *erecta* (L*er*) background. Seeds for wild-type Col-0 and L*er* were originally obtained from Arabidopsis Biological Resource Center (ABRC). Different T-DNA lines used in this study (Appendix I) were ordered either from ABRC or the European Arabidopsis Stock Center (NASC).

Seeds were sterilized in 70% ethanol for 45 sec, followed by 20% bleach with 0.1% sodium dodecyl sulfate (SDS) for 10 min with gentle shaking. Sterilized seeds were then rinsed with sterile distilled water four times and stored at 4°C in the dark for 48 h for stratification before sowing in soil, or after placing on Murashige and Skoog (MS) (Murashige and Skoog, 1962) agar.

For growing plants in soil after stratification, seeds were sowed into pots containing ProMix-BX (Premier Horticulture, Québec) soil. Plants were grown in either the growth room or chamber for 16 h light at 22°C followed by 8 h dark at 18°C.

For growing plants on MS agar, after surface sterilization, seeds were placed on MS agar containing 1X MS salts; 0.05% 2-N-morpholino-ethanesulfonic acid (MES); 3% sucrose; 0.8% agar; pH 5.8. Appropriate antibiotics or chemicals were added for selection or induction where necessary.

Nicotiana benthamiana seeds were obtained from Agriculture and Agri-Food Canada, London, Ontario, and grown in pots containing ProMix-BX under the same growth condition as described for Arabidopsis plants.

2.2 Crossing of Arabidopsis plants

To cross Arabidopsis plants from different genetic backgrounds, flower buds with their petals barely visible were used as pollen recipients. Using fine point tweezers, all the floral organs were carefully removed except for the carpel, which needs to be intact (Altmann et al., 1992). Plants were allowed to recover for 16-24 h. Then the stigma of the

recipient plant was pollinated by placing the pollen from the donor plant on the recipient stigma. The fertilized inflorescence was labeled and seeds from the corresponding silique were collected after being matured. These seeds represent the F_1 generation.

2.3 Histochemical assays

2.3.1 GUS staining

Two-week-old Arabidopsis seedlings were used for detection of ectopic GUS activity. Seedlings were immersed in GUS staining solution (80% distilled water; 20% methanol; 1 mM 5-bromo-4-chloro-3-indolyl glucuronide cyclohexylammonium salt (X-GLUC; Inalco); pH 7-7.5) and vacuumed for 15 min, then incubated at 37°C overnight. Destaining was performed with 75% ethanol followed by incubating at 37°C. Destaining process was repeated, if needed, to achieve a clear background.

2.3.2 Sudan red staining

Sudan red staining for visualizing fatty acid accumulation was performed by incubating three-week-old Arabidopsis seedlings with somatic embryo-like structures in a saturated solution of Sudan red 7B (Sigma) in 70% ethanol at 37°C overnight. Samples were rinsed with 70% ethanol at least three times to obtain a clear background (Bratzel et al., 2010; Tang et al., 2012b).

2.3.3 Aniline blue staining

Aniline blue fluorochrome (Biosupplies Australia PTY Ltd.) is a chemically synthesized fluorochrome which reacts with β-1,3-glucans to give a brilliant fluorescence under UV light. A stock solution of 0.1 mg/ml was prepared in distilled water. Stock solution can be stored at 4°C in the dark for at least one year. Prior to use, the stock solution was diluted 1:3 with 0.1 M K_3PO_4, pH 12.0. Roots of five- or seven-day-old Arabidopsis seedlings were incubated with fluorochrome staining solution (20 µl/root) for 30 min at room temperature then washed with 0.1 M K_3PO_4, pH 12.0 buffer and imaged on a Zeiss Axioscope 2 (Zeiss, Germany) compound fluorescence microscope using a UV laser. The

microscope was integrated with a Nikon DS-Ri2 digital camera using the ACT-1 software (Nikon, Japan).

2.3.4 Propidium iodide staining

Propidium iodide (PI) is a fluorescent intercalating agent with a molecular mass of 668.4 Da that can be used to stain cell walls and nuclei. PI binds to DNA between the bases, with little or no sequence preferences, and with a stoichiometry of one molecule per 4-5 base pairs of DNA. When PI is bound to nucleic acids, the fluorescence excitation and emission maximum are 535 nm and 617 nm, respectively. PI is the most commonly used dye to quantitatively assess DNA content (Suzuki et al., 1997). A typical use of PI in plant biology is to stain the cell wall. Cell membrane is impermeable to PI. Therefore, at low concentration, it is mostly used to identify dead cells. However, by increasing the concentration, it will diffuse into the cell and stains both the cell wall and nuclei.

Depending on the purpose, PI staining can be used for visualizing just cell walls or both cell walls and nuclei. A stock solution of 2 mg/ml of PI (Life Technologies) was prepared in distilled water. The stock solution was stored at 4°C in dark. To stain the cell walls, Arabidopsis roots were dipped in 1 µg/ml PI at room temperature for 3 min and then rinsed with distilled water. To visualize both the cell walls and nuclei, 100 µg/ml PI solution was used. Roots were stained for at least 5 min at room temperature and rinsed twice with distilled water. PI-stained roots were imaged on a Leica TCS SP2 Laser Scanning confocal microscope (Leica, Germany) using 543 nm excitation and 610-630 nm emission.

2.4 Next-generation mapping of *essp8*

For genetic mapping of the *essp8* mutation, M_2 plants from Col-0 background were crossed with wild-type plants of the L*er* accession. A total of 100 two-week-old seedlings with *essp8* dwarf phenotype were selected from the F_2 segregating population and used for bulked-segregant analysis (BSA) and rough-mapping. Genomic DNA (gDNA) extracted from these seedlings were pooled and used for BSA with 22 pairs of simple sequence length polymorphism (SSLP) markers (Lukowitz et al., 2000). After

identification of markers linked to the mutation using BSA, gDNA from individual plants were used for PCR-based rough-mapping to narrow down the genomic interval of *essp8* mutation (Appendix II). Pooled gDNA extracted from 64 seedlings were used as template for next-generation sequencing (NGS). NGS library was generated using NGS library preparation kit (Zymo Research). Sequencing was performed on the Illumina MiSeq (Illumina, USA) using 300 nt paired-end sequencing.

2.5 Plasmodesmata size exclusion limit assay

For PD SEL assay, wild-type (WT) Col-0 and *essp8* seeds were sown on MS agar plates. Seeds were allowed to germinate and grow in the dark for four or seven days. The hypocotyls of four- or seven-day-old seedlings were used for the assay. Dextran, Alexa Fluor® 488; 3,000 MW, Anionic (ThermoFisher Scientific) and Dextran, Fluorescein, 10,000 MW, Anionic (ThermoFisher Scientific) were dissolved in tris-ethylene diamine tetraacetic acid (Tris-EDTA) buffer, pH 8 at concentrations of 100 mg/ml and 50 mg/ml, respectively. Aqueous solution of dextrans were stored at -20°C and protected from light. Prior to use, the stocks were diluted in Tris-EDTA buffer at a ratio of 1:10.

The hypocotyls were obtained by cutting the seedlings at the hook. For each sample, 1 µl of the diluted probe was injected into the hypocotyl at the cut site using a Hamilton Gastight syringe (Hamilton). Movement of the probe was analyzed right after injection by imaging on a Leica TCS SP2 Laser Scanning confocal microscope (Leica) using 488 nm excitation and 515 to 530 nm emissions.

2.6 Generation of stable transgenic plants

Stable transgenic Arabidopsis plants were generated via *Agrobacterium*-mediated transformation using the floral dip method (Zhang et al., 2006). Plants with the genetic background of interest were allowed to bolt. The bolts were then removed to encourage more secondary inflorescences to proliferate from the axillary buds of the rosette. To increase the transformation efficiency, the older siliques were removed right before using the plants for transformation. A single fresh colony of *Agrobacterium tumefaciens* strain GV3101 (Koncz and Schell, 1986), harboring the binary vector, carrying the gene of

interest, was inoculated into 3 ml liquid Luria-Bertani broth (LB) medium (Bertani, 1951) containing the appropriate antibiotics. Cells were grown for 16-24 h at 28°C shaking at 225 rpm. This feeder culture can be stored at 4°C up to one month and was used to inoculate the transformation cultures. After preparation of liquid LB with appropriate antibiotics, 1 ml of feeder culture was used to inoculate 250 ml LB and grown at 28°C for 16-24 h, shaking at 225 rpm until the bacterial culture reached stationery phase (OD_{600}: 1.5-2.0). *Agrobacterium* cells were harvested by centrifugation at 4,000 g for 12 min at room temperature. Next, the cells were resuspended in one volume of freshly prepared 5% (wt/vol) sucrose solution. Just before dipping, Silwet L-77 (Lehle Seeds) was added to the transformation solution at a concentration of 0.02% (vol/vol) and mixed well. The plants were inverted and the aerial parts of the plants were dipped into the *Agrobacterium* cell suspension for 30 sec. The treated plants were gently drained. Dipped plants were wrapped with plastic bags to maintain high humidity. Covered plants were laid down horizontally and kept in the dark for 16-24 h. The cover was removed the next day. The treated plants were transferred back to the growth room. Seeds were collected after 4-5 weeks when the siliques tuned brown. These seeds were called T_1. Primary transformants were screened on selection media containing cefotaxime (100 µg/ml) and the appropriate amount of selection marker. Cefotaxime was used to inhibit *Agrobacterium* growth on the plate since harvested seeds are heavily covered with *Agrobacteria*. For each selective media plate (150 × 150 × 25 mm), around 2500 seeds were spread. After 7-10 days, transformants could be easily distinguished by their developing healthy green cotyledons, true leaves and roots which extended into the selective medium. Potential transformants were transferred to soil, and confirmed by genotyping (see section 2.7) for their corresponding transgene.

2.6.1 Generation of transgenic constructs

All transgenic constructs were generated using the Gateway™ system (Invitrogen) (Hartley et al., 2000). To create the translational construct for *SHR*, a 3 kb fragment upstream of the 5' untranslated region (UTR), the 5'-UTR and the genomic sequence except from the STOP codon was amplified from Arabidopsis gDNA (Appendix III), and cloned into the pMDC107 destination vector which does not have a promoter and carries

GFP reporter for C-terminal fusion (Curtis and Grossniklaus, 2003). *PDLP5* overexpression construct was generated by amplification of its coding sequence (CDS) from Arabidopsis cDNA (Appendix III), and its cloning into the pEarleyGate103 containing *CaMV35S* promoter and C-terminally-fused GFP reporter (Earley et al., 2006).

After confirming the constructs by DNA sequencing, the corresponding vectors were transferred to *Agrobacterium GV3101* using electroporation (Nagel et al., 1990), and later transformed to plants with floral dipping (Zhang et al., 2006). Transgenic *pSHR::SHR:GFP* plants were selected on MS agar media containing 50 µg/ml hygromycin B. *p35S::PDLP5:GFP* overexpression plants were screened on MS agar media containing 12 µg/ml glufosinate. At least ten independent transformants from T_1 generation were propagated to generate T_2 generation. Progeny of individual T_1 plants were screened for the segregation ratio of the transgene. Only T_2 populations which showed a 3:1 segregating ratio, indicating a single insertion of the transgene, were used for further analysis.

2.6.2 Generation of centromere-labeled transgenic plants

Transgenic seeds expressing the centromere labeling construct (*pSDS::CENH3:GFP*) were obtained from Ghent University (De Storme et al., 2013). Centromeric histone H3 (CENH3) replaces histone H3 in the nucleosomes of active centromeres in all eukaryotic cells (Lermontova et al., 2006). *SDS* encodes a mitotic cyclin-like protein and is constitutively expressed throughout the whole plant (De Muyt et al., 2009). Therefore, *pSDS::CENH3:GFP* construct is expressed in all plant cells. The labeling of the centromeres in *gsl8* mutants was carried out by crossing *GSL8/essp8*, *GSL8/gsl8-2* and *GSL8/gsl8-4* genotypes with homozygous plants expressing *pSDS::CENH3:GFP*. The F_2 population was used for imaging and quantifying the number of centromeres in different *gsl8* mutants.

2.6.3 Generation of miRNA165/6-sensor line

Homozygous seeds for miRNA165/6-sensor line were obtained from Seoul National University (Carlsbecker et al., 2010). The construct used to generate the sensor line

harbors miR165/6 target sequence from *PHB* under the control of *U2* promoter, providing ubiquitous expression, and C-terminally fused to GFP. To test the GFP expression in *gsl8* mutants, transgenic plants were crossed with heterozygous *GSL8/essp8* plants and F_2 seedlings were used for analysis and imaging.

2.6.4 Generation of artificial miRNA transgene constructs

The Web Micro Designer (WMD, http://wmd3.weigelworld.org/cgi-bin/webapp.cgi) was used for designing artificial miRNA (amiRNA) against both *GSL8* and *GSL10* genes. To generate the *XVE::aMIRGSL8/GSL10* construct, first the amiRNA sequence was introduced into pRS300 (Schwab et al., 2006) vector, containing the Arabidopsis miR319a precursor, as the backbone to create *aMIRGSL8/GSL10*. Then, *aMIRGSL8/GSL10* was subcloned into the pDONR221 vector (Invitrogen), and then recombined into pMDC7 Gateway-compatible destination vector (Curtis and Grossniklaus, 2003). In pMDC7, the *aMIRGSL8/GSL10* transgene is controlled by an estradiol-inducible promoter. Wild-type Col-0 plants were transformed with the construct using floral dip method (Zhang et al., 2006). Transgenic plants were selected for hygromycin B resistance (see section 2.6.1). T_2 transgenic seeds were sown on MS agar media containing 100 μM β–estradiol or Dimethyl sulfoxide (DMSO) as a mock control.

2.7 Polymerase chain reaction-based genotyping

PCR-based genotyping was used to identify homo and heterozygous plants for all T-DNA insertion lines. gDNA was isolated using a modified plant gDNA extraction protocol with cetyltrimethyl ammonium bromide (CTAB) (Tang et al., 2008). PCR was performed using both allele-specific and T-DNA insertion-specific primers (Appendix I and IV). EMS-based mutants were genotyped by PCR followed by sequencing to detect the single nucleotide polymorphism (SNP) of interest. Heterozygous plants were used for further analysis if homozygous mutations were lethal.

Transgenic plants were confirmed by testing the integration of the transgene by PCR with gene-specific and vector-specific primers.

2.8 Gene expression analysis

For quantitative reverse transcription-PCR (qRT-PCR), total RNA was isolated from ~ 100 mg of plant tissue using the RNeasy Mini Kit (Qiagen). The High Capacity cDNA Reverse Transcription kit (ABI) was used to reverse transcribe the total RNA into cDNA with random primers from the kit. qRT-PCR was performed using the SsoFast EvaGreen Supermix kit (Bio-Rad Laboratories, Inc.) with the Bio-Rad CFX96 real-time PCR detection system (Bio-Rad Laboratories, Inc. USA). The data shown in the figure are the average of three technical and three biological replicates. *GLYCERALDEHYDE-3-PHOSPHATE DEHYDROGENASE* (*GAPDH*) was used as the internal reference (Czechowski et al., 2005). PCR primers used in qRT-PCR are listed in Appendix V.

2.9 Förster resonance energy transfer

Förster resonance energy transfer (FRET) is one of the best methods available to identify and quantify protein-protein interactions. In FRET, the energy from an excited state donor fluorophore is transferred to a nearby acceptor, and it occurs only if the emission band of the donor displays overlapping spectra with the absorption band of the acceptor (Kaminski et al., 2014). FRET level can be quantified from potentially-interacting proteins using different methods including acceptor photobleaching, fluorescence lifetime and polarization resolving imaging (Van Munster and Gadella, 2005; Jares-Erijman and Jovin, 2006; Lakowicz, 2006).

To test the interaction of GSL8 with candidate partners, their CDSs were amplified from Arabidopsis cDNA and cloned into pEarleyGate101 and pEarleyGate102 (Earley et al., 2006) using Gateway system (Invitrogen) to generate YFP- and CFP-fusion proteins, respectively (Appendix III). Four-week-old *N. bentamiana* leaves were co-infiltrated, as described previously (Sparkes et al., 2006), with two constructs expressing GSL8-YFP and the candidate interactor fused to CFP. The reciprocal combinations were also tested. Three days post infiltration (dpi), the FRET between two proteins was quantified using acceptor photobleaching method by imaging on a Leica TCS SP2 Laser Scanning confocal microscope (Leica). Images of the CFP fluorescent, for donor protein, and YFP fluorescent images, for acceptor proteins, were captured using 458 nm excitation and 465

to 505 nm emissions, and 514 nm excitation and 525 to 600 nm emission, respectively. The fluorescence of the CFP and YFP channels were scanned before and after bleaching. Bleaching of the acceptor protein fluorescence was performed using 100% excitation of 514 nm beam for 50 frames. The energy transfer efficiency between the two potentially-interacting proteins was measured based on the fluorescence intensity change in the donor and acceptor, before and after photobleaching using following equation:

$$FRET_{efficiency}\% = (Donor_{postbleaching} - Donor_{prebleaching}) / Donor_{postbleaching}$$

$$0 < FRET_{efficiency} < 100$$

Three independent experiments with at least three biological replicates for each were used to calculate FRET efficiency.

2.10 Microscopy and image analysis

Images were captured by a Nikon SMZ1500 (Nikon) dissecting or Zeiss Axioscope 2 (Zeiss) compound light microscopes which were integrated with a Nikon DS-Ri2 digital camera using the ACT-1 software (Nikon). Nikon dissecting scope optical ranges varied between 0.75 and 11.5X, and the compound Zeiss microscope was used with 20 and 40X objectives. TIFF format at a resolution of 3840 x 3072 pixels was used for capturing all images.

2.11 Statistical analysis

In all cases, no less than three plants of each genotype per treatment were used to calculate the means. Pair-wise comparison of the means was done using a Student's t-Test assuming unequal variance. Unless otherwise stated, in all cases "*" and "**" symbols represent the 95% and 99% confidence interval of the means, respectively.

CHAPTER 3

3 RESULTS

3.1 Map-based cloning of the *essp8* mutation

As mentioned in section 1.8, the *essp8* mutant was identified in an unrelated genetic screen of an EMS mutant population that was intended to identify repressors of SSPs in Arabidopsis seedlings. The M_2 segregating population was screened to isolate mutant lines showing distinct ectopic *GUS* expression pattern in their vegetative tissues (Tang et al., 2008; Lu et al., 2010; Tang et al., 2012a; 2012b; Li et al., 2015).

3.1.1 Morphological phenotype of *essp8* seedlings

The *essp8* mutant was accidently identified in a screen for mutations affecting repression of seed storage protein genes. *essp8* seedlings exhibit an interesting phenotype with several developmental defects including dwarfism, formation of abnormally-developed cotyledons and true leaves, reduced growth of the root and hypocotyl, and generally delayed development compared to wild-type Col-0 (Fig. 3.1A-D). Segregation analysis showed reduced transmission of the mutant allele in *essp8* resulted in deviation from the expected 25% homozygous mutant seedlings for a normal recessive single locus Mendelian segregation (Table 3.1). Reduced transmission of the mutant allele can be due to embryo lethality as ~5% of the homozygous seeds were aborted and failed to germinate (Table 3.1). The abortion of *essp8* embryos was further confirmed by phenotypic analysis of the siliques from a heterozygous parent where ~25% of the seeds displayed defective phenotype as being smaller, darker and shrunk compared to wild-type seeds (Table 3.2) (Fig. 3.1E-F).

The *essp8* mutation is lethal in most of the mutant seedlings (~90%), leading to complete death of the seedlings after three weeks (Fig. 3.2A-C). However, it can induce formation of somatic embryo-like structures in the seedlings which survive longer at a low penetrance (~10%) (Fig. 3.2D-F). The somatic embryo-like structures were confirmed to be true embryos using GUS staining for ectopic *GUS* expression (Fig. 3.3A-B), and Sudan red staining for accumulation of seed storage-specific triacylglycerols (Fig. 3.3C-D). Screening different segregating population for *essp8* mutation, including F_2 and back cross 2 (BC_2),

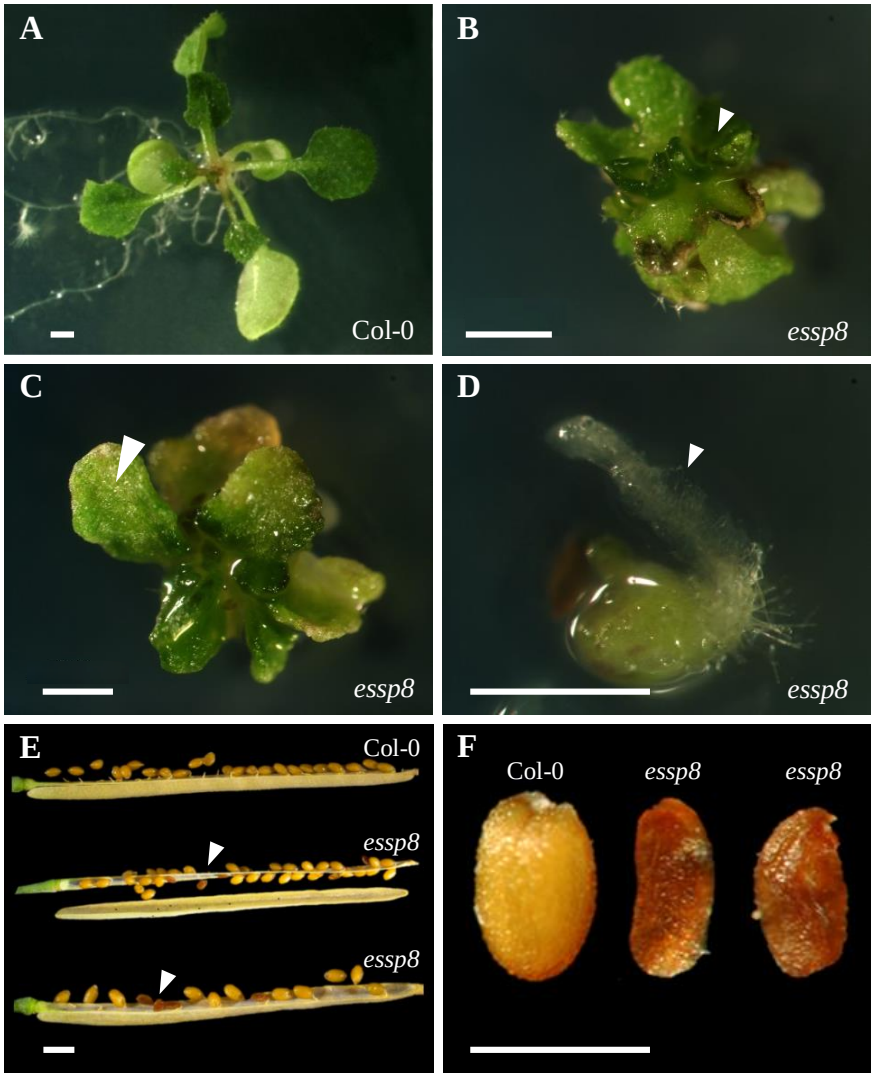

Figure 3.1 Morphological phenotype of the *essp8* mutant.

(A-D) Comparison of seedling phenotypes of wild-type Col-0 (A) and *essp8* mutants (B-D). (B-C) Fifteen-day-old *essp8* seedlings are very small and exhibit abnormally shaped true leaves (B) (white arrowheads). The surface of the *essp8* cotyledon epidermis is undulated (C) (white arrowheads). (D) The *essp8* roots and hypocotyls are shorter and thicker compared to the WT Col-0 (white arrowheads). (E-F) Morphological analysis of siliques from a heterozygous parent showed that the *essp8* mutation can cause formation of defective seeds (white arrowheads) (E) and seed lethality (F). Scale bars: A-E = 1 mm, F = 500 µm

Table 3.1 Segregation of homozygous *essp8* seedlings in the progeny of selfed *ESSP8/essp8* heterozygous plants

	Number of plants tested	**Percentage of homozygous seedlings**	**Percentage of non-germinating seeds**
essp8-1	132	15.9	9.1
essp8-2	112	21.4	8
essp8-3	142	16.2	4.9
essp8-4	132	19.7	5.3
essp8-5	125	20	4.8
essp8-6	123	22.8	4.1

Table 3.2 The percentage of defective seeds in one silique from selfed *ESSP8/essp8* heterozygous plants

	Number of seeds in one silique	**Percentage of defective seeds**
essp8-1	34	23.5
essp8-2	34	26.4
essp8-3	18	22.2
essp8-4	28	21.4
essp8-5	23	21.7
essp8-6	27	25.9

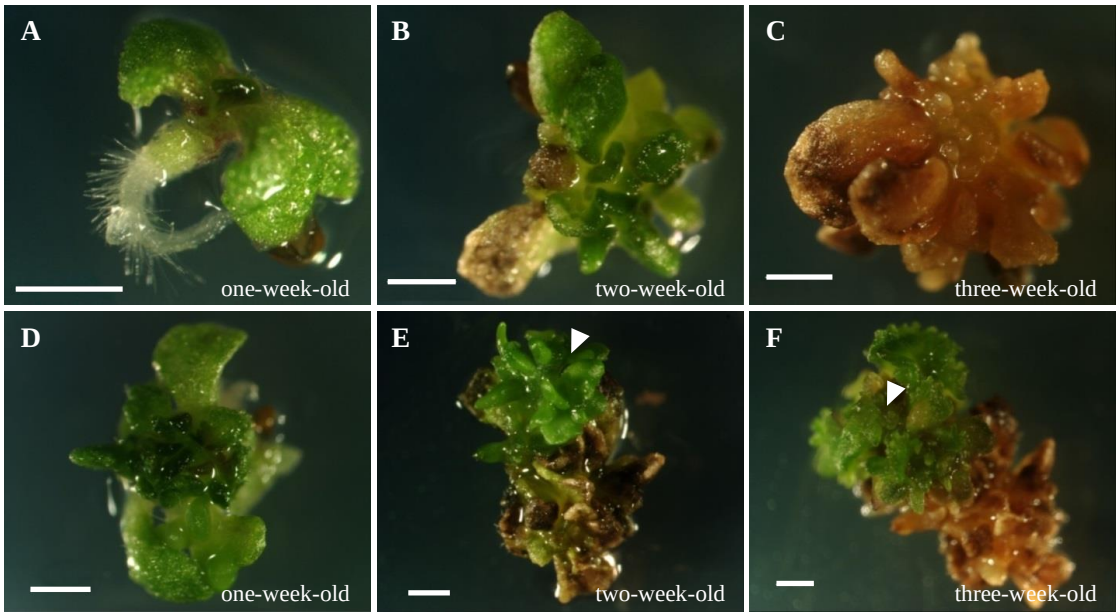

Figure 3.2 The *essp8* mutation causes somatic embryo formation with an incomplete penetrance.

(A-C) Developmental defects are observed in *essp8* mutant seedlings during the first three weeks after germination. It was also revealed that the *essp8* mutation is lethal in ~90% of the seedlings and leads to seedlings' death. (D-F) Around 10% of *essp8* seedlings show ectopic cell proliferation and formation of somatic embryo-like structures (red arrowheads) after two (E) and three weeks (F). Scale bars = 1 mm

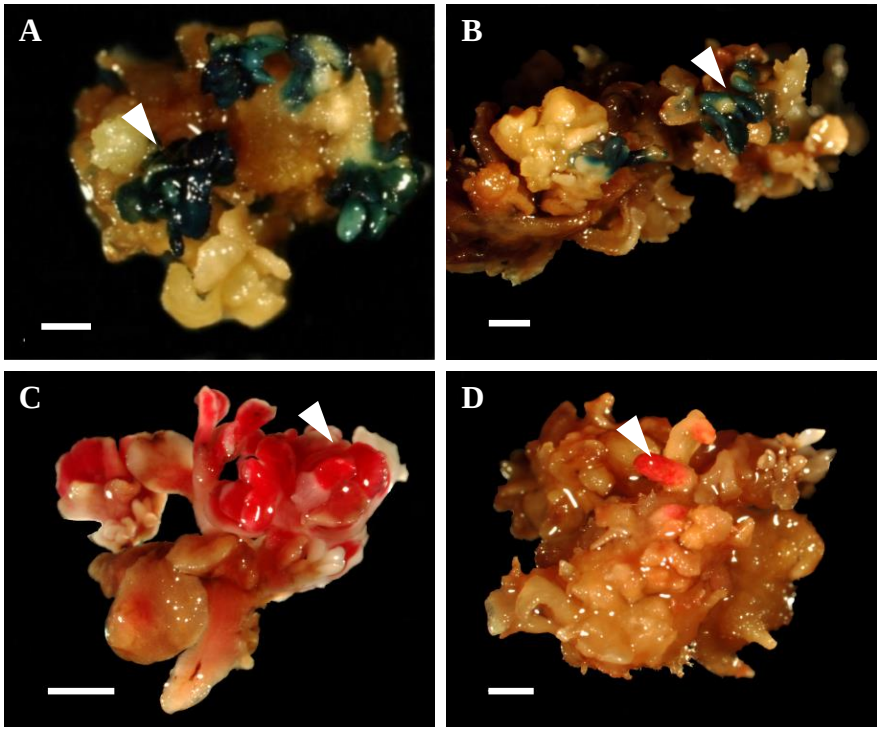

Figure 3.3 *essp8* mutant seedlings form somatic embryos.

(A-B) Histochemical GUS assay and (C-D) Sudan red staining confirmed ectopic *GUS* expression (red arrowheads) and accumulation of seed storage-specific triacylglycerols (white arrowheads), respectively, in four-week-old *essp8* seedlings showing somatic embryo-like structures. Scale bars = 1 mm

showed the same results (data not shown), confirming that *essp8* is a single recessive mutation inducing dwarfism, somatic embryo formation and seed abortion.

3.1.2 Next-generation mapping of *essp8* locus

In order to map the *essp8* mutation, M_2 *essp8* heterozygous plants were crossed with WT plants of the L*er* accession to generate a segregating F_2 mapping population. Using a small mapping population of 100 F_2 plants, BSA was performed with 22 pairs of SSLP markers (Lukowitz et al., 2000). BSA successfully located the *essp8* mutation on the bottom arm of chromosome II between the nga1126 and nga168 markers (Fig. 3.4A). Further mapping using more SSLP markers (Appendix II) roughly narrowed down the *essp8* mutation to a genomic interval of about 729 kb, covered by the F11F19 and F13M22 BAC clones (Fig. 3.4B).

To identify the SNP, caused by EMS in *essp8*, an NGM approach was used (Austin et al., 2011). After sequencing the pooled genomic DNA isolated from 64 two-week-old *essp8* F_2 seedlings, a SNP desert region, a non-recombinant block caused by linkage to the recessive mutation of interest, was detected on the bottom arm of chromosome II (Fig. 3.5). This result was consistent with both the BSA and rough mapping data. By combining the results from rough-mapping and NGS, all non-synonymous SNPs, caused by EMS, were identified within the candidate region on chromosome II using a web-based tool (http://bar.utoronto.ca/NGM/). Only one EMS-induced point mutation (GC to AT) (Kim et al., 2006) in the AT2G36850 (*GSL8*) was detected. The mutation disrupts a splice site of *GSL8* (Fig. 3.6).

According to gene structure modeling, *GSL8* is a large gene spanning a genomic region of 14,433 bp, consisting of 50 exons, and a coding sequence of 5712 bp (Fig. 3.7A). In *essp8*, the GC to AT substitution disrupts the splice site at intron 22. The retention of intron 22 alters the *GSL8* cDNA and results in introduction of a premature STOP-codon (Fig. 3.7B).

GSL8 encodes a large integral membrane protein with 1904 amino acids and is predicted to form sixteen transmembrane helices (Tsirigos et al., 2015). The transmembrane domains

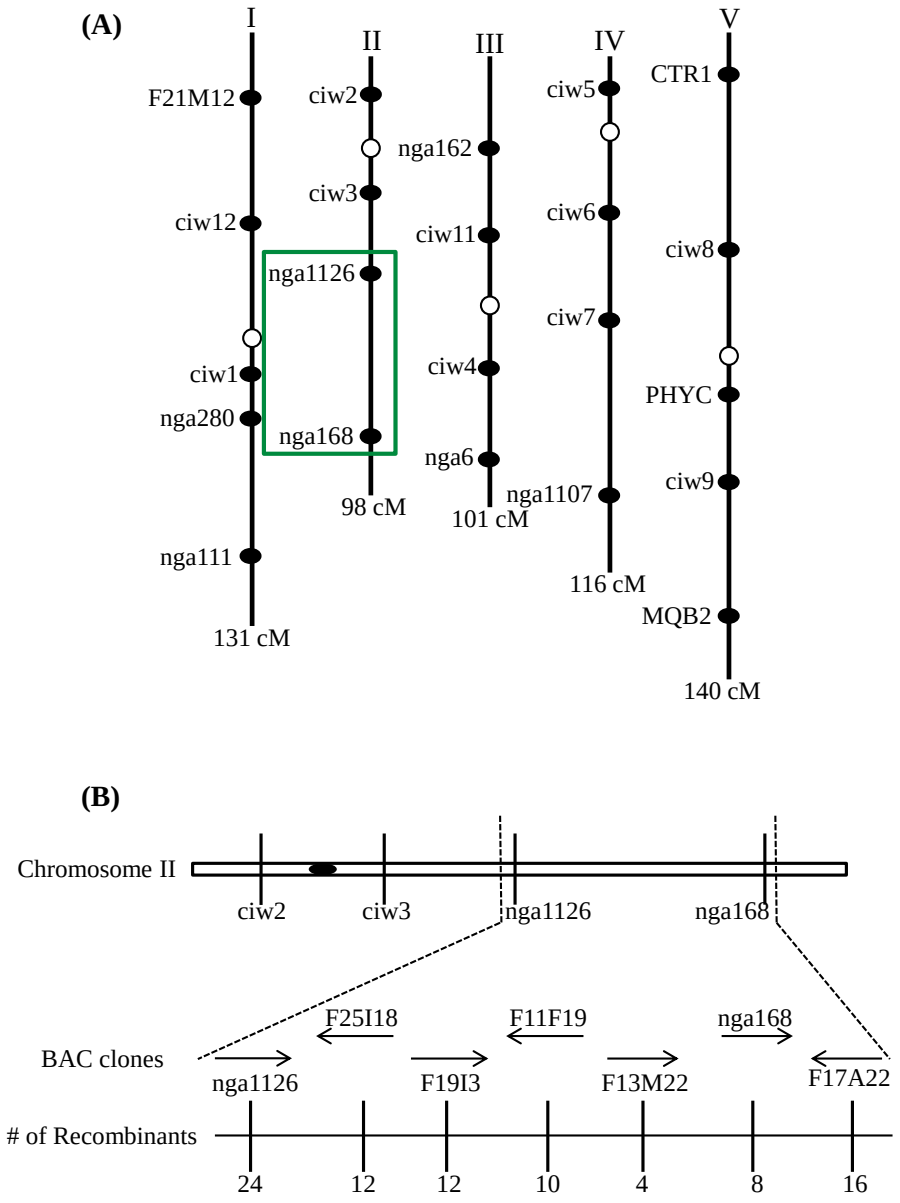

Figure 3.4 Rough mapping of the *essp8* mutation.

(A) Using BSA, the *essp8* mutation was located on the bottom arm of chromosome II between the nga1126 and nga168 markers (green square). (B) The position of the *essp8* mutation was narrowed down to a genomic interval of 729 kb, covered by the BAC clones F11F19 and F13M22, on chromosome II. The numbers of recombination events out of the total number of chromosomes examined (200) are indicated.

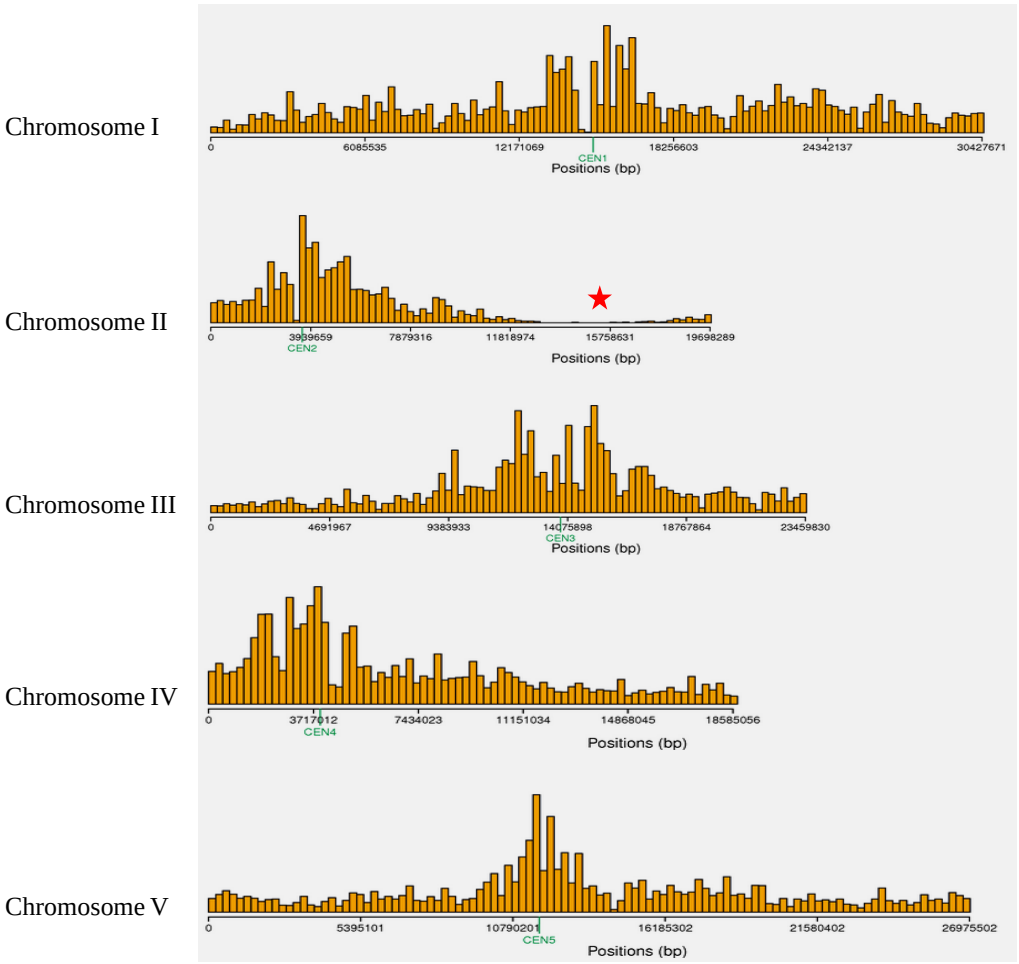

Figure 3.5 Identification of the *essp8* mutation using NGM.

NGM revealed one SNP desert region on the bottom arm of chromosome II (red star). The bars represent the natural polymorphism between wild-type Col-0 and L*er* accessions, used to generate the F_2 mapping population.

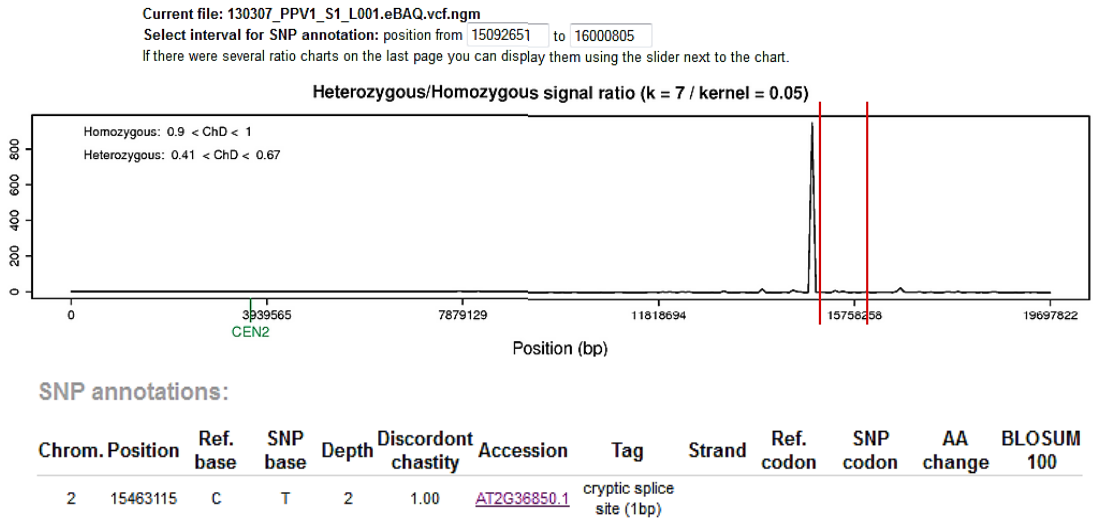

SNP annotations:

Chrom.	Position	Ref. base	SNP base	Depth	Discordont chastity	Accession	Tag	Strand	Ref. codon	SNP codon	AA change	BLOSUM 100
2	15463115	C	T	2	1.00	AT2G36850.1	cryptic splice site (1bp)					

Figure 3.6 Detection of SNPs within the candidate region for the *essp8* mutation.

The combination of rough mapping and NGM results identified one SNP caused by EMS within the candidate region (between the red lines) on chromosome II. The GC to AT mutation is located at an intron splice site of AT2G36850 (*GSL8*).

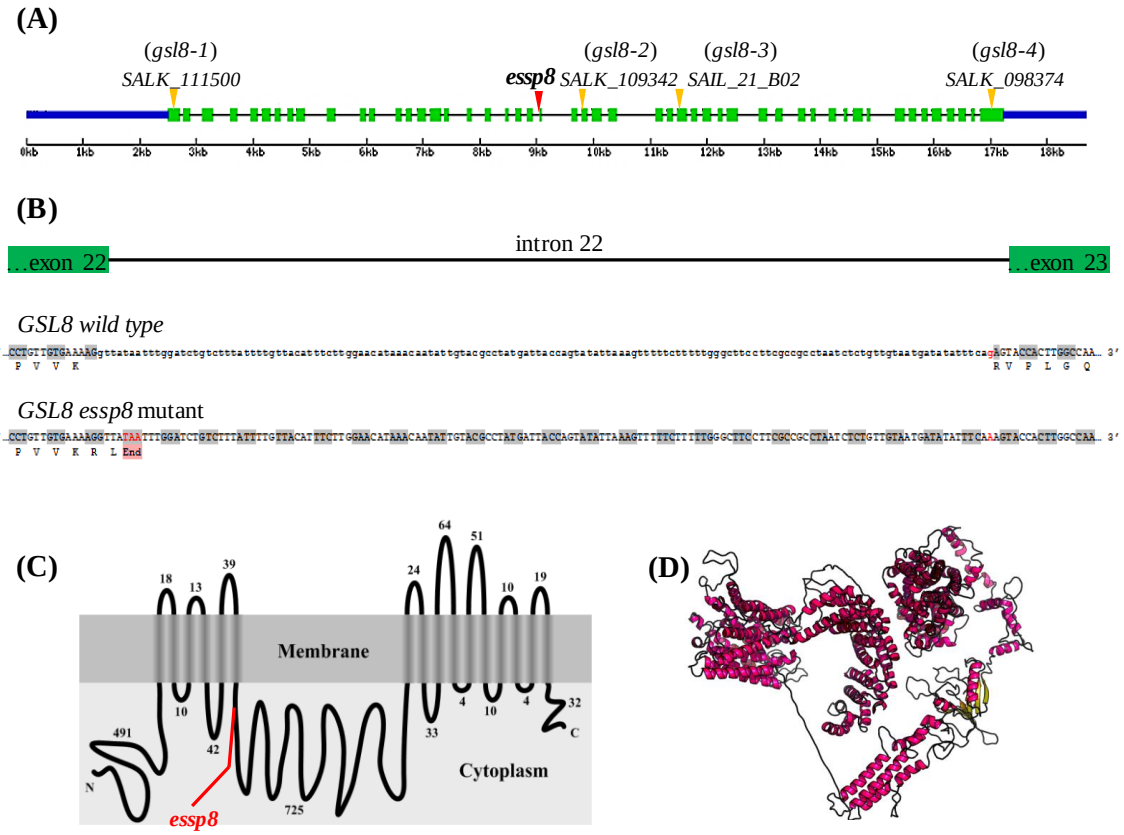

Figure 3.7 *GLUCAN SYNTHASE-LIKE 8* (*GSL8*) genomic and protein structure.

(A) *GSL8* consists of 50 exons and has a coding region of 5712 bp (GenBank Accession number GQ373182). The position of T-DNA insertions (yellow triangles) and EMS-induced mutation (red triangle) are indicated. (B) The splice site at intron 22 is disrupted in *essp8*. The retention of intron 22 in *essp8* establishes a premature STOP-codon downstream of exon 22. (C) *GSL8* encodes a large transmembrane protein. GSL8 has a large cytoplasmic central loop between the transmembrane domains. The *essp8* mutation results in the truncation of the GSL8 protein at the fifth cytoplasmic helix, indicated by the red line. (D) GSL8 secondary structure is predicted to mostly consist of helices and loops (Källberg et al., 2012).

are clustered into two N-terminal and C-terminal regions leaving a large hydrophilic central loop within cytoplasm (Fig. 3.7C). In *essp8*, introduction of the premature STOP-codon results in the truncation of the GSL8 protein at the fifth cytoplasmic helix (Fig. 3.7C). Based on RaptorX protein modeling (Källberg et al., 2012), GSL8 protein secondary structure is predicted to consist of 62% helices, 8% beta sheets and 29% loops (Fig. 3.7D).

3.1.3 *essp8* is allelic to *GSL8*

To confirm that *ESSP8* is indeed allelic to *GSL8*, four different T-DNA insertion lines, SALK_11500 (*gsl8-1*), SALK_109342 (*gsl8-2*), SAIL_21_B02 (*gsl8-3*) and SALK_098374 (*gsl8-4*), where the T-DNA is located either upstream or downstream of the *essp8* EMS mutation, were obtained from ABRC (Fig. 3.7A) (Appendix I).

Heterozygous plants were identified by PCR-based genotyping, and the segregation ratio of the homozygous plants with *essp8*-like phenotype was determined. Homozygous T-DNA mutant seedlings for all four insertion lines exhibited dwarfism as that of *essp8*. Similarly, the cotyledon and true leaves were thick and abnormally-developed (Fig. 3.8). Analysis of the root morphological phenotype in *gsl8* mutants revealed severe defects in their root tissue patterning as they have stunted roots with bloated cells, as well as short, swollen and often branched root hairs (Fig. 3.9). Similar to *essp8*, the segregation ratio of homozygous T-DNA mutants showed deviation from the expected 25% (data not shown), providing initial evidence that *gsl8* mutation can cause embryo lethality.

To further confirm that *ESSP8* is an allele of *GSL8*, an allelism test was performed. Heterozygous plants for three different T-DNA insertion lines (*GSL8/gsl8-1*, *GSL8/gsl8-3* and *GSL8/gsl8-4*) were crossed with *essp8* heterozygous plants (*GSL8/essp8*). F_1 seedlings that were heterozygous for two different mutant alleles of *GSL8*, i.e., one of the T-DNA insertions and the EMS mutation (*gsl8-1/essp8*, *gsl8-3/essp8* and *gsl8-4/essp8*), recapitulated the morphological phenotype of homozygous *gsl8* and *essp8* mutants (Fig. 3.10). The genotype of the seedlings was confirmed using PCR-based genotyping for T-DNA insertion and sequencing for EMS mutation (data not shown). The genotyping results proved that the seedlings with *essp8*-like phenotype were

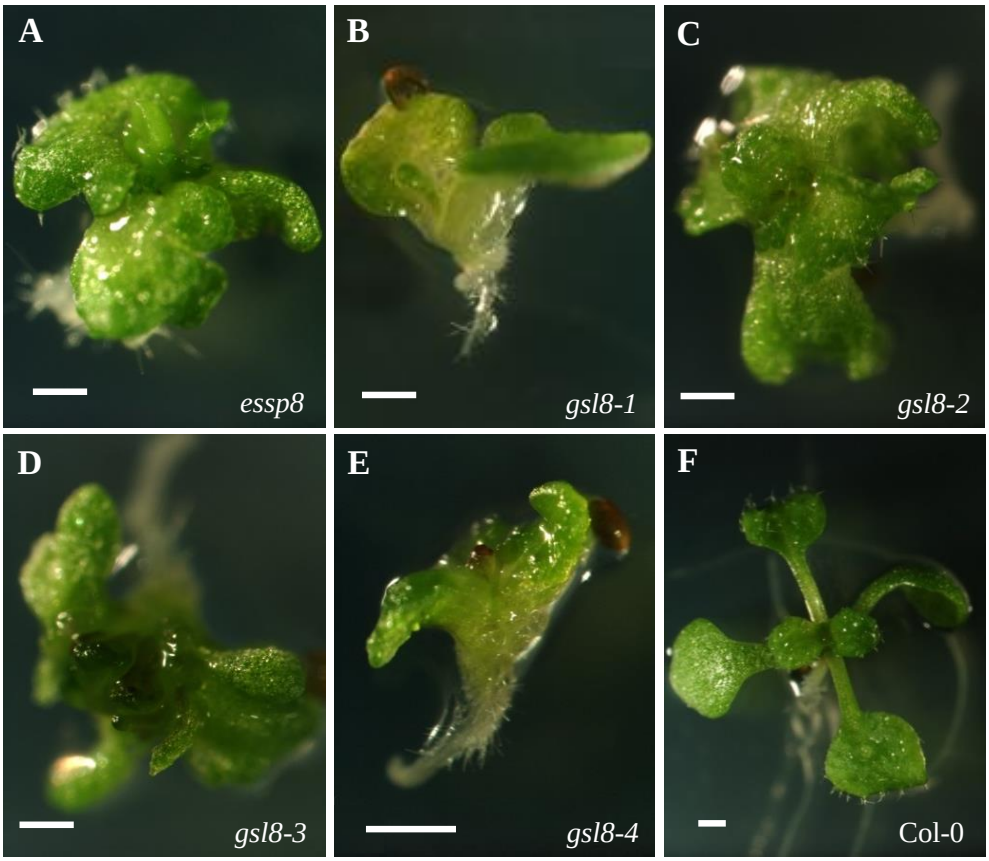

Figure 3.8 Morphological phenotypes of *gsl8* T-DNA mutant seedlings compared to *essp8*. (A) Ten-day-old *essp8* seedling phenotype, (B-E) phenotypes for *gsl8* T-DNA mutants of the same age: SALK_11500 (*gsl8-1*) (B), SALK_109342 (*gsl8-2*) (C), SAIL_21_B02 (*gsl8-3*) (D) and SALK_098374 (*gsl8-4*) (E).Each of the mutant lines contains a T-DNA insert upstream or downstream of the *essp8* mutation. *gsl8* T-DNA insertion mutants exhibited similar phenotypes by forming dwarf seedlings, developing thick cotyledon and true leaves as well as short and thick hypocotyl and roots. (F) Ten-day-old wild-type Col-0 seedling is shown as control. Scale bars = 500 µm

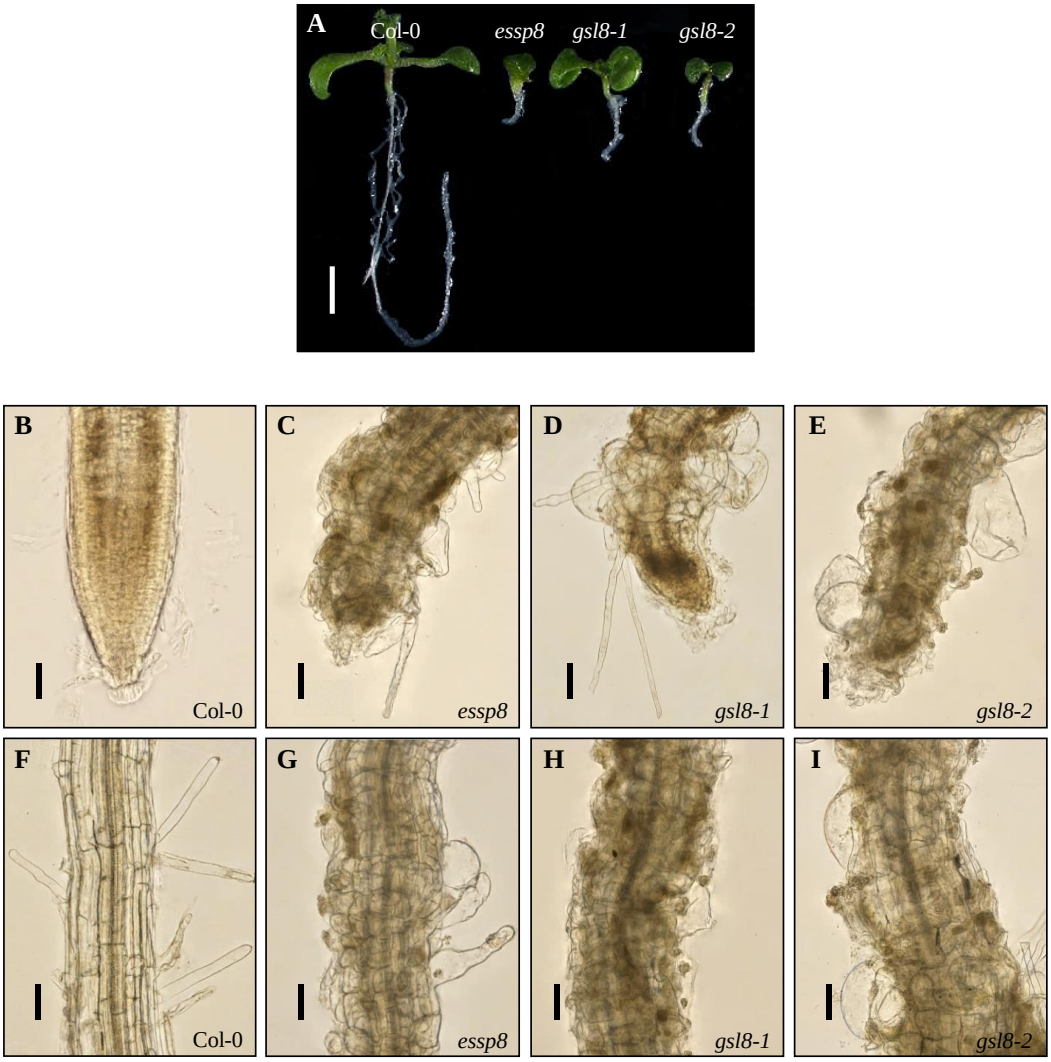

Figure 3.9 Analysis of the root morphological phenotype of *gsl8* mutants showing severe defects in root tissue patterning.

(A) Ten-day-old *gls8* mutant seedlings (*essp8*, *gsl8-1* and *gsl8-2*) develop stunted roots compared to the wild type. (B-I) Comparison of the root phenotype between five-day-old wild-type and *gsl8* mutant seedlings at the root tip and elongation zone of the root. (C-E) *gsl8* mutants showed abnormally-developed root tips with having bloated cells. (G-I) Morphological phenotype of the elongation zone of the primary roots in *gsl8* mutants revealed formation of short, swollen, and often branched root hairs. Scale bars: A = 200 µm, B-I = 50 µm

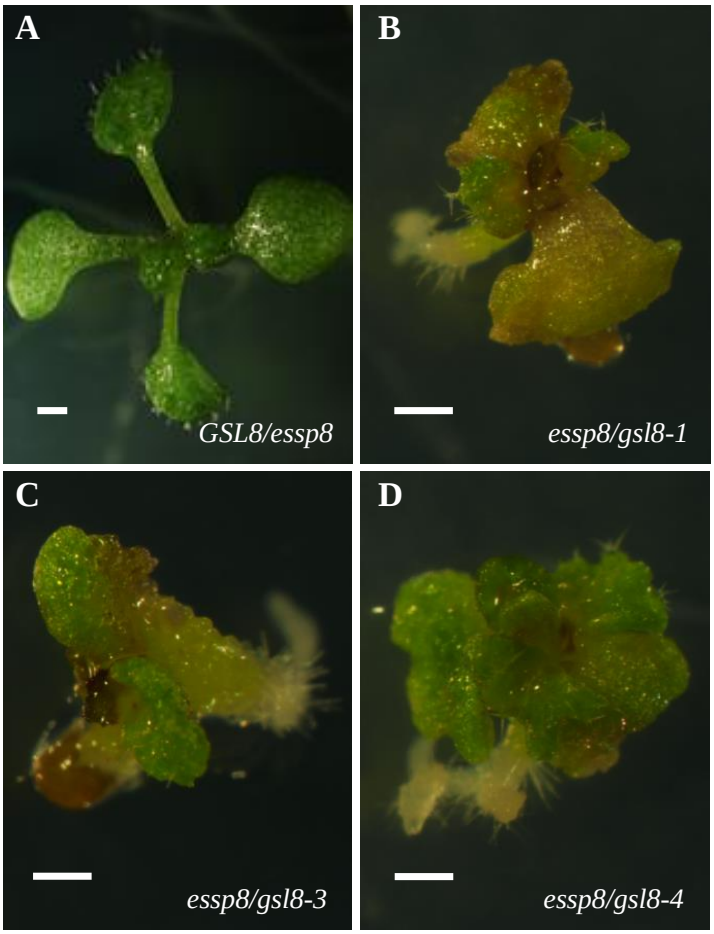

Figure 3.10 Allelism test confirms that *ESSP8* is an allele of *GSL8.*

(A) *GSL8/essp8* seedlings show no recognizable phenotypic defects. (B-D) Ten-day-old seedlings that were heterozygous for two different mutant alleles of *GSL8*, *essp8* mutation and *gsl8-1* (B), *gsl8-3* (C) and *gsl8-4* (D) T-DNA insertions, respectively, exhibited a phenotype similar to that of homozygous *gsl8* mutants. Scale bars = 500 µm

heterozygous for both mutant alleles. Taken together, the morphological phenotype of four different T-DNA insertion lines for *GSL8* and the allelism test demonstrated that *ESSP8* is indeed a new allele of *GSL8* (AT2G35850) and, therefore, the cause of the developmental defects in Arabidopsis seedlings.

3.2 Phylogenetic analysis of Arabidopsis GSLs

To comprehend the relationship among the twelve members of the GSL family in Arabidopsis, a phylogenetic tree of the family was generated. Putative protein sequences of Arabidopsis GSL1-12 and callose synthase from *Phytophthora infestans*, as outgroup, were obtained from the national center for biotechnology information (NCBI) at the time (Appendix VI). A phylogenetic tree was generated with MEGA6 (Tamura et al., 2013) program, using the maximum likelihood method. Alignment of all twelve Arabidopsis GSLs positioned these proteins into three distinct groups (Fig. 3.11). According to the phylogenetic analysis, GSL8 is more closely related to GSL10 as they are clustered into the same subfamily and share 63.7% and 63.4% identities at the DNA and protein sequences levels, respectively. Although there are several lines of evidence suggesting a partial redundancy between the members which belong to the same subfamily (Jacobs et al., 2003; Nishimura et al., 2003; Enns et al., 2005), GSL8 and GSL10 have not yet been shown to be functionally redundant. As was previously predicted (see section 1.2.2), GSL1 and GSL5 were positioned into a different group, reconfirming that GSL1 and GSL5 are different from the other member of the Arabidopsis GSL family.

3.2.1 The cytoplasmic domains of Arabidopsis GSLs are highly conserved

To predict which domain(s) in the GSL proteins are responsible for their enzymatic activity, the amino acid sequences from all twelve members in Arabidopsis were further analyzed by performing an alignment using PRALINE, a web-based tool for multiple sequence alignment (Simossis and Heringa, 2005). It has been classically assumed that the cytoplasmic domain of GSLs contains the catalytic site (Cui et al., 2001; Doblin et al., 2001; Hong et al., 2001a; Østergaard et al., 2002). Multiple sequence alignment of GSLs shows that GSLs' amino acid sequences are mostly semi- to fully-conserved among all

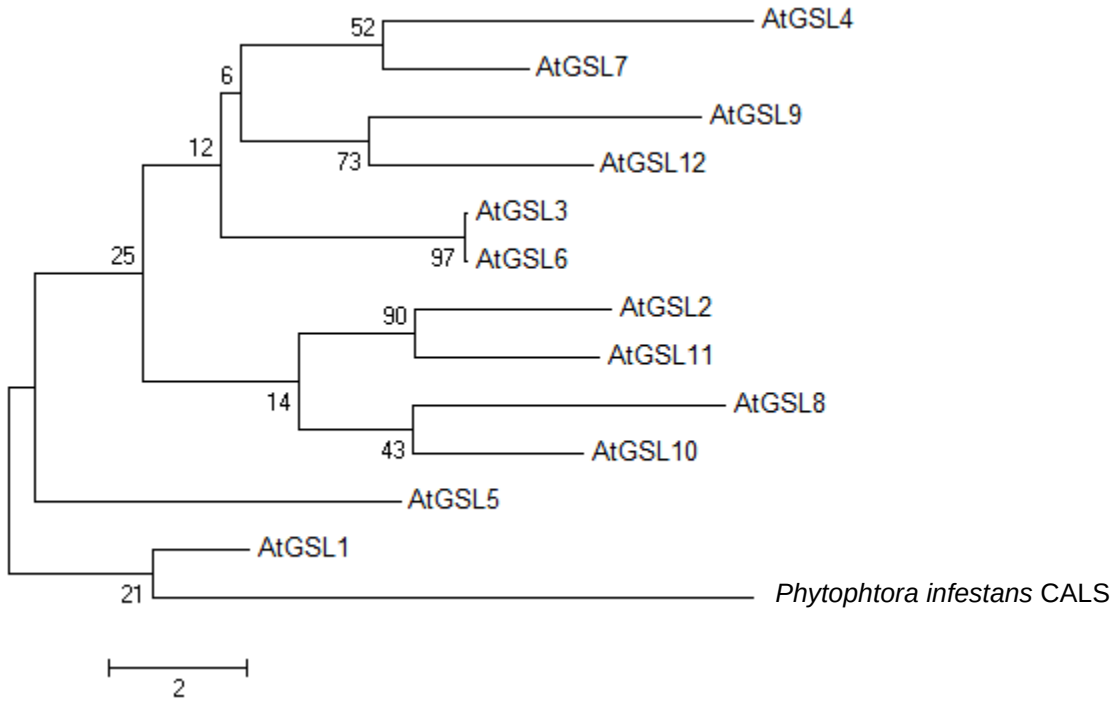

Figure 3.11 Phylogenetic tree of Arabidopsis GSLs.

The unrooted tree is based on an amino acid alignment of full-length sequences from Arabidopsis (Appendix VII).The evolutionary history was inferred by using the maximum likelihood method. The tree with the highest log likelihood (-62692.0592) is shown. The percentage of trees in which the associated taxa clustered together is shown next to the branch points. The tree is drawn to scale, with branch lengths reflecting the number of substitutions per site. There were a total of 1768 positions in the final dataset. The phylogenetic tree was generated with MEGA6 using a bootstrap value of 500.

twelve members of the family with very short non-conserved regions (Appendix VII). As has been predicted, the conserved residues are mainly found in the cytoplasmic domains. The largest number of conserved residues was found in the ninth cytoplasmic loop of GSL8, suggesting that this domain can potentially act as a catalytic and/ or interacting site of these enzymes with other proteins or co-factors (Fig. 3.12).

3.3 Callose deposition at both cell plate and PD is decreased in *essp8* root

As GSL8 has been suggested to be involved in callose biosynthesis, the effect of the *gsl8* mutation on callose deposition at the cell plate and PD was further investigated. Callose accumulation was visualized using a callose-specific dye, aniline blue fluorochrome, in WT Col-0 and *essp8* roots. Two T-DNA insertion lines (*gsl8-1* and *gsl8-2*), which contain insertion sites upstream and downstream of the EMS mutation, respectively (Fig. 3.7A), were also analyzed (Fig. 3.13). In the WT Col-0 root tip, bright, linear signals represent the callose deposited at the cell plate in dividing cells (Fig. 3.13A). Furthermore, punctate fluorescent signals were detected on the cell walls in the elongation zone of the roots, root hairs and vascular tissues, which indicate characteristic callose deposition at the PD (Fig. 3.13E). In contrast to the WT Col-0, *essp8*, as well as *gsl8-1* and *gsl8-2* roots showed almost no signal from callose either at the cell plate in the root tip (Fig. 3.13B-D) or PD in the elongation zone of the root (Fig. 3.13F-H). Absence of callose deposition was also noticed in the root hairs and vasculature tissues in *gsl8* mutants. Based on these findings, it can be concluded that GSL8 is required for proper deposition and accumulation of callose at the cell walls, cell plates and plasmodesmata.

3.4 *essp8* is a cytokinesis-defective mutant

Formation of defective cell plate during cytokinesis can cause abortion of cell division. Depending on the stage that mitosis is aborted, separation of the newly-formed nuclei or duplicated chromosomes is disrupted, resulting in generation of multi-nucleated cells or cells with doubled number of chromosomes (Joubès and Chevalier, 2000) (Fig. 1.2).

3.4.1 *GSL8* is required for the completion of plant cytokinesis

Callose has already been characterized as an essential component of the cell plate (see

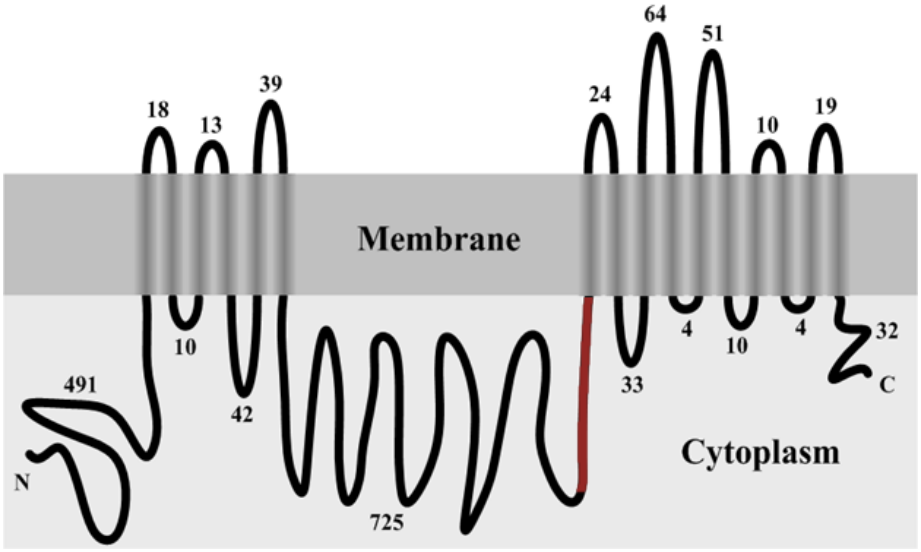

Figure 3.12 The predicted conserved domains of the GSL8 protein.

According to the alignment result (Appendix VII), the conserved residues are mainly located in the cytoplasmic domains. The longest conserved stretch of residues corresponds to the ninth cytoplasmic loop in GSL8, shown in red. The numbers indicate the predicted number of amino acids forming different domains.

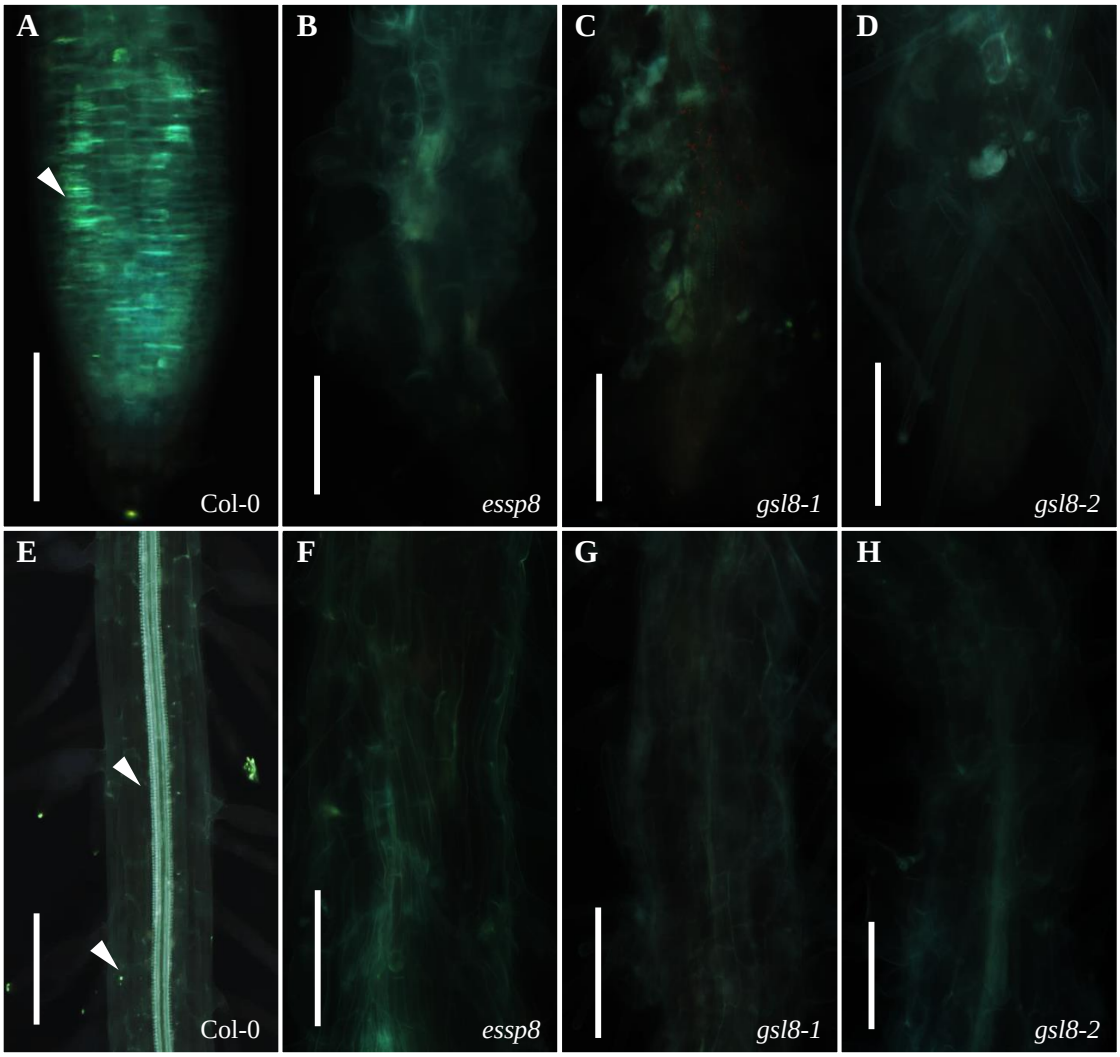

Figure 3.13 Callose deposition in the primary roots of *gsl8* mutants.

Callose accumulation was visualized using aniline blue staining in five-day-old seedlings of WT Col-0, *essp8*, and two T-DNA insertion lines, *gsl8-1* and *gsl8-2*. (A-D) Bright lines (white arrowhead) at the root tip represent callose deposition at the cell plate in WT Col-0 (A) and *gsl8* mutants. (E-H) In the elongation zone of the primary root, callose deposition at plasmodesmata is detected as dots (white arrowheads) in the root hairs, cell wall and vascular tissue in the WT Col-0 (E) and *gsl8* mutants. Scale bars = 100 µm.

section 1.1.5). To investigate if severe phenotypic defects in *essp8* seedlings are caused by incomplete cytokinesis, different known cytokinesis-defective mutants including *hinkel* (Strompen et al., 2002), *knolle* (Touihri et al., 2011), *keule* (Waizenegger et al., 2000), *korrigan* (Sato et al., 2001) and *stomatal cytokinesis-defective 1* (*scd1*) (Falbel et al., 2003) were screened for their morphological phenotypes.

Previous studies have shown that mutations in genes that are required for cytokinesis execution, such as *HINKEL*, *KNOLLE* and *KEULE*, induce formation of multi-nucleated cells which are characterized by having gapped or incomplete cell walls (Assaad, 2001). *HINKEL* encodes a kinesin-like protein which is required for cytoskeletal formation (Strompen et al., 2002). *KNOLLE* and *KEULE* encode a syntaxin and a Sec1/Munc18 proteins, respectively, and are required when vesicles are fusing to form the cell plate (Lukowitz et al., 1996; Waizenegger et al., 2000). *KORRIGAN* belongs to a different class of genes required for cytokinesis. It encodes a membrane-bound endo-1,4-β-glucanase (Sato et al., 2001). Cell wall formation is disrupted in *korrigan* mutants whose mutant seedlings are identified as having cell-wall stubs and swollen cells (Söllner et al., 2002). *SCD1* is involved in vesicle trafficking during cytokinesis (Falbel et al., 2003). Epidermal and guard cells in *scd1* mutants are binucleated and have cell wall stubs, indicating that *scd1* plants are cytokinetically defective (Falbel et al., 2003).

T-DNA insertion lines for all five selected cytokinesis genes were obtained from ABRC (Appendix I). After germinating seeds on MS agar media, the phenotypes of the homozygous seedlings were compared to that of *essp8*. Two of the mutants, *hinkel* and *scd1*, showed more similar phenotype to *essp8* by having small seedlings, fairly short roots and thicker leaves (Fig. 3.14A-C). However, even though *knolle*, *keule* and *korrigan* also form tiny seedlings, they develop fused cotyledons and fail to form true leaves, which are different characteristics compared to *essp8* seedlings (Fig. 3.14D-F). The possibility of somatic embryo formation by cytokinesis-defective mutants was also investigated. Despite the fact that *hinkel* and *scd1* show elevated cell proliferation, and form somatic embryo-like structures, none of them were confirmed to be true somatic embryos by Sudan red staining (data not shown).

To explore if *essp8* mutant seedlings show any secondary effects of cytokinesis defects such as formation of binucleated cells, PI staining was used to visualize the cell wall and nuclei of cells in the elongation zone of roots. Analysis of these cells was performed by confocal microscopy to detect bi- or multi-nucleated cells in which two daughter nuclei do not seem to be separated by a cross-wall. As expected, confocal imaging confirmed the presence of binucleated cells in cytokinesis-defective mutants including *scd1*, *keule*, *korrigan* and *knolle* (Fig. 3.15E-H). Similar to cytokinesis-defective mutants, *gsl8* mutant seedlings including *essp8*, *gsl8-1* and *gsl8-2* have cells with more than one nucleus, suggesting that *gsl8* can also be defined as a cytokinesis-defective mutant (Fig. 3.15B-D). A very frequent defect observed in *essp8* roots was enlarged disorganized cells with abnormal shapes, compared to the WT Col-0, which could not be detected in the cytokinesis mutants, indicating that *essp8* morphological and developmental defects are only partially caused by cytokinesis impairments.

3.4.2 Cytokinesis impairment in *essp8* induces ectopic endomitosis

Identification of binucleated cells in somatic tissue of *essp8* root organs prompted me to assess the possibility of another cytokinesis-related defect. To investigate whether *essp8* mutation also induces ectopic endomitosis in the root, the expression of a centromere-labeling construct, *pSDS::CENH3:GFP* (De Storme et al., 2013), in the *gsl8* background was analyzed. Since this construct is expressed in all plant tissues and organs, the absolute number of chromosomes can be quantified *in vivo* by detection of fluorescent GFP in the tissue of interest.

The primary roots of homozygous *essp8*, *gsl8-2* and *gsl8-4* mutant seedlings expressing *pSDS::CENH3:GFP* were used for analysis. The diploid status of the root cells in WT Col-0 was confirmed by detection of 5 to 10 centromeric dots (Fig. 3.16A). Interestingly, the *espp8*, *gsl8-2* and *gsl8-4* root cells have nuclei carrying higher number of chromosomes (ranging from 11 to 15), indicating the presence of triploid, and potentially polyploid cells in these mutants (Fig. 3.16B-D). A comparison of the distribution pattern as well as number of centromeres between WT Col-0 and *gsl8* mutants revealed a significant difference for all three *gsl8* mutants (*essp8*, *gsl8-2* and *gsl8-4*) compared to WT, whereas the difference among the *gsl8* mutants was found not to be significant (Fig. 3.16E).

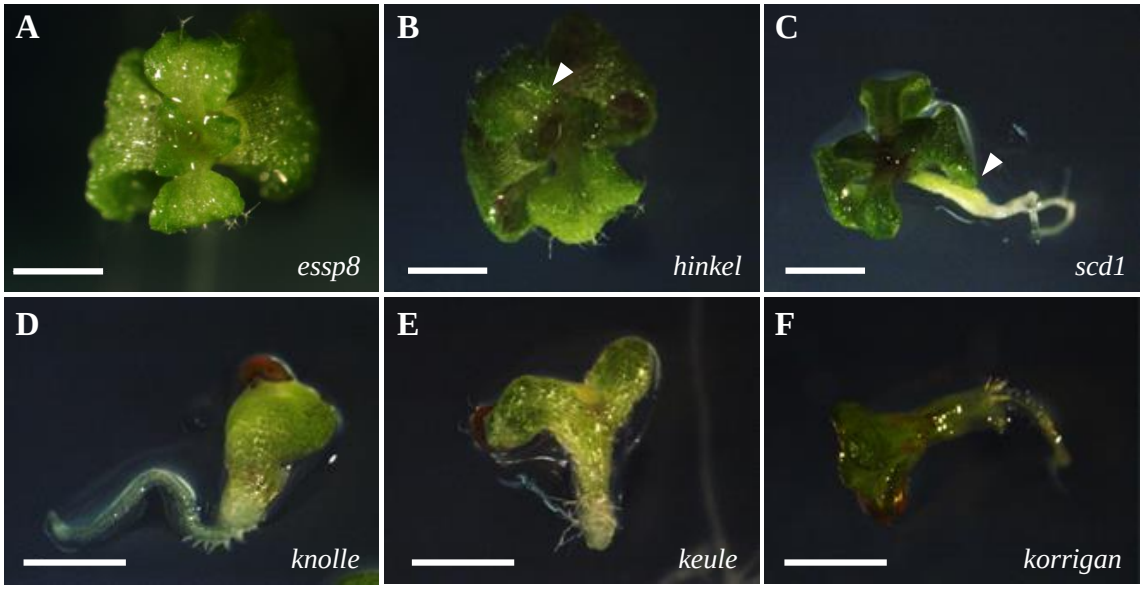

Figure 3.14 Morphological phenotypes of cytokinesis-defective mutants.
(A-F) Comparison between *essp8* (A) and cytokinesis-defective mutant seedlings: *hinkel* (B), *scd1* (C), *knolle* (D), *keule* (E) and *korrigan* (F). All cytokinesis-defective mutants develop dwarf seedlings, but *hinkel* and *scd1* are morphologically more similar to *essp8* with having abnormally-developed cotyledons and true leaves (B), and thicker roots and hypocotyls (C) (red arrowheads). Scale bars = 1 mm

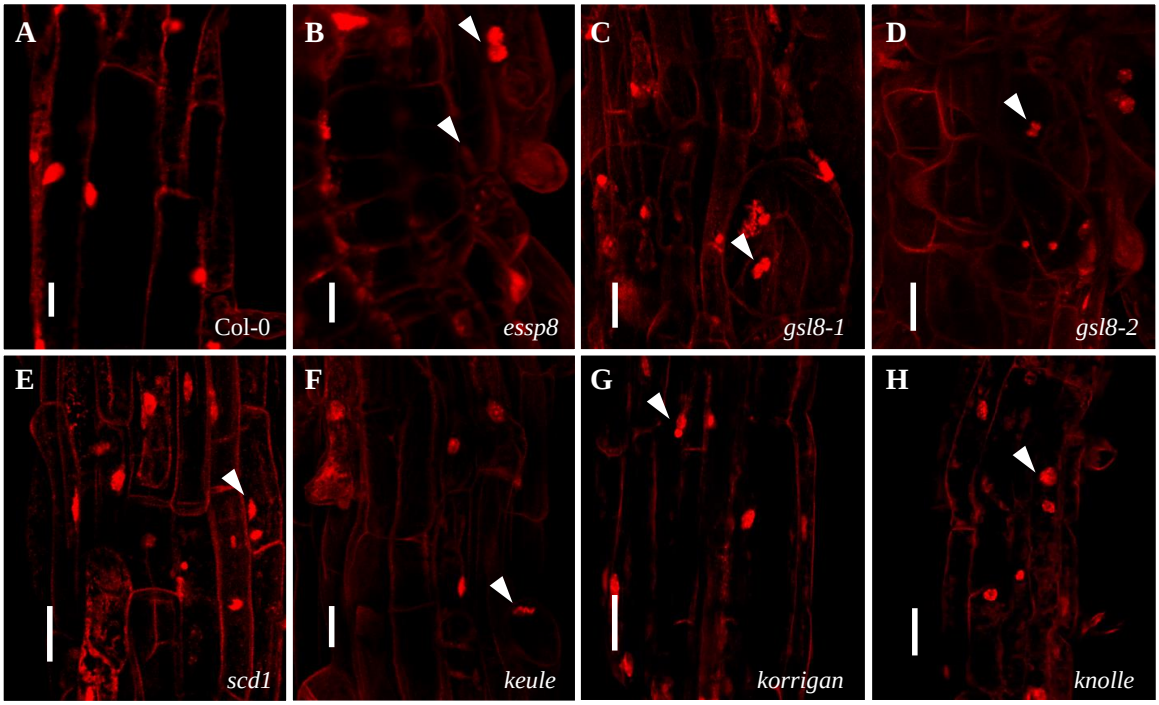

Figure 3.15 Formation of binucleated cells in the primary roots of *gsl8* and cytokinesis-defective mutants.

(A-D) Comparison of the number of nuclei per cell in the elongation zone of the root between wild-type Col-0 (A) and *gsl8* mutants: *essp8* (B), *gsl8-1* (C), *gsl8-2* (D). (E-H) The primary roots of cytokinesis-defective mutants harbor binucleated cells: *scd1* (E), *keule* (F), *korrigan* (G) and *knolle* (H). Examples of binucleated cells are indicated by white arrowheads in *gsl8* and cytokinesis-defective mutants. Propidium iodide was used to stain both nuclei and cell walls. Scale bars = 20 µm

Therefore, it was concluded that the *essp8* mutation can induce not only ectopic endomitosis in reproductive cells (previously shown by De Storme et al., 2013), but also in the somatic cells in the root at early stages of development.

Ectopic polyploidization and endomitosis in *essp8* seedlings were further confirmed by detection of enlarged cells. In contrast to wild-type roots which always show homogeneously sized cells containing equally sized single diploid nuclei (Fig. 3.15A), *gsl8* roots have enlarged abnormally-shaped cells with polyploid nuclei (Fig. 3.15B-D). Interestingly, the frequency of these enlarged polyploid cells increases with age. Analyzing the root cells and nuclei at five and ten days using the centromere labeling construct revealed that, at five days, *essp8* root tissues often contained scattered single enlarged endomitotic and/or polyploid cells, as only five days later, clusters of enlarged polyploid cells could be found (Fig. 3.17A-D). This result indicates that with age, as the seedlings start deteriorating, the polyploidization defects significantly increase (Fig. 3.17E).

3.5 GSL8 regulates symplastic connectivity through plasmodesmata

Plant cells are interconnected with each other via narrow channels of PD, facilitating cell-to-cell communication (Rinne and van der Schoot, 1998). Callose deposition at the PD plays an important role in symplastic movement of various substances (see section 1.1.6) (Levy et al., 2006; Lucas et al., 2009; Xu and Jackson, 2010; Maule et al., 2011; Zavaliev et al., 2011; Xie et al., 2012). Callose deposition is a highly-regulated dynamic process, which is required for adjustment of PD SEL in response to endogenous and exogenous signals (De Storme and Geelen, 2014).

3.5.1 Loss of GSL8 induces an increase in plasmodesmata size exclusion limit

Since aniline blue staining results have already indicated the requirement of GSL8 for callose deposition at both cell-plate and PD (Fig. 3.13), it was postulated that lack of callose deposition at the PD in *essp8* causes an increase in SEL of the PD. To test this hypothesis, alteration of cell-to-cell symplastic movement was investigated in the *essp8* hypocotyls. Two different fluorescent probes, Alexa Flour and fluorescein (see section 2.5), with different sizes (3 kDa and 10 kDa, respectively) were used as markers

Figure 3.16 Comparison of centromere numbers in the primary roots of wild-type Col-0 and *gsl8* mutants shows an increase in *gsl8* mutants.

(A-D) The number of centromeres per nucleus in the primary roots in the WT Col-0 (A) and *gsl8* mutants: *essp8* (B), *gsl8-2* (C) and *gsl8-4* (D). Quantification revealed up to ten centromeres per nucleus in the WT Col-0, reflecting a basic diploid status, whereas all three *gsl8* mutants have more centromeric dots indicating the occurrence of endomitotic polyploidization. Sample nuclei are marked by circles. (E) Quantification of centromere numbers in the WT Col-0 and *gsl8* mutants shows a significant difference. The boxes signify the upper (purple) and lower (green) quartiles, and the median is represented by a short black line within the box for each plant line. The upper and lower "whiskers" represent the entire spread of the data. Data were acquired from at least ten cells in an individual seedling and three seedlings per genetic background were examines. Dotted lines show which samples were compared pairwise and significant differences at $P < 0.01$ using Student's t-Test are indicated by **. Scale bars = 10 μm

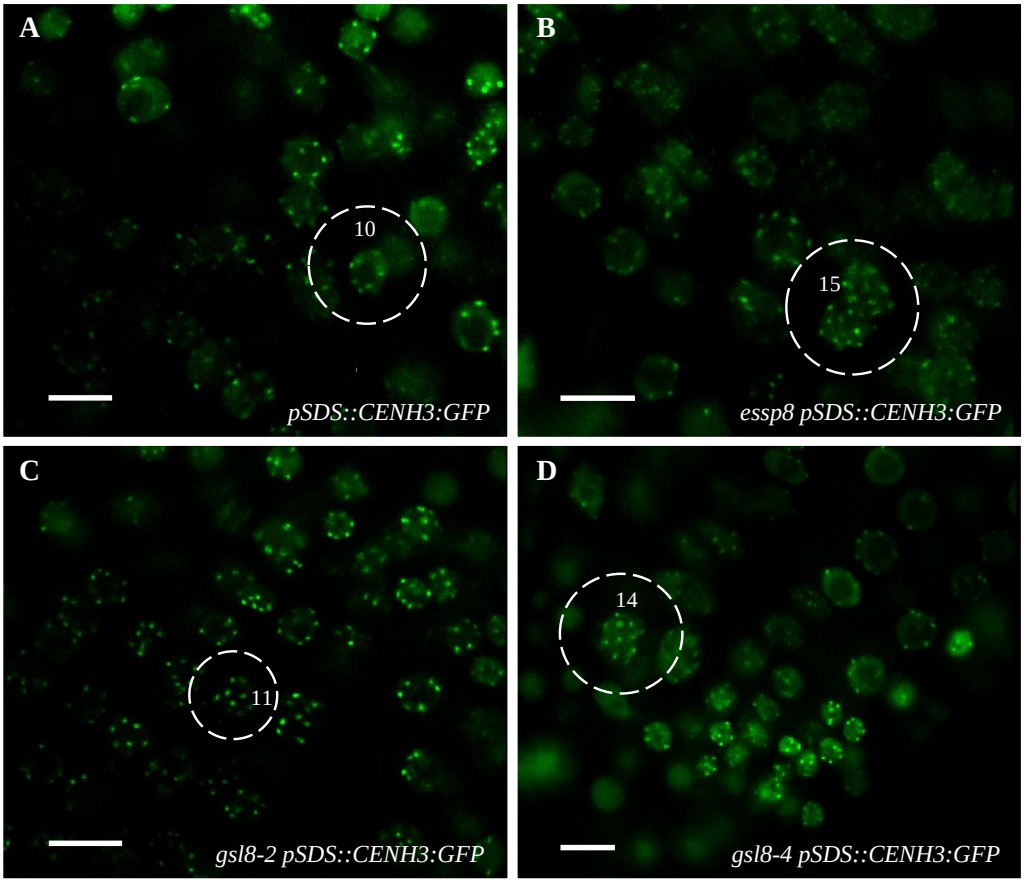
A
10
pSDS::CENH3:GFP
B
15
essp8 pSDS::CENH3:GFP
C
11
gsl8-2 pSDS::CENH3:GFP
D
14
gsl8-4 pSDS::CENH3:GFP

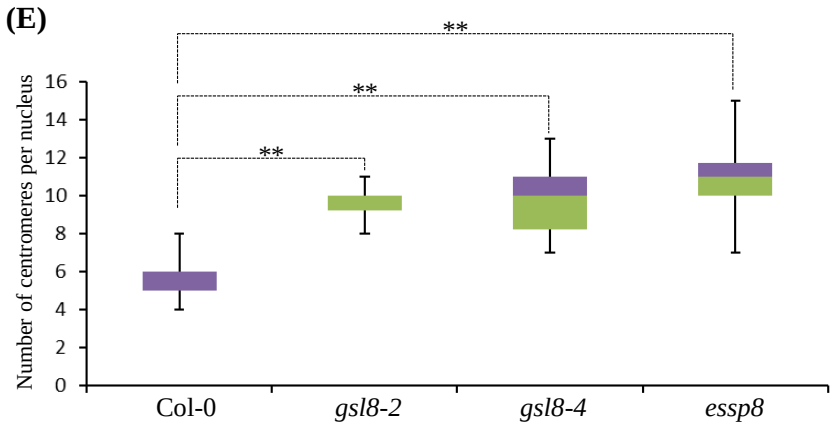
(E)
Number of centromeres per nucleus
0
2
4
6
8
10
12
14
16
**
**
**
Col-0
gsl8-2
gsl8-4
essp8

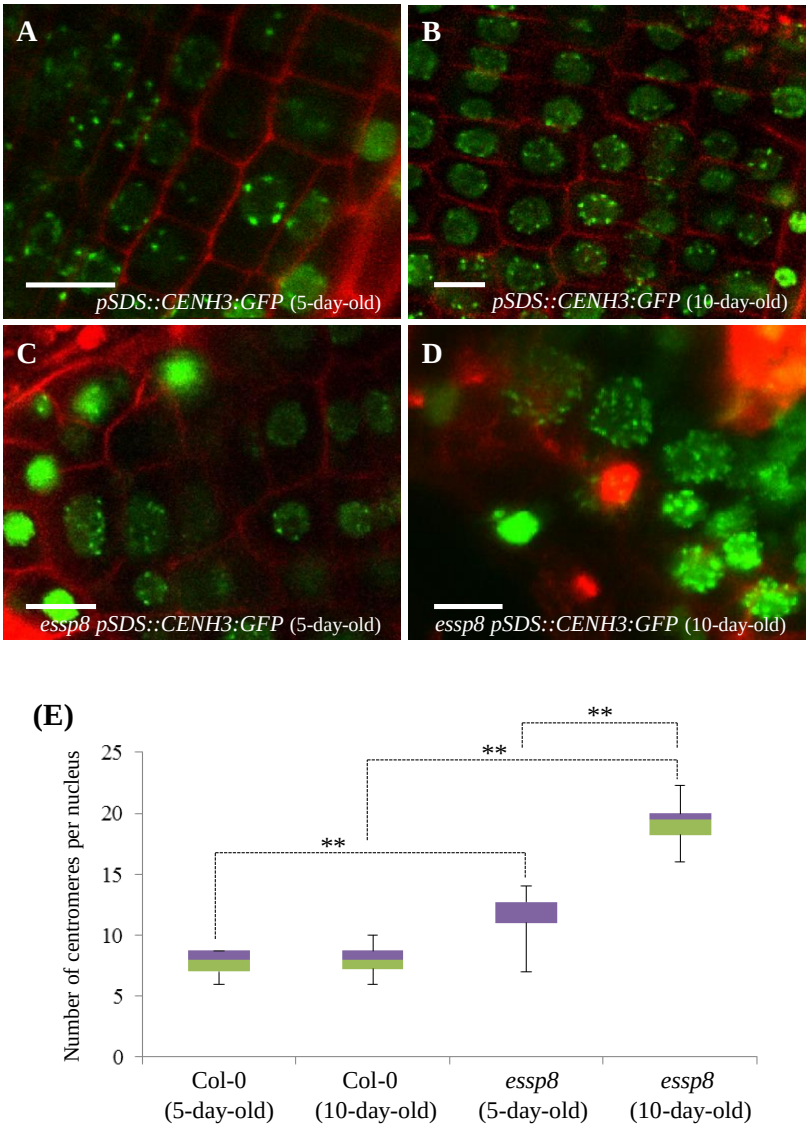

Figure 3.17 Comparison of polyploid cells in *essp8* mutant at different ages shows an increase in ploidy level with age .

(A-B) The number of centromeres in the primary root cells of five- and ten-day-old wild-type Col-0, and (C-D) *essp8*, respectively. (E) In *essp8*, the number of endomitotic cells significantly increases with age and clusters of polyploid cells with higher number of chromosomes are formed in ten-day old (D) compared to five-day-old primary roots (C). (E) Quantification of centromere numbers shows no significant difference in WT Col-0 seedlings. The data obtained from at least ten cells in each individual seedling with three biological replicates. Dotted lines show pairwise significant differences at **P < 0.01 using Student's t-Test. Scale bars = 10 µm

to monitor passive cell-to-cell diffusion.

Fluorescent probes were separately injected to the hypocotyls after the seeds have been germinated for four days in the dark (Fig. 3.18A-B). Diffusion of fluorescent signal, from the point of initial injection, was assayed by measuring their distance between the injection site and the furthest detected signal. For the smaller probe, in both WT and *essp8*, the fluorescent signal was detected at the site of injection and surrounding cells (Fig. 3.18C-D); however, the distance of its movement was significantly longer in *essp8* (Fig. 3.18G). In contrast, the larger probe (fluorescein) was only detected at the site of injection in nearly all cases in WT. Only a few surrounding cells showed a dim fluorescent signal, indicating its minor diffusion in the WT hypocotyls (Fig. 3.18E). Contrary to the WT, *essp8* hypocotyl cells showed strong fluorescent signal in many more surrounding cells (Fig. 3.18F) as well as significantly longer distance of movement (Fig. 3.18G).

Diffusion patterns of Alexa Fluor in both WT and *essp8* hypocotyls indicate that its size (3 kDa) is below the SEL. Lack of fluorescein diffusion in the WT suggests that 10 kDa is possibly beyond the SEL of hypocotyl. On the contrary, the fluorescent signal in surrounding cells in *essp8* was detected significantly further away from the injection sites compared to the WT, which indicates that larger molecules were able to spread into neighboring cells in the *essp8* hypocotyl. These results suggest that in the *essp8* mutants, reduction of callose deposition at the PD is likely to be associated with an increase in SEL and, therefore, alteration of symplastic connectivity between hypocotyl cells.

3.5.2 Dysregulation of SHORT ROOT movement through PD in the *essp8* roots

Arabidopsis root is composed of concentric cell layers including epidermis, cortex and endodermis, which surround the stele that comprises the vascular tissues and pericycle (Dolan et al., 1993). To gain a better understanding of the downstream effects of PD defects in the *essp8* mutants on PD-mediated intercellular signaling during root development, SHR, an important developmental regulators in roots, was used as a molecular marker (see section 1.5.2). During root development in Arabidopsis, the endodermis, middle cortex (MC), and cortex are formed by timely and spatially regulated

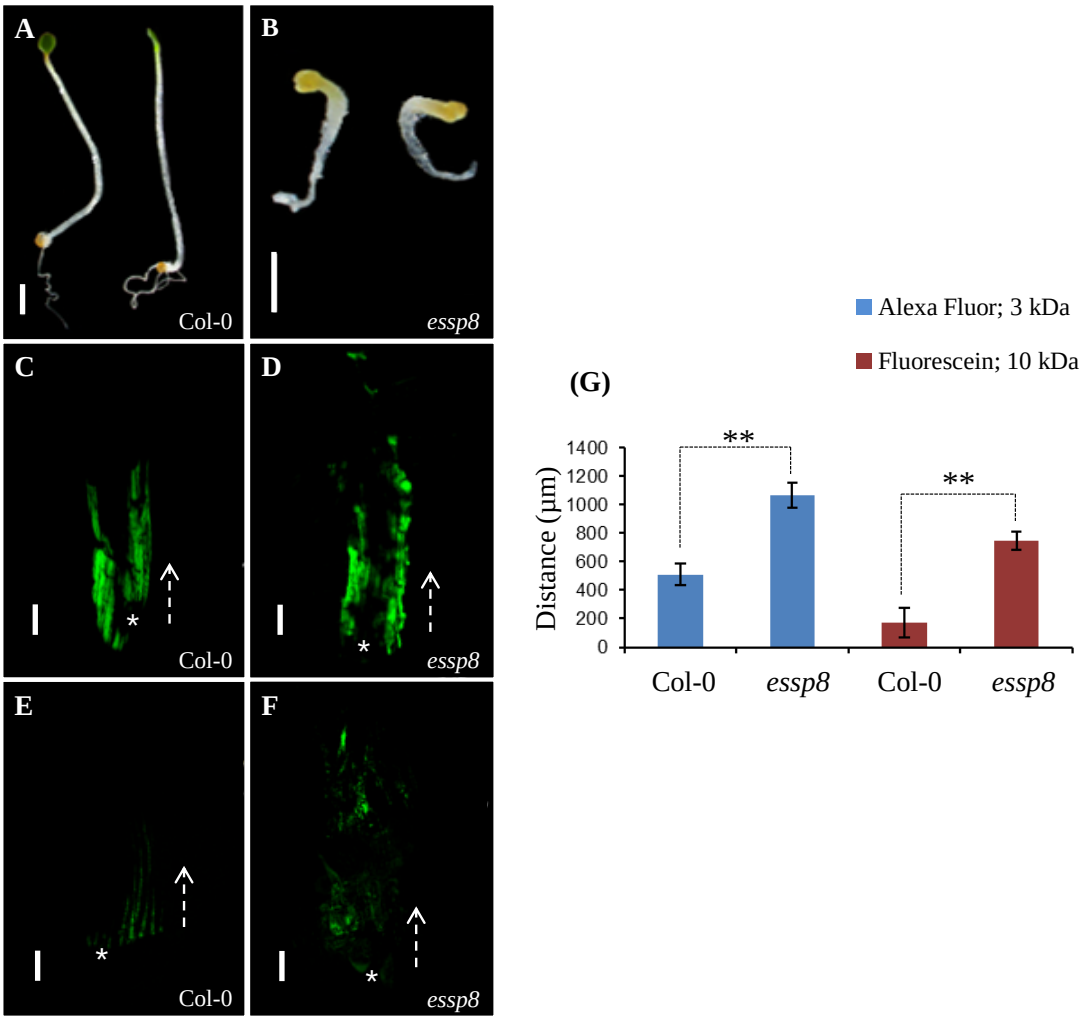

Figure 3.18 Quantitative measurement of the fluorescent probes movement in *essp8* hypocotyl.

(A-B) The hypocotyls of wild-type (A) and *essp8* (B) etiolated seedlings were used for the assay. (C-F) Using two fluorescent probes, Alexa Fluor (3 kDa) (C-D) and fluorescein (10 kDa) (E-F), the symplastic connectivity was quantitatively measured in wild-type (C and E) and *essp8* (D and F) hypocotyls. The injection sites are shown by single asterisks. (G) For both the Alexa Fluor and fluorescein probes, the distance of the probes' movement in WT Col-0 was significantly less than that in *essp8*. In all cases, values reported are the mean ± S.E (n = 5). The double asterisks denote significant differences (Student's t-Test, **P < 0.01). Scale bars: A-B = 1 mm, C-F = 100 µm

periclinal cell divisions. The formation of endodermis and cortex occurs continuously by parallel division of the cells surrounding the QC at the root tip, and is mediated by the activity of two transcription factors SHR and SCR (Di Laurenzio et al., 1996; Helariutta et al., 2000; Wysocka-Diller et al., 2000). It has been previously suggested that the intercellular movement of SHR is PD-mediated (Vatén et al., 2011).

essp8 mutant seedlings display severe defects in root tissue patterning with cell identity change and increased number of cell layers resembling the phenotype of *SHR* ectopic expression. Since it was already shown that the *essp8* mutation causes reduced callose accumulation at the PD (Fig. 3.13E-H) accompanied by an increase in PD SEL (Fig. 3.18G), it was hypothesized that the movement of SHR is altered during root development as a consequence of the PD defects in *essp8*.

To determine whether the root phenotype in *essp8* is, at least partially, SHR-dependent, the *pSHR::SHR:GFP* expression construct was introduced into WT Col-0 and *essp8* heterozygous plants. In five-day-old WT seedlings, SHR is localized into nuclei and cytoplasm in the stele cells, while in the neighboring cell layers including the QC, CEI, and endodermis, SHR specifically resides in the nucleus (Fig. 3.19A). Contrary to the WT, in *essp8* five-day-old seedlings, SHR-GFP fusion protein signal was detected in both nucleus and cytoplasm in the stele cells and the neighboring layers including the QC, CEI and endodermis, as well as cortex (Fig. 3.19B). Although severe defects in root tissue patterning in ten-day-old *essp8* roots make the recognition of different cell layers and tissues challenging, the SHR-GFP fusion protein signal was detected in the outer cell layers, indicating an increase in intercellular movement of SHR in the *essp8* roots compared to the wild type (Fig. 3.19C-D).

This result reconfirms that SHR cell-to-cell trafficking is PD-mediated. Defects in PD aperture in the *gsl8* mutants interfere with the highly-regulated movement of SHR. Dysregulation of SHR symplastic movement leads to its ectopic localization to the cortex and outer cell layers, as well as ectopic subcellular localization into the cytoplasm in the embryonic roots of *gsl8* mutant. Similar results were obtained using two other *gsl8* mutants (*gsl8-1* and *gsl8-2*) (data not shown), which further confirmed that *gsl8* mutants are PD-defective.

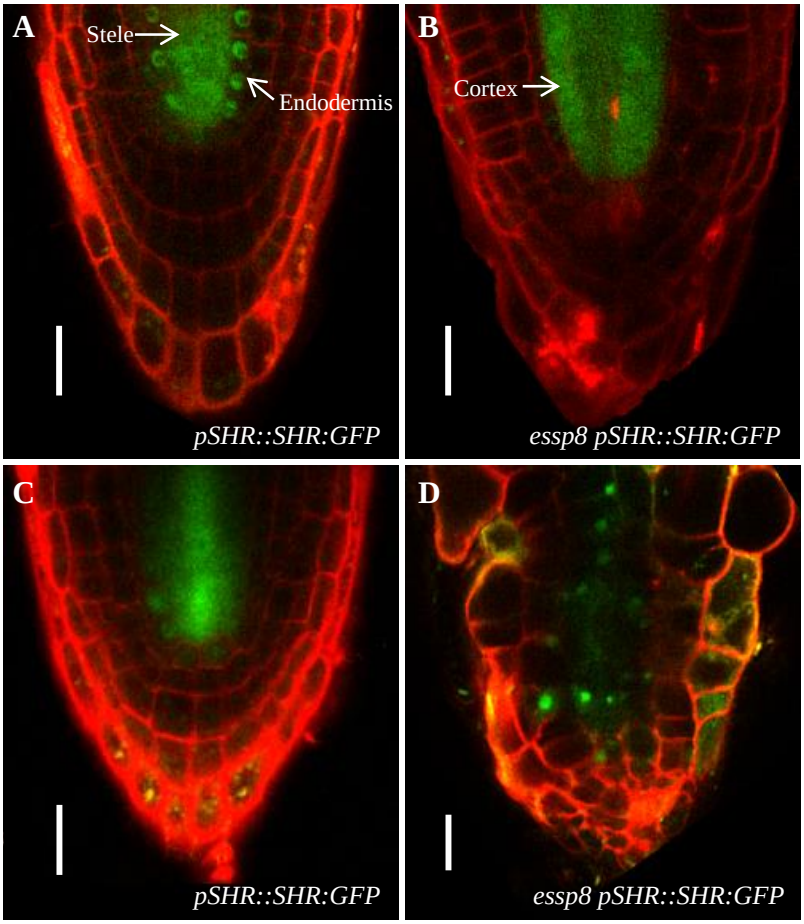

Figure 3.19 Symplastic movement of SHR is altered in *essp8*.

(A-B) Localization of SHR-GFP fusion proteins in five-day-old wild-type Col-0 (A) and *essp8* (B) primary roots. SHR movement and subcellular localization are dysregulated in *essp8* roots as early as five days. (C-D) Localization of SHR-GFP fusion protein in the root tips of ten-day-old wild-type Col-0 (C) and *essp8* (D). Dysregulation of SHR movement and its localization become more severe over time as the root tissue pattern deteriorates with age. Roots were stained with PI to visualize the cell wall. Scale bars = 20 µm

3.5.3 The movement of miR165/6 is altered in the *essp8* root

It has been shown that the miR165/6 species (see section 1.5.4) are transcribed in the endodermis outside of the stele, where SHR is required for their transcription, and then move from the endodermis into the stele where they target the transcripts of class III homeodomain leucine zipper (*HD-ZIP III*) family genes (Carlsbecker et al., 2010; Miyashima et al., 2011). To further understand if the defective root tissue patterning in *essp8* is, at least partially, the result of an increase in PD SEL and impaired symplastic signaling, miR165/6 activity in the endodermis and stele in *essp8* roots was investigated using a 'miRNA-sensor' system (Carlsbecker et al., 2010). In this system, lower GFP signal is an indicator of higher miR165/6 activity (see section 2.6.3).

In WT Col-0 roots, the detected GFP signal was weak but consistent in the stele and endodermis in both five- and ten-day-old seedlings, indicating miR165/6 activity in these cell layers as expected (Fig. 3.20A and C). The GFP signal was more obvious in the QC as well as lateral and collumella root cap, confirming the absence of miR165/6 activity. In five-day-old *essp8* roots, the miR165/6 activity pattern was similar to that of the WT with weak GFP signal in the stele and endodermis (Fig. 3.20B). However, the detected signal in the QC, lateral and collumella root cap was weaker compared to WT Col-0, suggesting that miR165/6 might also be present and active in these cell layers (Fig. 3.20B). In the ten-day-old *essp8* seedlings, miR165/6 was found to be ectopically active in the outer cell layers, which was confirmed by the detection of very weak GFP signals in the stele, endodermis, epidermis, as well as lateral and collumella root cap cells (Fig. 3.20D). Taken together, these results suggest that lack of callose accumulation at the PD in *essp8* possibly dysregulates PD-mediated intercellular signaling and, therefore, results in ectopic activity of miR165/6 in the outer cell layers of the root in *essp8* mutant.

3.5.4 WUSCHEL symplastic movement might be dysregulated in *essp8* shoot apical meristem

WUS (see section 1.5.3) is required for stem cell specification (Laux et al., 1996). WUS activates *CLV3* transcription in the adjacent cell layers of SAM by directly binding its

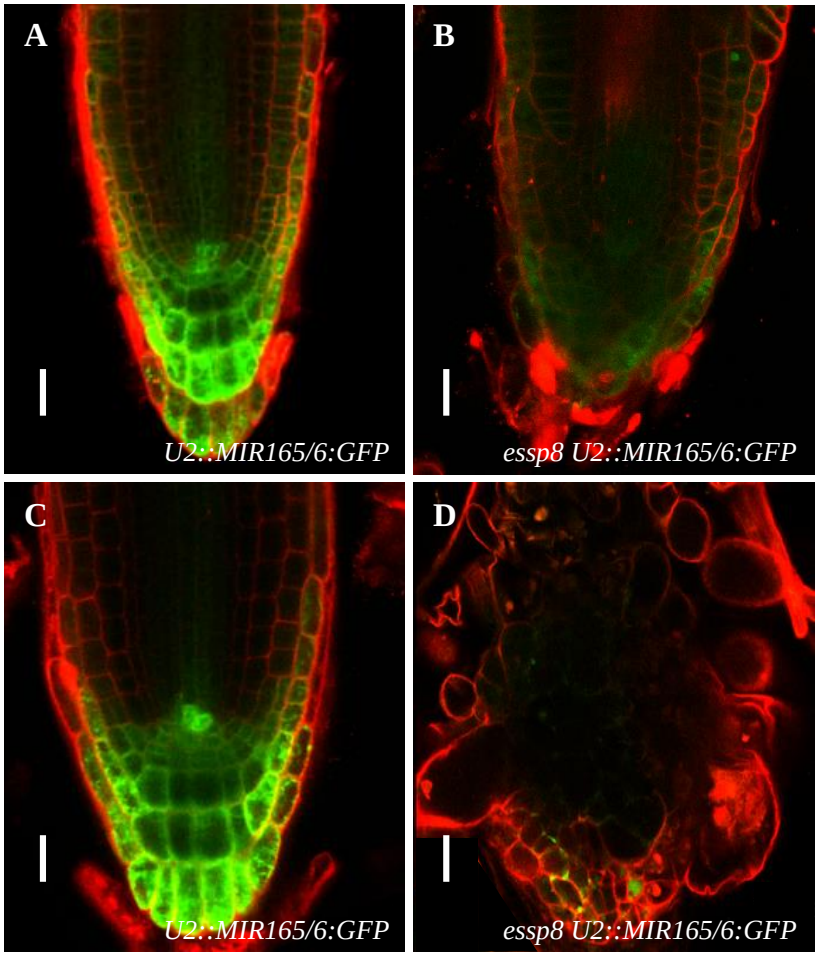

Figure 3.20 Cell-to-cell movement of miR165/6 is dysregulated in *essp8*.

miR165/6 activity in five-day-old wild-type Col-0 (A-B) and ten-day-old seedlings (C-D) in wild-type Col-0 (A, C) and *essp8* (B, D) primary roots, respectively. In the WT, the activity of miR165/6 in the stele and endodermis cells shows a weak GFP signal, whereas in the root cap, absence of miR165/6 activity results in a strong GFP signal (A). In five-day-old *essp8* roots (B), the GFP signal in the root cap is weaker compared to the WT. The detected GFP signal in the ten-day-old *essp8* root cap is noticeably weaker compared to the WT (C and D). Scale bars = 20 µm

genomic region (Yadav et al., 2011). Restricted movement of WUS for two cell layers in SAM is critical for stem cell activity and specification. Mislocalization of WUS in the neighboring cells of SAM induces expansion of the stem cells and proliferation of meristematic cells (Yadav et al., 2010). There is supporting evidence that WUS trafficking is more likely to occur through PD (Daum et al., 2014). Given the possibility that movement of WUS in SAM is mediated through PD and the observation of defective PD in *essp8* mutants, it was postulated that WUS is mislocalized into adjacent cell layers of SAM in *espp8* mutants, leading to up-regulation of *CLV3* in the *essp8* seedlings compared to the WT.

To address this hypothesis, the expression level of *CLV3* was determined by qRT-PCR in wild-type and *essp8* seedlings at two different ages (five- and 10-day-old). Interestingly, a significant increase was found in expression of *CLV3* in *essp8* in both five- and ten-day-old seedlings, with being more significant in ten-day-old seedlings (Fig. 3.21). Taking into consideration that WUS activates *CLV3* transcription, the up-regulation of *CLV3* in *essp8* seedlings indirectly indicates the possibility of WUS ectopic movement and, therefore, ectopic activation of *CLV3* transcription. This result suggests that in SAM, similar to RAM, PD defects may cause an alteration in intercellular communication.

3.6 Attempts to rescue *essp8* mutant phenotype

To examine whether the reduced callose at the PD and consequently increased SEL of the PD are related to the *essp8* defective mutant phenotype, genetic approaches were used to, at least partially, rescue the *essp8* phenotype. Based on our current understanding of the PD regulation and identified proteins in PD proteome (Table 1.1), two candidates, AtBG_PPAP (Levy et al., 2007; Zavaliev et al., 2013) and PDLP5 (Lee et al., 2008; Thomas et al., 2008; Lee et al., 2011; Wang et al., 2013) were chosen for the tests to rescue the *espp8* mutant phenotype and, specifically, its PD defects.

3.6.1 Knocking out AtBG_PPAP cannot restore callose balance at the PD in *essp8*

Deposition of callose is a reversible process which occurs both during developmental processes (Rinne and van der Schoot, 1998; Ruan et al., 2004) and in response to stress

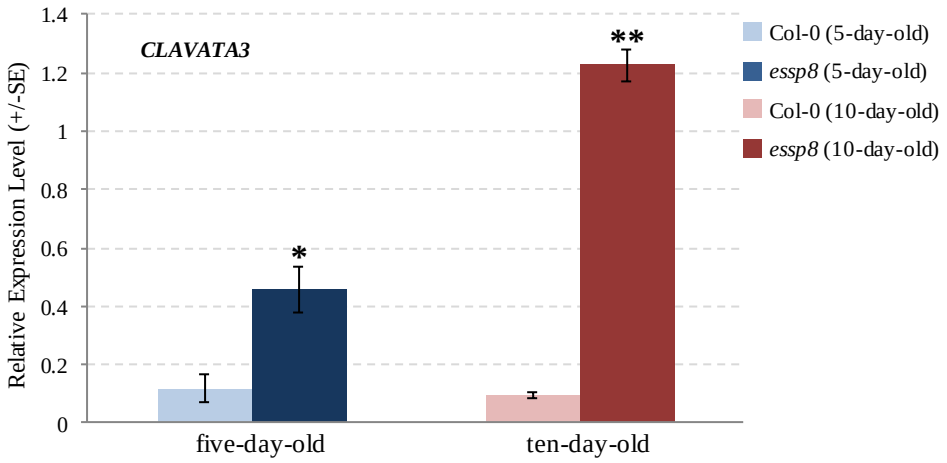

Figure 3.21 Analysis of *CLAVATA3* transcript levels by qRT-PCR.

The expression level was normalized to that of *GAPDH*. Error bars indicate standard deviation for three biological replicates. The asterisks denote significant differences using Student's t-Test, * $P < 0.05$, ** $P < 0.01$.

(Radford et al., 1998; Sivaguru et al., 2000). *AtBG_PPAP* encodes a β-1,3-glucanase (see section 1.4.2) which is associated with PD and is localized to the cell membrane (Levy et al., 2007). It has been previously shown that knocking out β-1,3-glucanase results in an increase in callose accumulation around PD and reduces SEL. Based on these results, it has been proposed that callose turnover, as a result of its synthesis vs. hydrolysis, is responsible for regulating PD SEL (Levy et al., 2007). Therefore, a balance between the activities of β-1,3-glucanases and callose synthases (GSLs) is required to variably deposit callose at the neck of PD, and regulate PD's symplastic flow by adjusting the channel size (Fig. 1.5) (Maule et al., 2012).

essp8 is a *GSL8* loss-of-function mutant. Therefore, it was assumed that the balance between callose synthases and β-1,3-glucanases is disrupted in *essp8*, presumably with higher callose hydrolysis activity than callose synthesis. It was hypothesized that knocking out *AtBG_PPAP* partially restores the balance between the activity of the enzymes hydrolyzing and synthesizing callose, and, consequently, rescues *essp8* mutant phenotype and PD defects moderately. To address this hypothesis, a T-DNA insertion line for *AtBG_PPAP*, *atbg-1*, was ordered from ABRC (Appendix I). After genotyping, individual plants that were homozygous for the T-DNA insertion were crossed with heterozygous *GSL8/essp8* and *GSL8/gsl8-1* plants, and F_2 population was screened to identify the double mutants (*atbg-1 essp8* and *atbg-1 gsl8-1*). Double mutants were identified using PCR-based genotyping and sequencing to confirm the *atbg-1*, *gsl8-1* and *essp8* genotypes. *atbg-1 essp8* and *atbg-1 gsl8-1* double mutants were identified at the ratios of around 5% and 6% in the F_2 population, respectively.

Interestingly, knocking out *AtBG_PPAP* in *essp8* and *gsl8-1* genetic backgrounds could not rescue the morphological defects of *gsl8* mutants (Fig. 3.22A-D). To investigate whether the *atbg-1* mutation can rescue PD defects, the callose accumulation was visualized using aniline blue staining. Callose visualization showed an increase in the amount of callose deposited at PD in *atbg-1* compared to the WT, and in *atbg-1 essp8* double mutant compared to *essp8* single mutant (Fig. 3.22E-H). No obvious change was detected at the cell plate (data not shown). This result indicates that only a minor

elevation of the callose deposited at PD is not sufficient to rescue the PD defects and subsequently, the *gsl8* mutant phenotype.

3.6.2 *PDLP5* overexpression induces callose deposition at PD

It was been previously suggested that PDLPs (see section 1.4.1) can induce callose deposition at PD and, therefore, might negatively regulate SEL of PD (De Storme and Geelen, 2014). *PDLP5* overexpression can elevate plants' resistance against viral infection, which is achieved through an increase in callose deposition at PD and thus, restricts the symplastic movement of the viral genome MPs (Lee et al., 2008; 2011). It was previously shown that in *essp8*, callose deposition at PD is reduced (Fig. 3.13F-H), and cell-to-cell communication is impaired (Fig. 3.18), supposedly due to an increase in SEL of PD. Thus, it was hypothesized that *PDLP5* overexpression in *gsl8* mutant background partially rescues PD defects and, therefore, the altered symplastic signaling.

To test my hypothesis, the *p35S::PDLP5:GFP* expression construct was introduced into WT Col-0 and *GSL8/essp8* heterozygous plants to generate *PDLP5*-overexpression lines (*PDLP5-OE*). Wild-type seedlings overexpressing *PDLP5* exhibited yellowish color compared to the wild-type Col-0 (Fig. 3.23A-B), consistent with a previously published observation (Lee et al., 2011). *PDLP5* overexpression did not rescue the *gsl8* phenotypic defects in *essp8* background (Fig. 3.23C). To confirm that PDLP5 in transgenic plants is indeed localized at the PD, its localization was examined in the roots of five-day-old seedlings. PDLP5-GFP signals were detected at punctate particles at the cell membrane of root cells, suggested to be associated with the PD apertures, which is consistent with previous reports on PDLP5 (Lee et al., 2011) and its homolog, PDLP1 (Thomas et al., 2008) (Fig. 3.23D-E). Additionally, in *essp8 PDLP5-OE* root cells, PDLP5-GFP signal could occasionally be detected inside the cell periphery (Fig. 3.23F), suggesting that PDLP5 localization might be disrupted in *essp8* plants.

To determine if PDLP5 can induce callose deposition at the PD, aniline blue staining was used to visualize the callose accumulated at the PD in the *PDLP5-OE* lines in wild type and *essp8* backgrounds. Staining of the primary roots in seven-day-old seedlings showed

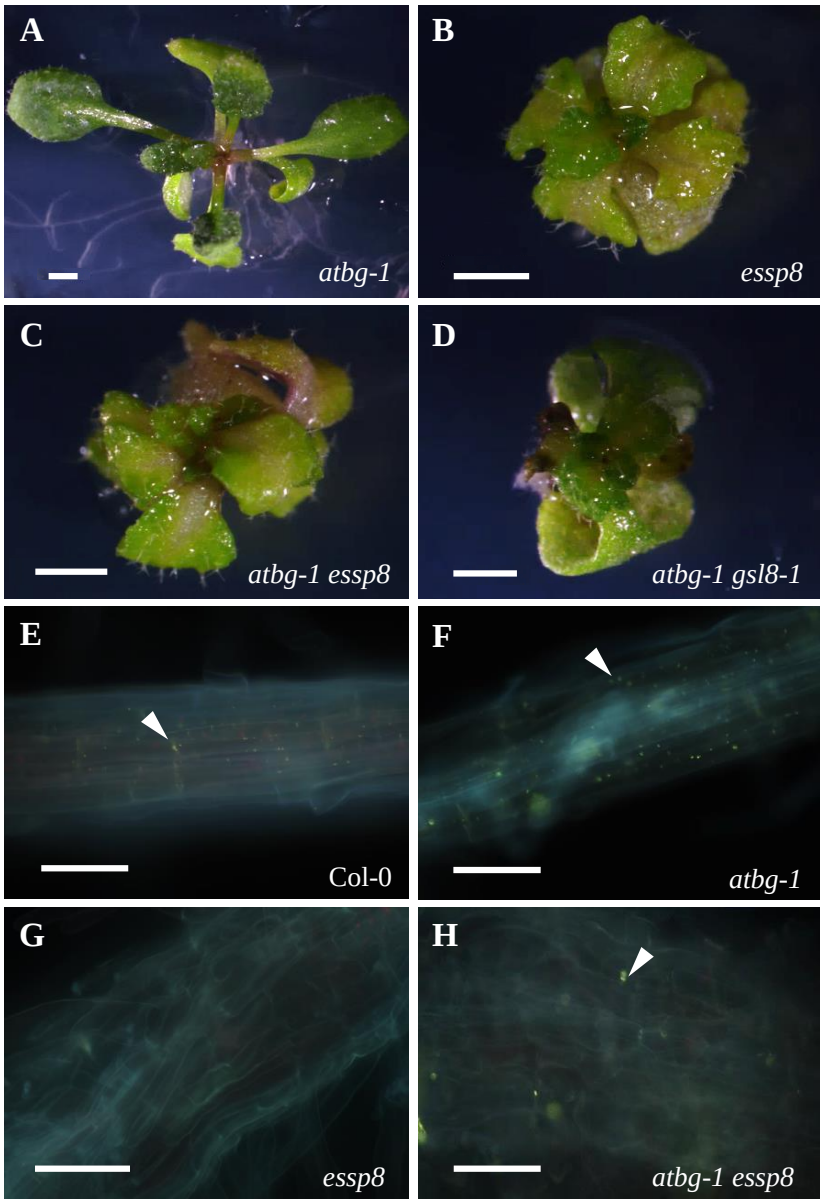

Figure 3.22 Phenotypes of *atbg-1 gsl8* double mutants.

(A-D) The morphological phenotypes of *atbg-1* (A), *essp8* (B), *atbg-1 essp8* (C) and *atbg-1 gsl8-1* (D) two-week-old seedlings. *atbg-1* seedlings do not exhibit distinguishable phenotypic defects. Knocking out *AtBG_PPAP* in the *gsl8* background does not rescue the defective phenotype of *gsl8* mutants compared to an *essp8* single mutant. (E-H) Visualization of callose deposition at the PD using aniline blue staining in seven-day-old primary roots of wild-type Col-0 (E), *atbg-1* (F), *essp8* (G) and *atbg-1 essp8* (H) seedlings. Callose deposited at the PD is indicated by white arrowheads. Scale bars: A-D = 1mm, E-H = 50 µm

that *PDLP5* overexpression in the WT background induces an increase in callose accumulation at the PD (Fig. 3.23G-H), while no change was detected in *essp8 PDLP5-OE* roots (Fig. 3.23I).

3.6.3 PDLP5 and AtBG_PPAP regulate PD's SEL

To further elucidate if modulation of callose deposition at the PD, induced by *PDLP5* overexpression and/or knocking out *AtBG_PPAP*, can indeed affect the SEL, cell-to-cell communication was tested using the SEL assay (see section 2.7). Measuring the extent of fluorescein probe movement in seven-day-old hypocotyls confirmed that an increase in callose deposition, induced by *AtBG_PPAP* knockout or *PDLP5* overexpression, modulates the SEL in *atbg-1* and *PDLP5-OE* compared to wild-type Col-0. Cell-to-cell movement of probe showed a reduction in both *atbg-1* and *PDLP5-OE* hypocotyls compared to wild-type Col-0, with *PDLP5-OE* displaying a significant decrease. Knocking out *AtBG_PPAP* in *essp8* background could significantly decrease the SEL. However, no difference could be detected between *essp8 PDLP5-OE* and *essp8* seven-day-old hypocotyls (Fig. 3.24). This result confirms that knocking out *AtBG_PPAP* slightly restores the accumulation of callose at the PD in both WT and *gsl8* hypocotyls, similar to what was observed in primary roots (Fig. 3.22). Moreover, *PDLP5* overexpression induces callose deposition at the PD in WT, but, surprisingly, not in the *gsl8* mutant.

3.7 Identification of GSL8 interacting partners

It has been predicted that GSL might be part of a complex called CalS complex (see section 1.2.4). At least four potential candidates have been suggested as components of this complex including at least one of the GSLs, UGT1, ROP and SuSy (Andrawis et al., 1993; Shin and Brown, 1999; Hong et al., 2001a; Hong et al., 2001b).

Additionally, it has been indicated that a balance between β-1,3-glucan synthase and glucanase activities is required to achieve a dynamic modulation of callose deposition at the PD, and consequently regulate the SEL of the PD in response to exogenous and endogenous stimuli (Fig. 1.5) (Yadav et al., 2014). PDLPs have also been characterized as PD-localized proteins and, in theory, they can interact with other proteins that are similarly-

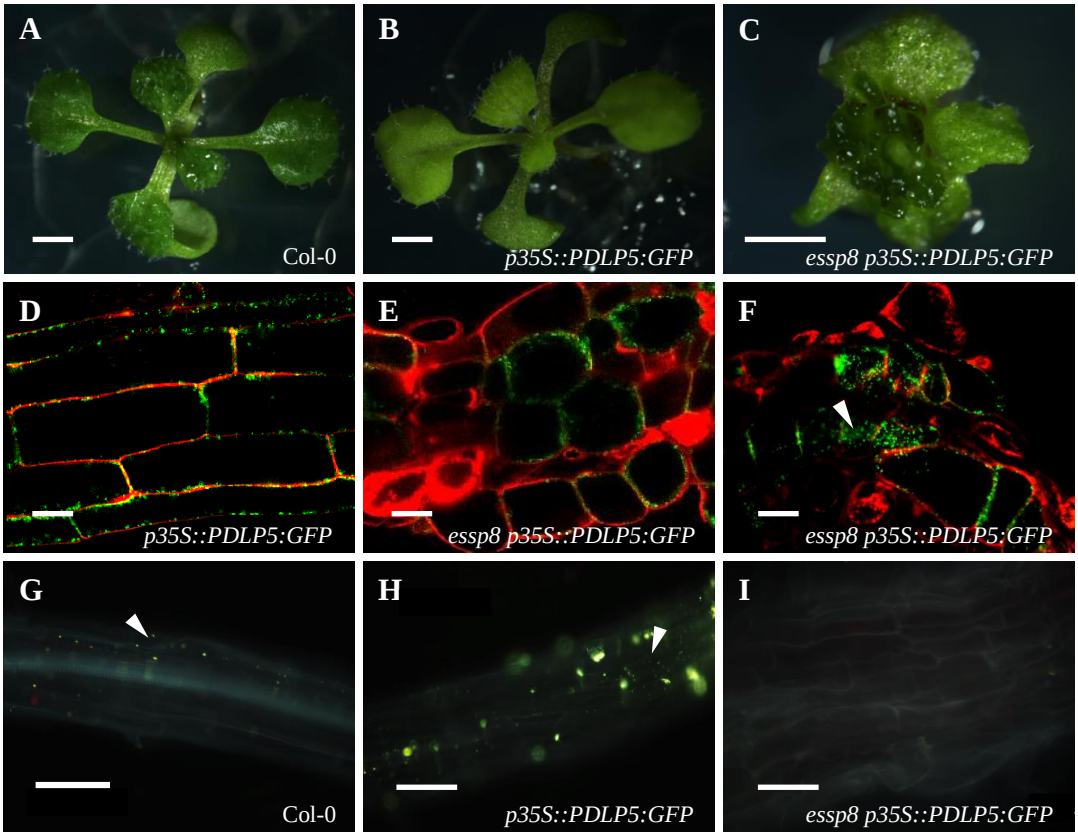

Figure 3.23 Phenotype of *PDLP5-OE* seedlings and PDLP5 subcellular localization. (A-C) Morphological phenotypes of wild-type Col-0 (A), *PDLP5-OE* (B) and *essp8 PDLP5-OE* (C) two-week-old seedlings. *PDLP5-OE* seedlings show chlorosis compared to the WT. *essp8* seedlings overexpressing *PDLP5* display a similar phenotype as *essp8*. (D-F) Subcellular localization of PDLP5 in *PDLP5-OE* (D) and *essp8 PDLP5-OE* (E and F) five-day-old primary roots. In the WT background, PDLP5 is localized at the cell membranes in a dotted pattern. In the *essp8* background, the PDLP5-GFP signal can also be detected inside the cell periphery (white arrowhead). (G-I) Visualization of callose deposition at the PD (white arrowheads) using aniline blue staining in WT Col-0 (G), *PDLP5-OE* (H) and *essp8 PDLP5-OE* (I). Scale bars: A-C = 1 mm, D-F = 20 µm, G-I = 50 µm

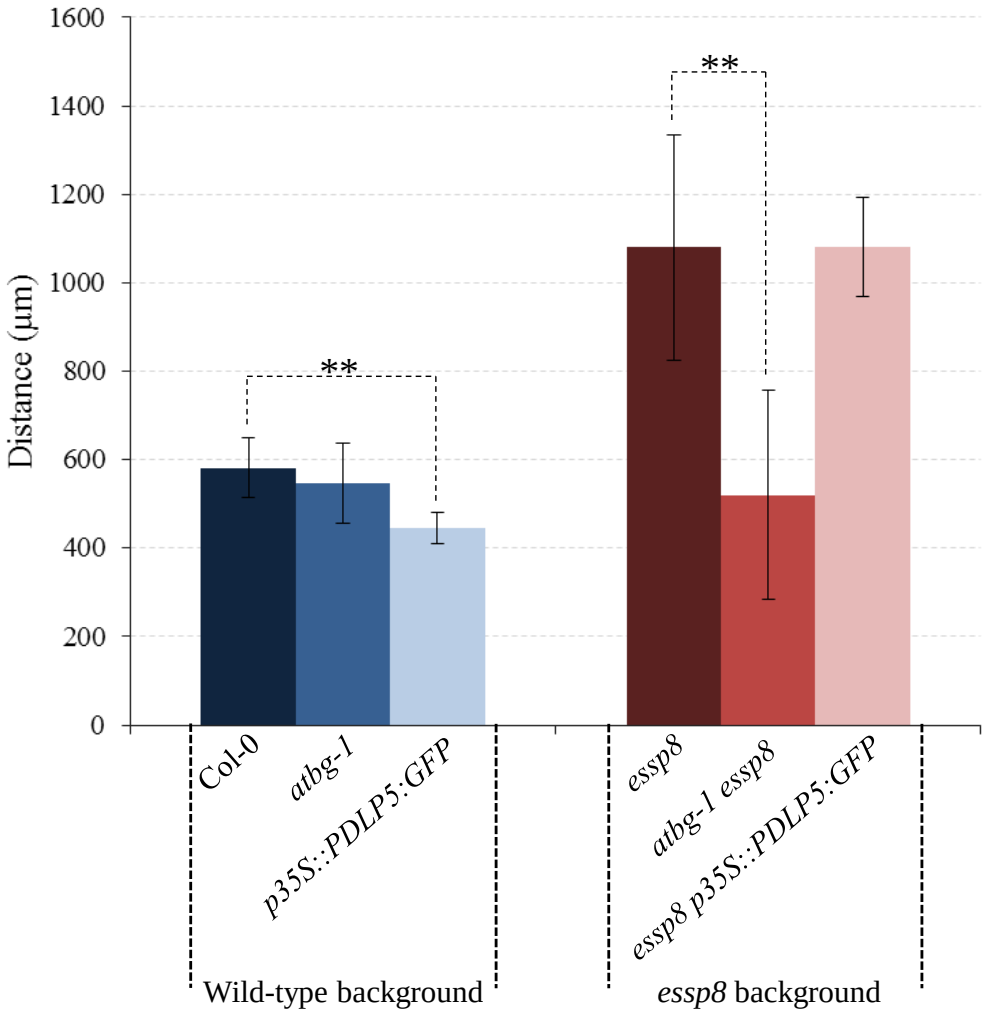

Figure 3.24 Measurement of symplastic movement in various genetic and transgenic backgrounds.

Cell-to-cell communication was quantified in hypocotyls of seven-day-old seedlings using a 10 kDa fluorescent probe (fluorescein) in corresponding genetic backgrounds as indicated. In all cases, values represent the mean ± S.E. (n = 5) and dotted lines indicate which samples were pairwise compared. Significant differences at $P < 0.01$ using Student's t-Test are shown with **.

localized (Thomas et al., 2008). The receptor-like characteristics of PDLPs suggests that they might be involved in the regulation of symplastic trafficking. Additionally, earlier reports demonstrated that GSL8 is required for cytokinesis completion and proper callose deposition during cell plate formation (see section 3.4) (Chen et al., 2009; Thiele et al., 2009). SCD1 has been known to function in membrane trafficking during cytokinesis and cell expansion and, together with SCD2, is associated with clathrin-mediated membrane transport and plasma membrane endocytosis (McMichael et al., 2013). SCD1 was chosen as one of the candidate to investigate its possible interaction with GSL8 at cell plate and/or plasma membrane.

To determine the components of the callose synthase complex, firstly a hypothetical interactome was generated for GSL8 using a web-based tool (Franceschini et al., 2013) (Fig. 3.25). By combining the results from the hypothetical interactome and previous studies, six candidates, SUCROSE SYNTHASE 1 (SUS1), UDP-GLYCOSYL TRANSFERASE (UDPG), ROP4, PDLP5, AtBG_PPAP and SCD1, were chosen to investigate their physical interaction with GSL8 *in vivo*.

FRET was used to test these protein-protein interactions. The acceptor photobleaching approach (see section 2.9) was used to quantify FRET efficiency. FRET analysis showed an *in vivo* interaction between GSL8 and SUS1, AtBG_PPAP, PDLP5 and SCD1. However, no direct interaction could be detected between GSL8 and UDPG or ROP4 (Fig. 3.26). Testing the swapped fluorophores, in which GSL8 was used as the donor, generated similar results (data not shown), confirming the observed molecular interactions.

These results suggest that, similar to cellulose synthase complex, SuSy is likely to provide the UDP-Glc for callose synthase, e.g. GSL8, confirmed by identification of their interaction. The interaction of PD-localized β-1,3- glucanase (AtBG_PPAP) with GSL8 provides evidence that the balance between the activity of enzymes synthesizing and degrading callose might occur through their direct interaction. Based on our results as well as the previous prediction (De Storme and Geelen, 2014), induction of callose deposition at the PD by PDLP5 is suggested to be mediated by GSL8 as shown by their interaction. An earlier study had predicted the possible interaction of SCD1 and callose synthase during cell plate formation (Hong et al., 2001a) as was confirmed here.

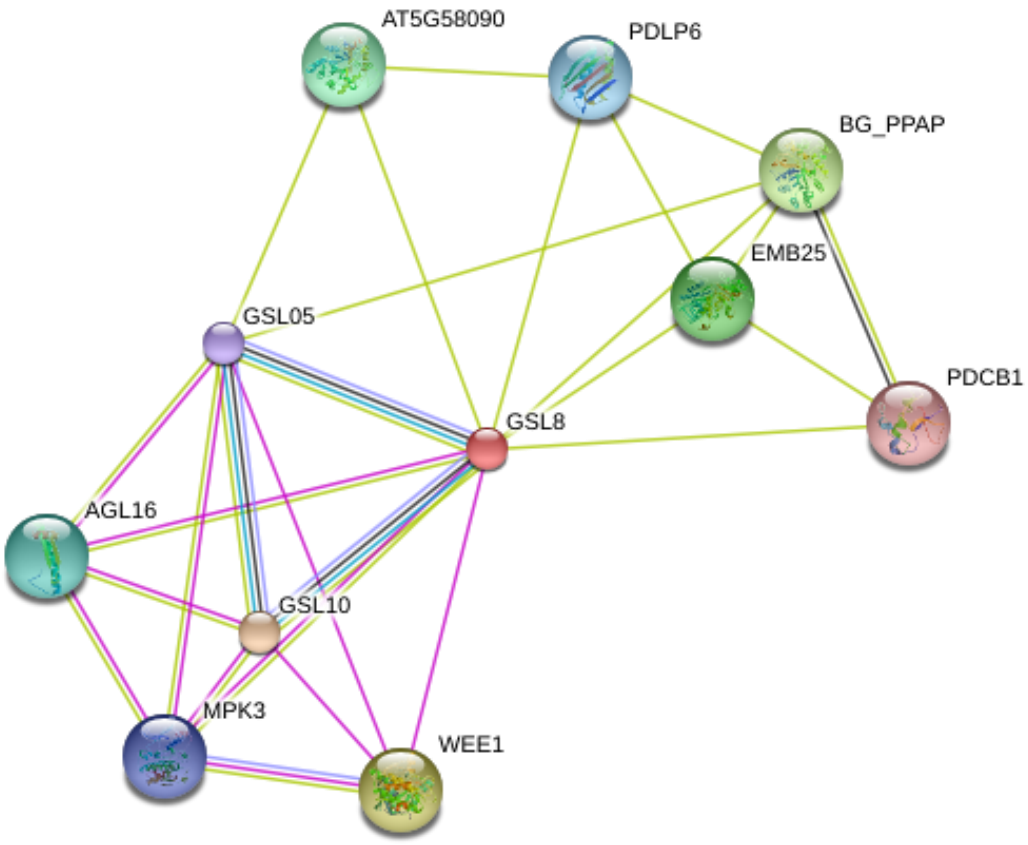

Figure 3.25 A hypothetical interactome network for GSL8.

Potential interactors of GSL8 were identified using a web-based tool (Franceschini et al., 2013). Different line colors represent the type of evidence used to identify the association. Functional partners of GSL8 were identified based on co-expression (grey), experimental data (pink), database (blue), text mining (green) and sequence homology (purple) (Franceschini et al., 2013).

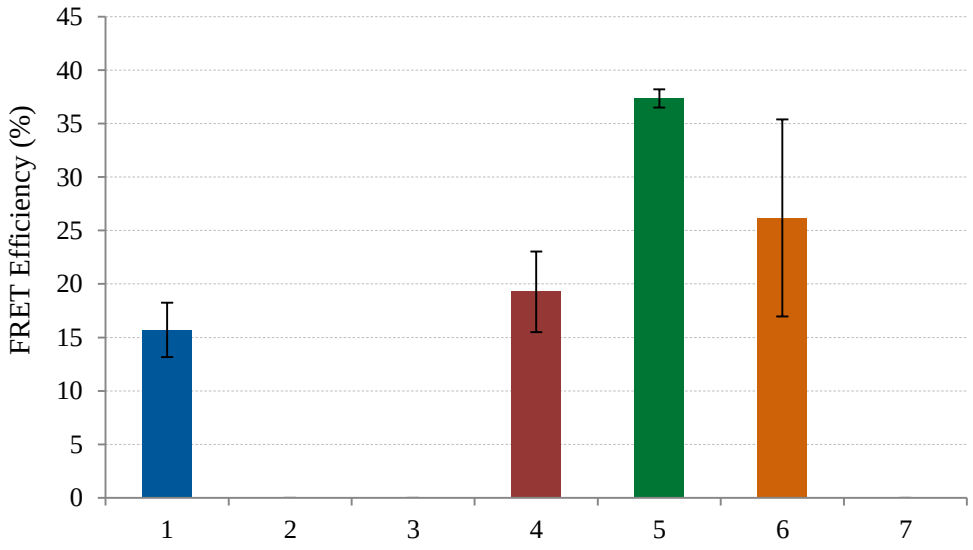

1. SUS1-CFP + GSL8-YFP
2. UDPG-CFP + GSL8-YFP
3. ROP4-CFP + GSL8-YFP
4. AtBG_PPAP-CFP + GSL8-YFP
5. PDLP5-CFP + GSL8-YFP
6. SCD1-CFP + GSL8-YFP
7. CFP + GSL8-YFP

Figure 3.26 GSL8 interacts with sucrose synthase, AtBG_PPAP, PDLP5 and SCD1. The acceptor photobleaching FRET showed an interaction between GSL8 and SUS1, PD-localized callose degrading enzyme (AtBG_PPAP), PDLP5 and SCD1. According to the FRET results, no direct interaction could be identified between GSL8 and UDPG, and ROP4. Free CFP was used as the negative control. The data used for FRET efficiency calculation and statistical analyses were obtained from at least three independent experiments and three biological replicates for each experiment. In all cases values reported are the mean ± S.E., n = 9.

3.7.1 GSL8 cytoplasmic domain is required for its interaction with SUS1, AtBG_PPAP, PDLP5 and SCD1

The alignment of GSLs' amino acid sequence revealed that the conserved residues mostly belong to the cytoplasmic domain with the longest conserved region located on the C-terminal end of the cytoplasmic loop in GSL8 (Appendix VII, Fig. 3.12). Based on the GSLs' alignment, it was hypothesized that the cytoplasmic loop of GSL8 acts as its catalytic site and is required for the interaction with its identified partners. Therefore, truncation of GSL8 in *essp8*, leading to the absence of the cytoplasmic loop, should negatively affect GSL8 function. To assess this hypothesis, YFP and CFP fusions were made with the truncated version of GSL8 to use for interaction analysis. The interaction of truncated GSL8 with SUS1, AtBG_PPAP, PDLP5 and SCD1, which was proved with full-length GSL8, was investigated using FRET. For all four interactions, FRET quantification revealed significant decrease compared to the full length version (Fig. 3.27). Thus, it can be concluded that the GSL8 cytoplasmic loop is indeed required for its interaction with its partners and, therefore, for its activity.

3.7.2 GSL10 might be part of the callose synthase complex

GSL8 and GSL10 are the most closely-related members of the GSL family, at both their genomic and amino acid sequence levels, and clustered into the same subfamily in the phylogenetic tree of the Arabidopsis GSL family (Fig. 3.11). Additionally, their loss-of-function mutants show similar phenotypes during microspore mitosis and sporophyte development (Töller et al., 2008). The hypothetical interactome for GSL8 also suggested high likelihood of its interaction with GSL10 (Fig. 3.25). These results led to the speculation that GSL8 and GSL10 form a heterodimeric complex, in which the absence of one member disrupts the complex functionality. This is similar to what has been shown for cellulose synthase (CESA) complexes which consist of three different CESA proteins (Taylor et al., 2000; Gardiner et al., 2003).

A previous study reported dwarf phenotypes for both *gsl8* and *gsl10* knockdown lines, generated using dsRNAi approach, with *gsl10* exhibiting more severe dwarfism (Töller et al., 2008). Therefore, it was hypothesized that *gsl8 gsl10* double mutants show similar

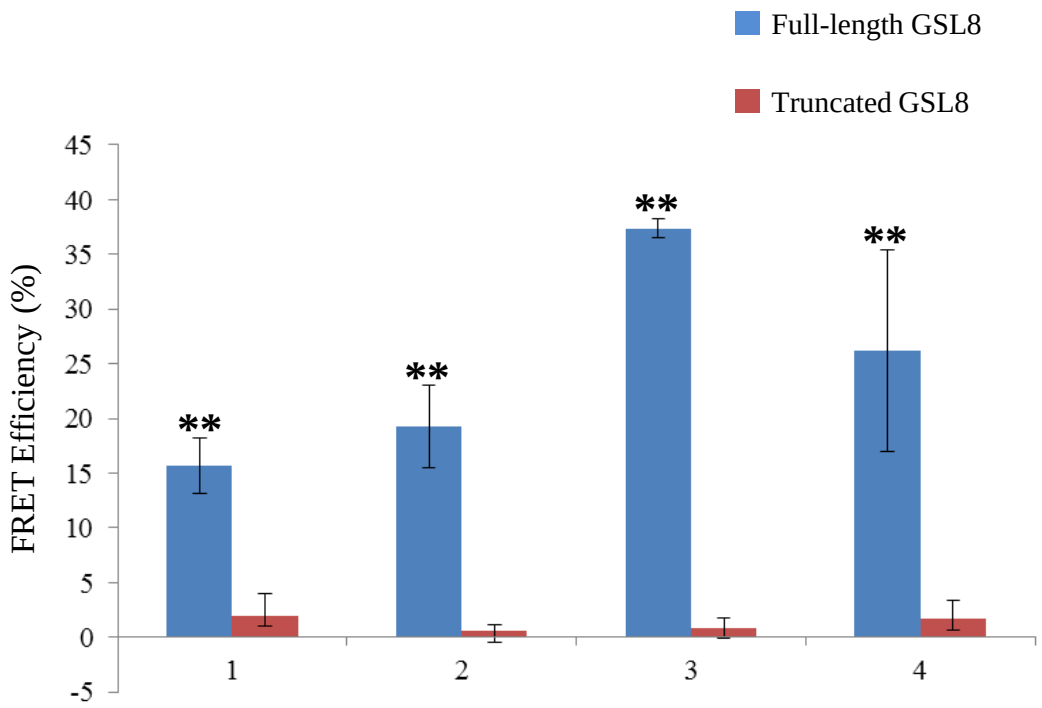

1. SUS1-CFP + GSL8-YFP
2. AtBG_PPAP-CFP + GSL8-YFP
3. PDLP5-CFP + GSL8-YFP
4. SCD1-CFP + GSL8-YFP

Figure 3.27 The GSL8 cytoplasmic loop is required for its interaction with SUS1, AtBG_PPAP, PDLP5 and SCD1.

Using a truncated GSL8 as the acceptor in FRET quantification for GSL8 showed significant reduction of FRET efficiency for all four interactions with SUS1, AtBG_PPAP, PDLP5 and SCD1 compared to full-length GSL8. The data used for FRET efficiency calculation and statistical analysis were obtained from at least three independent experiments and three biological replicates for each experiment. In all cases values reported are the mean ± S.E., n = 9. The double asterisks denote significant differences using Student's t-Test, $P < 0.01$.

phenotype to that of *gsl8* or *gsl10* single mutants if GSL8 and GSL10 indeed form a heterodimeric complex.

Due to the essential role of GSL10 in gametophytic development, no homozygous *gsl10* mutants could be recovered after screening several T-DNA insertion lines for *GSL10* (Appendix I). Therefore, *gsl8 gsl10* double mutant was generated using an artificial miRNA under the control of an estradiol-inducible promoter (see section 2.6.4). *XVE::aMIRGSL8/GSL10* transgenic seeds were germinated and induced on MS media containing 100 μM β-esteradiol or mock-treated on MS media containing DMSO. The mock treated fourteen-day-old *XVE::aMIRGSL8/GSL10* transgenic seedlings did not show any obvious defects compared to the WT Col-0 (Fig. 3.28A-B), whereas the transgenic seedlings treated with β-esteradiol phenocopied the phenotype of *gsl8-1* mutant seedlings. Similar to *gl8-1*, *XVE::aMIRGSL8/GSL10* transgenic seedlings show dwarfism and develop abnormally-shaped true leaves. Additionally, the primary roots and root hairs of *XVE::aMIRGSL8/GSL10* seedlings are shorter, thicker, and the root tips are swollen compared to the wild-type, but similar to those of *gsl8-1* (Fig. 3.28C-D).

This result suggested that GSL8 and GSL10 are unlikely to be functionally-redundant, as their single mutants have strong phenotypes, although it is possible that they become functional by forming a complex. Hence, the *XVE::aMIRGSL8/GSL10* seedlings do not exhibit more severe defects compared to *gsl8* single mutants. Further investigation is required to determine whether GSL8 and GSL10 physically interact *in vivo*.

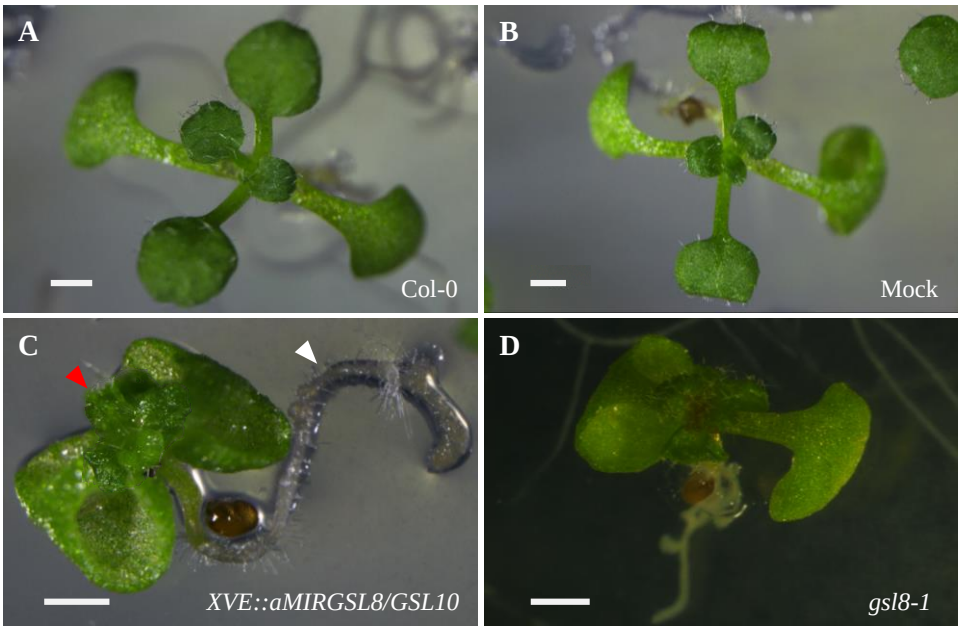

Figure 3.28 Morphological phenotype of *XVE::aMIRGSL8/GSL10* seedling.
Comparing the morphological phenotypes of two-week-old WT Col-0 (A), mock-treated (B), *XVE::aMIRGSL8/GSL10* transgenic (C) and *gsl8-1* (D) seedlings. *XVE::aMIRGSL8/GSL10* transgenic seedlings phenocopy the *gsl8-1* single mutant developmental defects: dwarf seedlings with short and thick roots (white arrowhead), and abnormally-shaped true leaves (red arrowhead). Scale bars = 1 mm

CHAPTER 4

4 DISCUSSION

4.1 *essp8* is a new allele of *GSL8*

In this study, an Arabidopsis mutant named *essp8*, initially identified through an unrelated genetic screen (see section 1.8), was discovered to have an interesting phenotype. *essp8* mutant forms tiny seedlings, having short and thick roots and hypocotyls. The cotyledons and true leaves are thicker and undulated in *essp8* seedlings compared to the WT. In addition, the *essp8* mutation can ectopically induce somatic embryo formation with incomplete penetrance. The first evidence for the biological role of *essp8* was discovered when *essp8* was identified as a novel allele of Arabidopsis *GSL8*. GSL8 has been characterized as a callose synthase. Callose plays important roles in cell division, growth and differentiation in plants (Piršelová and Matušíková, 2013), and accounts for up to 80% of the plant cell walls' dry mass (Xie and Hong, 2011). Hence, this study was focused on characterization of *essp8* mutant.

The observed *essp8* seedling phenotype is similar to the defects previously reported for the other *GSL8* alleles, such as showing dwarfism, short roots with defects in root tissue patterning (Chen et al., 2009; Thiele et al., 2009; Guseman et al., 2010), swollen, branched root hairs (Guseman et al., 2010), and disorganized epidermal cells in cotyledon and true leaves (Chen et al., 2009). However the ectopic somatic embryo phenotype had not been documented for *gsl8* mutants. An elevation of cell proliferation in the root cap collumella, hypocotyl cortex, endodermis and phloem (Chen et al., 2009), stomatal-lineage cells (Guseman et al., 2010), and cotyledon and first leaves (De Storme et al., 2013) was mentioned in previously characterized alleles of *GSL8*. My different observation might be due to the unique mutation site in *essp8* leading to the truncation of GSL8. Alternatively, it cannot be excluded that it might be simply caused by slightly different growth conditions such as difference in sucrose concentration in the growth media compared to what were used in other studies (3% vs. 1%). Dependence of aerial and root morphological phenotype, and cell expansion on external sucrose level has been previously reported (Benfey et al., 1993; Roldán et al., 1999; Caño-Delgado et al., 2000; Takahashi et al., 2003). This study also showed the dependence of somatic embryo phenotype induction on the sucrose concentration. As such, *essp8* seedlings develop

somatic embryos only on MS media containing 3% sucrose (Fig. 3.3), whereas, no somatic embryo could be identified when the sucrose content was decreased to 1.5% (data not shown). This is the first report on induction of somatic embryo formation and cell identity change in a *gsl8* mutant. The somatic embryo phenotype of *essp8* mutant provides new insight into GSL8 requirement during early seedling development in Arabidopsis.

4.1.1 *gsl8* mutation causes embryo defects and seedling lethality

Poor germination was observed, regardless of sucrose concentration, in all the *GSL8* mutants studied, including *gsl8-1*, *gsl8-2*, *gsl8-3*, *gsl8-4* and *essp8*. Germination failure in about 5% of the homozygous *essp8* seeds resulted in a segregation ratio of approximately 20%, instead of 25% (Table 3.1), the ratio expected in the case of Mendelian segregation for a recessive mutation at a single locus. The morphological analysis of the siliques from a heterozygous parent showed that homozygous *gsl8* seeds are reduced in size compared to the WT and carry defective embryos (Fig. 3.1E-F), which is consistent with previous reports (Chen et al., 2009; Thiele et al., 2009).

The lethality for the *gsl8* knockout lines has already been documented (Töller et al., 2008; Chen et al., 2009; Thiele et al., 2009; Guseman et al., 2010). The lethal phenotype of *essp8* mutant seedlings excludes the possibility of GSL8 functional redundancy with the other eleven identified GSLs in Arabidopsis, at least at the seedling stage. Additionally, it indicates that GSL8 plays a specific and substantial role in callose biosynthesis during plant growth and development. High correlation of *GSL8* and *GSL10* expression profiles and their similar mutant phenotypes during microspore mitosis and sporophyte development have raised the question of whether they are functionally-related, or have overlapping roles (Töller et al., 2008). It still needs to be further investigated if GSL8 and GSL10 can form a heteromeric callose synthase complex, similar to what have been shown for cellulose synthase complexes (Taylor et al., 2000; Gardiner et al., 2003). The existence of such a complex can potentially explain their similar mutant phenotypes, caused by disruption of the complex activity in the absence of one component (see section 4.5.4).

4.2 *gsl8* phenotypic defects are partially caused by cytokinesis impairment

Endopolyploidization, defined as the cell-specific nuclear DNA content multiplication, in both plants and animals is either the result of endomitosis or endoreduplication during mitotic cell cycle processes (Joubès and Chevalier, 2000). In endoreduplication, due to a complete absence of mitotic chromosomes condensation and their subsequent division, while the total number of the chromosomes won't be affected, polytenal chromosomes are generated (Edgar and Orr-Weaver, 2001; Lee et al., 2009). In endomitosis, in contrast to endoreduplication, cells enter mitosis but do not complete the process. Depending on the stage when the M-phase is aborted, division of the duplicated chromosomes and cytokinesis might be missing, resulting in the generation of cells that will have doubled absolute number of chromosomes (D'Amato, 1984).

Although callose biosynthesis occurs in different species, accumulation of callose at the cell plate during cell division is plant-specific, and has been confirmed for all plant taxa (Scherp et al., 2001). Callose is known as a major component of cell plate and cell wall and, therefore, is required for completing plant cytokinesis and proper cell wall formation (Verma, 2001; Chen and Kim, 2009; Vatén et al., 2011; Piršelová and Matušíková, 2013). It has been shown that loss-of-function mutations in GSL8 cause defects in cell plate and cell wall formation (Töller et al., 2008; Chen et al., 2009; Thiele et al., 2009; Guseman et al., 2010; De Storme et al., 2013). Thiele et al. (2009) for the first time reported severe cell division defects and a significant decrease in callose deposition at the cell plates in a *GSL8* knockdown line. This result provided the evidence supporting the important role of GSL8 in callose biosynthesis during cytokinesis. Additionally, defects in the cell walls accompanied with formation of endomitotic cells were detected in flower tissues of *et2*, a weak allele of *GSL8* (De Storme et al., 2013). Taken together, callose biosynthesis by GSL8 plays a substantial role during cell plate formation and is thus required for maintaining the basic ploidy level, especially in reproductive tissues. My findings are in agreement with the previous studies and reconfirm the cytokinesis defects in the newly identified allele of *GSL8*, *essp8*. The *essp8* mutation causes reduction of callose deposited at the cell plates in actively dividing cells in the RAM. Determination of the ploidy level in the root cells of three different *gsl8* mutants, *essp8*, *gsl8-1* and

gsl8-2 revealed that *gsl8* mutation induces ectopic polyploidization and endomitosis, both in the meristematic tissue and elongating cells of the root (Fig. 3.15 and 3.16). This result, for the first time, provides the evidence that cytokinesis defects in *gsl8* mutants are beyond the reproductive tissues and affect both somatic and reproductive cells.

4.2.1 Cytokinesis defects might cause lethality of *essp8* seedlings

The cause(s) of *gsl8* knockout mutants' lethality is still under debate. Loss of proper chromosome condensation and segregation during successive cell divisions has been suggested as one of the potential reasons leading to growth arrest (De Storme et al., 2013). Segregation of the replicated chromosomes becomes too complicated in polyploid or endomitotic nuclei as they go through consecutive cell divisions (Sugimoto-Shirasu and Roberts, 2003). Therefore, it is expected that with progression of *gsl8* seedling development, the number of polyploid and/or endomitotic cells and the ploidy level increases. Comparing *essp8* seedlings at different ages confirmed that more cells display cytokinesis defects as the number of polyploid and/or endomitotic cells significantly increases in older seedlings (Fig. 3.17). It is plausible that accumulative polyploidization caused by defects in cell plate formation induces a premature arrest of cell division in proliferating tissues and, consequently, cell death. Death through mitotic catastrophe and polyploidization has already been reported in different species (Doelling et al., 2001; Tzafrir et al., 2002; Castedo et al., 2004; McCall, 2004; Vakifahmetoglu et al., 2008; Pritchett et al., 2009).

4.2.2 Cytokinesis-defective mutants do not exhibit severe tissue impairments

Ectopic polyploidization is known as a general characteristic of cytokinesis-defective mutants and has been detected in different organisms and cell types (Hatzfeld and Buttin, 1975; Thompson and Lindl, 1976; Karess et al., 1991; Castrillon and Wasserman, 1994; Neufeld and Rubin, 1994; Liu et al., 1997; Spielman et al., 1997; Lordier et al., 2008; Pampalona et al., 2012; Serres et al., 2012; De Storme and Geelen, 2013). Through forward genetic screens, several cytokinesis-defective mutants have been isolated. Comparing the phenotypic defects of three *gsl8* alleles to five different cytokinesis-defective mutants including *hinkel*, *scd1*, *knolle*, *keule* and *korrigan* showed that

dwarfism is shared among all the analyzed mutants. As was expected, all cytokinesis-defective mutants induce ectopic polyploidization in the root somatic cells similar to that observed for *gsl8* mutants. However; root tissue patterning and root-hair morphogenesis do not exhibit severe impairments as seen in *gsl8* (Fig. 3.14 and 3.15). For example, the *keule* mutant roots are stunted (Söllner et al., 2002; Thiele et al., 2009), but bloated cells and branched swollen root hairs, characteristic for *essp8*, could not be detected in *keule* seedlings. Additionally, none of the cytokinesis-defective mutants showed somatic embryo formation.

With the exception of *KORRIGAN*, the remaining cytokinesis-defective mutants analyzed in this study are required for vesicles transport and fusion, known as the first step of cell-plate formation (Samuels et al., 1995; Lukowitz et al., 1996; Waizenegger et al., 2000; Strompen et al., 2002). Callose deposition, however, mainly occurs during the second step of cell-plate formation where the cell wall is assembled within the network generated in the first step as a result of vesicle fusion (Thiele et al., 2009). Therefore, part of the phenotypic differences might be caused by the disparate timing of their involvement during cytokinesis completion. *KORRIGAN* encodes a membrane-bound endo-1,4-β-glucanase that plays a role during the second step (Sato et al., 2001). Surprisingly, in spite of their related functions during cytokinesis, *GSL8* and *KORRIGAN* mutants display different phenotypes. My findings suggest that *essp8*, similar to the other reported *GSL8* alleles (Chen et al., 2009; Thiele et al., 2009; De Storme et al., 2013), is a cytokinesis-defective mutant, as indicated by its lack of callose deposition at the cell plates and ectopic induction of multi-nucleated and endomitotic somatic cells. Nevertheless, *essp8* phenotypic defects and seedling lethality are likely to be caused only 'partially' by cytokinesis impairments.

It was previously proposed that GSL6 is a cell plate-specific callose synthase (see section 1.2.2). In tobacco BY-2 cells, GFP-GSL6 fusion proteins are localized to the cell plate when expressed under the control of the *CaMV35S* promoter (Hong et al., 2001a; Hong et al., 2001b). Interestingly, *gsl6* knockout lines do not show any phenotypic and/or cytokinesis defects (Dong et al., 2008; Chen et al., 2009). Therefore, considering the severity of cytokinesis defects as well as the observed lethality in different *gsl8* mutants,

tested in this study, it is tempting to propose that GSL8 is the callose synthase essential for depositing callose at the cell plate to complete cytokinesis.

4.3 Cell-to-cell communication is relaxed in *essp8* hypocotyls

Intercellular signaling is required for regulation of developmental programs in any multicellular organism. In plants, PD channels interconnect the cells and provide the path for movement of nutrients and regulatory molecules such as mobile transcription factors (Rinne and van der Schoot, 1998; Koizumi et al., 2011; Xu et al., 2011). Callose deposition at the neck of the PD plays a critical role in regulating cell-to-cell communication in plants (Vatén et al., 2011). Symplastic signaling is a dynamic process and is achieved through a balance between the activity of callose synthases and β-1,3-glucanases (Levy et al., 2007). However, it is still not clear how callose synthases regulate PD and what other molecular components are required for this regulation.

Expression analysis of *GSL8* indicated that *GSL8* is highly expressed in most organs during plant development with the maximum transcript level in the vasculature and actively dividing cells (Schmid et al., 2005; Chen et al., 2009). In the vasculature, callose is mostly deposited at the PD to regulate its SEL. Therefore, GSL8 was suggested to be associated with PD regulation. In agreement with the predicted role of GSL8 in PD regulation, a mutant allele of *GSL8*, called *chorus*, showed PD defects as indicated by an increase in passive diffusion of CFP and a trimeric GFP (3×GFP) molecules in leaf epidermis (Guseman et al., 2010). In agreement with Guseman at al. (2010), the histochemical assay to visualize the callose deposited at the PD showed that, in all *gsl8* mutants, almost no callose is accumulated at the PD in the elongation zone of the root, in the root hairs and vasculature tissue compared to the wild-type Col-0 (Fig. 3.13E-H). Furthermore, the cell-to-cell diffusion assay using fluorescent probes demonstrated that the *essp8* mutation results in an increase in symplastic movement in hypocotyls, likely due to lack of callose accumulation at the PD, which consequently boosts the passive diffusion (Fig. 3.18). Therefore, not only my finding is consistent with PD defects previously documented in *chorus* epidermal cells by Guseman et al. (2010), but also it indicates that PD defects in *gsl8* mutants occur in different somatic tissues. Hence, it can

be concluded that GSL8 is required for callose deposition at the PD and regulation of their size exclusion limit.

Two other members of the Arabidopsis GSL family, GSL7 and GSL12, were recently shown to be involved in callose biosynthesis at the PD (Barratt et al., 2011; Vatén et al., 2011; Xie et al., 2011). Compared to GSL12, GSL7 callose biosynthesis activity is more tissue-specific. *GSL7* is expressed in the vasculature system and is required only for callose deposition at the phloem PD and sieve plates. Vaten et al. (2011) suggested a role for GSL12 in PD regulation using an inducible expression system for *GSL12* gain-of-function mutants. Although, a *GSL12* gain-of-function mutant seedlings develop shorter roots compared to the WT, the defect is not as severe as those of *essp8* (Vatén et al., 2011; Yadav et al., 2014). The lethality of *essp8* single mutant rules out the possibility that GSL8 and GSL12 are functionally redundant during early seedling development and suggests that they are likely to be independently required for callose biosynthesis at the PD with GSL8 playing a more critical role.

4.3.1 GSL8 is required for highly-regulated trafficking of SHR

To gain a better understanding of the effect of *essp8* mutation on PD aperture and trafficking of various mobile factors, SHR (see section 1.5.2) was chosen as a candidate for NCATFs, and its symplastic movements in *essp8* roots was investigated. *SHR* is specifically expressed in the stele cells and the SHR protein moves from stele into the neighboring cells including the QC, the CEIs, the CEIDs and the endodermis (Nakajima et al., 2001). In the endodermis, SHR transcriptionally activates several target genes including *SCR*. Physical interaction of SHR and SCR suggests that a transcription activation complex might be formed by the two proteins (Nakajima et al., 2001; Levesque et al., 2006; Cui et al., 2007).

Vaten et al. (2011) suggested that SHR movement is likely to be PD-mediated as callose induction, in either the endodermis or the stele, could impair its trafficking (Vatén et al., 2011). Disruption of SHR movement in *essp8* root meristematic zone suggests dysregulation of SHR signaling pathway. This finding, for the first time, provides evidence that *essp8* mutation indeed alters the movement of SHR protein as its trafficking

increases by an extra cell layer. This increase could be detected as early as in five-day-old *essp8* roots. In *essp8*, SHR ectopically moves to the cortex, the neighboring cells to endodermis (Fig. 3.19B). In wild-type seedlings, SHR is localized into both nucleus and cytoplasm of stele cells, but only to the nucleus in the endodermis (Fig. 3.19A) where it activates *SCR* as a transcription factor (Cui et al., 2007). Contrary to the WT, in *essp8* seedlings, SHR was localized into both, nucleus and cytoplasm, in stele, endodermis and cortex cells (Fig. 3.19B). Previous studies have shown that restricted movement of SHR for only one cell layer and its nuclear localization in the endodermis are critical regulatory mechanisms for endodermis differentiation (Nakajima et al., 2001), and are evolutionarily conserved (Cui et al., 2007). Reduction of SHR nuclear localization and its movement outside of the endodermis induces cell divisions and an increase in the number of cell layers, where the cells ectopically exhibit endodermal characteristics (Cui et al., 2007; Welch et al., 2007; Miyashima and Nakajima, 2011).

SHR plays a substantial role during embryonic root development by regulating radial patterning of the Arabidopsis root (Nakajima et al., 2001). Transport of SHR from the stele into the endodermis acts as an initiator of cell communication network in the meristematic zone of the root. SHR is required for cell division and endodermis differentiation (Benfey et al., 1993; Helariutta et al., 2000). Highly-regulated movement of SHR and its well-defined subcellular localization are both crucial for ground tissue formation. Furthermore, it has been previously shown that SHR abundance changes dynamically during root development, and its dose regulates MC formation. An increase in SHR level prevents MC formation, whereas its abundance at intermediate level promotes MC formation (Koizumi et al., 2012). Additionally, overexpression of *SHR* using *CaMV35S* promoter induces disorganized cell divisions in the root meristem (Helariutta et al., 2000; Nakajima et al., 2001). Similarly, ectopic expression of *SCR* in the supernumerary cell layers leads to development of extra endodermal layers (Cui et al., 2007). Collectively dysregulation of SHR symplastic movement in *gsl8* mutants suggests that GSL8 is required for careful regulation of SHR trafficking via PD. Therefore, it is tempting to speculate that *essp8* root defects such as increased number of cell layers and cell identity changes are, at least partially, caused by impairment of SHR cell-to-cell movement caused by loss of GSL8 and disruption of PD aperture. These results suggest a

new role for GSL8 as a critical factor required for regulation of cell communication network during early seedling development in Arabidopsis.

4.3.2 Loss of GSL8 dysregulates symplastic movement of microR165/6

Transcription activation of three *MICRORNA165/6* genes, *MIR165A, MIR166A* and *MIR166B* is SHR-mediated in the QC, CEIs, CEIDs and endodermis (Carlsbecker et al., 2010; Miyashima et al., 2011). SHR directly binds to the 5' upstream regions of *MIR165A* and *MIR166B* to activate their transcription (Carlsbecker et al., 2010). After activation, the mature miR165/6 will move from endodermis to stele, and suppress the *HD-ZIP III* family genes, such as *PHB*, by targeting their transcripts (McConnell et al., 2001; Prigge et al., 2005; Hirakawa et al., 2011). Suppression of the *HD-ZIPIII* genes by miR165/6 plays important roles in establishing apical-basal polarity during embryogenesis, patterning of leaf primordia and shoot vascular organization (McConnell et al., 2001; Emery et al., 2003; Smith and Long, 2010). However, it is not yet clear whether miR165/6 acts as a non-cell-autonomous factor during the other developmental events, or if it is root-specific.

Similar to SHR, symplastic movement of miR165/6 has been shown to be PD-mediated (Vatén et al., 2011). The symplastic movement of mature miR165/6 was investigated in *essp8* roots to confirm whether PD defects and the increase in their SEL affect miR165/6 signaling. The analysis revealed that the movement of mature miR165/6 is impaired in *essp8* roots (Fig. 3.20). Even though the difference in miR165/6 activity between wild type and *essp8* in five-day-old seedling roots was minor, the ectopic activity of miR165/6 in the outer cell layers and root collumella cells increases markedly in ten-day-old roots as the root tissue patterning develops a more severe defect. This is the first report on the alteration of miR165/6 intercellular movement in *gsl8* mutants. This new finding suggests that GSL8 is required for regulation of miR165/6 PD-mediated trafficking.

The mRNAs of five *HD-ZIPIII* genes, including *PHABULOSA* (*PHB*), *PHAVOLUTA* (*PHV*), *REVOLUTA/INTERFASCICULAR FIBERLESS1* (*REV/IFL1*), *CORONA/ INCURVATA4* (*CNA/ICU4)* and *ATHB8,* are targeted by miR165/6 (Baima et al., 1995; Talbert et al., 1995; McConnell et al., 2001; Green et al., 2005; Prigge et al., 2005;

Ochando et al., 2006). Although single mutants for any of these five genes do not display distinguishable defects in their root tissue patterning, quadruple mutants for the *HD-ZIPIII* genes, as well as overexpression lines for miR165 develop excessive cell layers in their vasculature tissue (Carlsbecker et al., 2010). The dose of miR165/6 in the ground tissue precisely regulates the PHB distribution across the stele, known to be essential for xylem differentiation in vasculature tissue (Miyashima et al., 2011). Interestingly, miR165/6 and HD-ZIPIII have also been found to be involved in regulation of xylem secondary cell wall (SCW) formation (Du and Wang, 2015). Alternatively, miR165/6 seems to have a bidirectional movement pattern, moving both, to the inside and outside, of the endodermis (Carlsbecker et al., 2010). Therefore, miR165/6-mediated suppression of the *HD-ZIPIII* genes in the endodermis and stele is not only restricted to xylem cell specification, but also plays a broader role in cell layers differentiation in Arabidopsis roots (Miyashima et al., 2011). The defects in meristematic root tissue patterning in *essp8* mutants are similar to the phenotype of miR165/6 overexpression lines and quadruple mutants of *HD-ZIPIII* genes, particularly the extra cell layers observed in the root and vasculature tissue (Carlsbecker et al., 2010). Therefore, it can be suggested that ectopic miR165/6 activity in the outer cell layers in the root meristem might be, at least partially, responsible for the *essp8* root phenotype and loss of vasculature tissue in ten-day-old seedlings.

Significant decrease of miR165/6 levels in both *shr* and *scr* mutants have suggested that the SHR/SCR transcription complex is likely to regulate *MIR165/6* expression (Carlsbecker et al., 2010; Miyashima et al., 2011). Therefore, it still needs to be further investigated whether elevated miR165/6 activity in the outer cell layers in *essp8* is a direct result of an increase in its bidirectional PD-mediated symplastic movement from endodermis to stele, cortex, epidermis and collumella cells, or the ectopic presence of SHR in the outer cell layers up-regulates miR165/6, or it is caused by both.

4.4 PDLP5 function is likely to be GSL8-dependent

PDLP isoforms were first identified in the cell wall proteome of Arabidopsis (Table 1.1) (Thomas et al., 2008). PDLPs are small proteins with a predicted size of 30 to 35 kDa. They contain a very short tail at the C-terminus, two conserved Cys-rich repeats at the N-

terminus and a connecting transmembrane domain (TMD) (see section 1.4.1). Thomas et al. (2008) showed that all PDLPs localize to the cell periphery with punctate structures which represent PD. There are reports indicating that overexpression of PDLP1 and PDLP5 leads to the reduction in PD permeability and, therefore, improves plants' resistance against pathogens, and concomitant elevation of callose deposition at the PD (Lee et al., 2008; Thomas et al., 2008; Lee et al., 2011; Wang et al., 2013). It is still unknown how PDLPs induce callose deposition at the PD and control symplastic trafficking in response to both internal and external signals. Contrary to PDLPs positive regulation of callose deposition at the PD, Amari et al. (2010) found that PDLPs might act as endogenous factors required for virus infection and movement of the virus MP. It was found that in a *pdlp* triple mutant, the virus association with the PD and its MP movement is inhibited (Amari et al., 2010).

To investigate whether the *gsl8* phenotypic defects can be partially rescued by induction of callose deposition at the PD, *PDLP5* was overexpressed in a *gsl8* genetic background. Seedlings overexpressing *PDLP5* look slightly yellowish, and their adult plants show evident growth inhibition and chlorosis compared to the WT (Fig. 3.23A-B). This result is consistent with previous reports on the phenotype of *PDLP5* overexpression lines (Lee et al., 2011; Carella et al., 2015). Similar to the other members of the PDLP family (Thomas et al., 2008; Lee et al., 2011), the localization analysis in the root showed that PDLP5 is localized at the cell wall as punctate structures, correspond to PD, in the WT and *gsl8* five-day-old seedlings (Fig. 3.23D-E). Interestingly, serial z-section images revealed that in *essp8* seedlings overexpressing *PDLP5*, the punctate localization pattern is missing in some of the cells. Instead, PDLP5-GFP signal was detected in the cytoplasm (Fig. 3.23C).

Dysregulation of PD aperture in *gsl8* mutant seedlings was previously observed as it affects the symplastic movement of non-cell autonomous factors including SHR and miR165/6 (see sections 4.3.1 and 4.3.2). Mislocalization of PDLP5 to cytoplasm in five-day-old *gsl8* seedlings raised the question whether PDLP5 localization at the PD is GSL8-dependent, or this occurs only as an indirect effect of cell wall and PD defects in *gsl8* mutants.

Lee et al. (2011) showed that overexpression of *PDLP5* induces callose accumulation at the PD for up to fourfold higher than the wild type. They proposed that PDLP5 controls PD permeability through modulation of callose accumulation at the PD. In agreement with their finding, WT seedlings overexpressing *PDLP5* display an increase in callose deposited at the PD compared to the wild type. Furthermore, over accumulation of callose at the PD in *PDLP5-OE* lines indeed affects the SEL of PD and restricts passive diffusion through PD (Fig. 3.24). This finding supports the notion of Lee et al. (2011) that PDLP5 adjusts callose accumulation at the PD to control PD permeability.

In contrast to the *PDLP5-OE* data in wild type, surprisingly, overexpression of *PDLP5* in a *gsl8* mutant background did not alter callose accumulation at the PD compared to the *gsl8* loss-of-function mutants. Moreover, no significant difference could be detected in intercellular movement of fluorescein in the hypocotyls of *gsl8 PDLP5-OE* seedlings (Fig. 3.24). Taken together, these results explain why overexpression of *PDLP5* in *gsl8* background cannot rescue their phenotypic defects as persistent lack of callose at the PD in *gsl8 PDLP5-OE* lines does not lead to discernible restoration of the PD size exclusion limit. Therefore, it can be concluded that loss of GSL8 might negatively affect PDLP5 function and subcellular localization.

De Storme and Geelen (2014) proposed that negative regulation of PD by PDLPs might occur through their interaction with enzymes synthesizing callose such as GSLs; however, no evidence was provided to support this hypothesis. This study provides novel insight into a putative cross talk between GSL8 and PDLP5, and the significance of this cross talk in PD regulation. Based on PDLP5 mislocalization and absence of callose induction in *gsl8 PDLP5-OE* seedlings, it can be argued that PDLP5 is likely to require GSL8 for its localization at the PD and this might happen through their direct interaction. This assumption needs to be further confirmed by testing the possibility of PDLP5 and GSL8 physical interaction, and if truncation of GSL8, in case of *essp8*, affects this putative interaction (see sections 4.5.2 and 4.5.5).

4.5 GSL8 forms a complex to synthesize callose and regulate its deposition

Callose biosynthesis and its deposition need to be highly-regulated. Hence it has been proposed that GSLs, e.g. GSL8, are integrated into an extremely specialized protein complex, hypothetically named CalS complex, to carry out callose synthesis.

4.5.1 SUCROSE SYNTHASE 1, a provider of UDP-Glc to GSL8

Callose is synthesized from hundreds of glucose residues linked by β-1,3- glycosidic bridges (Piršelová and Matušíková, 2013). Thus, glucose molecules need to be provided to GSLs, where they are used by GSLs as precursors to synthesize β-1,3-glucan polymers. SuSy, known as a sugar metabolic enzyme involved in sucrose synthesis and degradation, can potentially act as the glucose provider for GSLs. It has been previously shown that in cellulose synthase complexes, SuSy is in charge of UDP-Glc delivery to the enzyme (Baroja-Fernández et al., 2012).

The FRET analysis (see section 3.7) revealed a physical interaction between GSL8 and SUS1 (Fig. 3.26). This result suggests that, similar to the case of the cellulose complex, SuSy is likely to be incorporated into the callose synthase complex to channel UDP-Glc into glucan synthesis. SUS1 is traditionally predicted to be localized into cytosol (Hooper et al., 2014). However, several studies have suggested that, depending on the metabolic environment, SUCROSE SYNTHASE can adjust its cellular localization, and interact with membranes, organelles and cytoskeletal actin (Winter and Huber, 2000; Etxeberria and Gonzalez, 2003; Subbaiah et al., 2006; Zheng et al., 2011). Several lines of evidence have highlighted posttranslational modification as an important regulatory mechanism for SUS1 association with membranes. For example, SUS1 phosphorylation at Ser-15 in *Zea mays* and Ser-11 in *Glycine max* enhances its association with the membrane (Komina et al., 2002; Hardin et al., 2004). Although the molecular mechanisms by which SUS1 can bind to the membranes are not yet known, based on this finding, it is plausible to conclude that SUS1 integration into CalS complex might occur at its membrane-associated status where it interacts with GSL8 to provide UDP-Glc monomers, required for callose biosynthesis.

4.5.2 A PD-localized β-1,3-glucanase and PDLP5 regulate PD through GSL8

AtBG_PPAP, a PD-localized enzyme degrading callose, is required for maintaining callose balance at the PD (Levy et al., 2007; Zavaliev et al., 2011). AtBG_PPAP is localized in the ER membrane and at the cell periphery where it is associated with PD (Zavaliev et al., 2013). As was previously predicted in the hypothetical interactome network for GSL8 (Fig. 3.25), results of the FRET experiment support interaction of GSL8 and AtBG_PPAP (Fig. 3.26). The physical interaction of GSL8 and PD-associated β-1,3-glucanase suggests that GSL8 is likely to be the PD-associated callose synthase required for retaining the equilibrium between callose synthesis and hydrolysis.

My results already showed that PDLP5 functionality and subcellular localization are disrupted in *essp8* mutant seedlings (Fig. 3.23). This finding led me to investigate whether PDLP5 and GSL8 physically interact. The FRET result proved the interaction of GSL8 and PDLP5 (Fig. 3.26). PDLPs have their N-terminal domain exposed to the apoplast and a very short cytoplasmic domain with unknown role. Therefore, it has been proposed that the extracellular domains are likely to act as the interacting domains (Thomas et al., 2008). The FRET analysis suggests that the cytoplasmic domain of PDLP5 might be the one involved in its interaction with GSL8. Furthermore, the identified interaction between GSL8 and PDLP5 supports an earlier proposal that the induction of callose deposition at the PD by PDLP5 might happen through its interaction with callose synthase enzymes (De Storme and Geelen, 2014). Here, I have demonstrated that GSL8 is, if not the only one, the callose synthase regulating callose deposition at the PD.

Cumulatively, the physical interaction of GSL8 with two PD-localized proteins, with roles in PD regulation, provides the first evidence for an earlier prediction by Töller et al. (2008) as GSL8 might have regulatory roles, apart from its enzymatic function. This study gives new insight into the role of GSL8 in PD regulation, the mechanisms underlying the regulation of PD aperture and/or their size exclusion limit, and how they are linked to callose biosynthesis.

4.5.3 SCD1, an interacting partner of GSL8

SCD1 is required for vesicular trafficking to the equator of the dividing cell (Falbel et al., 2003), where the vesicles are fused together to form a tubulovesicular network (Söllner et al., 2002). Callose deposition converts the network into a fenestrated plate (Samuels et al., 1995; Verma, 2001).

A recent study has shown that SCD proteins, including SCD1, are involved in different membrane trafficking events required not only for cytokinesis, but also for cell expansion (McMichael et al., 2013). It is already known that the secondary PD are formed post-cytokinesis, possibly during cell expansion. However, how this happens has remained unclear (Brunkard et al., 2013). The observed interaction between GSL8 and SCD1 provides new views on the role of GSL8, both in cytokinesis and PD regulation. Therefore, it raises new questions on whether this interaction is restricted to cell plate formation and is required for callose deposition at the cell plate, and/or it is somehow linked to secondary PD formation.

4.5.4 GSL8 and GSL10 interplay might be required for proper function of callose synthase complex

The effort to clone GSL10 cDNA was unfortunately not successful, thus the interaction of GSL10 and GSL8 could not be tested. Furthermore, although five different T-DNA insertion lines for *GSL10* were screened (Appendix I), no homozygous seedlings could be recovered, indicating that *gsl10* mutation causes gamethophytic lethality. Hence, the seedling phenotype of a conditional *gsl8 gsl10* knockdown remains as the only evidence for the hypothetical GSL8 and GSL10 interaction.

The similar phenotype of *gsl8 gsl10* double mutant to that of *gsl8* single mutant supports an earlier prediction made by Töller et al. (2008). They hypothesized that GSL8 and GSL10 might form a complex where both are required for the complex to be functional. The assumption that GSL8 and GSL10 form a complex, where the absence of one of them disrupts the complex function, was supported by *gsl8 gsl10* morphological phenotype. Two-week-old *gsl8 gsl10* seedlings' phenotypic defects are similar to *gsl8-1*

by having dwarf seedlings with short roots and abnormally-shaped true leaves (Fig. 3.28). To further confirm this assumption, the physical interaction of GSL8 and GSL10 should be tested in the future. Due to requirement of both GSL8 and GSL10 in early seedling development, efforts to generate *gsl8 gsl10* double mutants have not been successful. Hence, this study can be considered as the first report on GSL8 and GSL10 interplay in early seedling development in Arabidopsis.

4.5.5 GSL8 cytoplasmic loops are required for its interaction with the partners

GSL8 encodes a large integral membrane protein with sixteen predicated transmembrane helices and seventeen non-transmembrane loops. GSL8 comprises a large hydrophilic cytoplasmic loop in the middle (Käll et al., 2007). It has been previously suggested that the cytoplasmic loop is required for GSLs interaction with other regulatory proteins (Verma and Hong, 2001; De Storme and Geelen, 2014). The alignment of Arabidopsis GSLs' amino acid sequence revealed that the conserved regions mostly belong to the cytoplasmic loop (Fig. 3.12). In *essp8*, GSL8 is truncated at the fifth cytoplasmic loop. The findings demonstrated a loss of GSL8 interaction with SUS1, AtBG_PPAP, PDLP5 and SCD1 where an *essp8* version of *GSL8* cDNA was used for interaction analysis (Fig. 3.27). These data support the assumption that GSL8 cytoplasmic loop is required for its interaction with the identified partners and, possibly, its regulatory role(s). Taken together, it is predicted that truncation of GSL8 in *essp8* disrupts the CalS complex at the PD and, therefore, PD regulation (Fig. 4.1).

It has been predicted that the cytoplasmic loop should contain a UDP-Glc catalytic site and a glucosyltransferase domain (Verma and Hong, 2001). Furthermore, GSLs show a high substrate specificity for UDP-Glc (Brownfield et al., 2009; Zavaliev et al., 2011). Although FRET results confirm that SUS1 may provide the UDP-Glc substrate to GSL8, no UDP-Glc binding site has been identified on the cytoplasmic loop of GSL8 yet. Therefore, further investigation should be performed to identify the specific domain(s) required for GSL8 interaction with regulatory proteins including AtBG_PPAP and PDLP5.

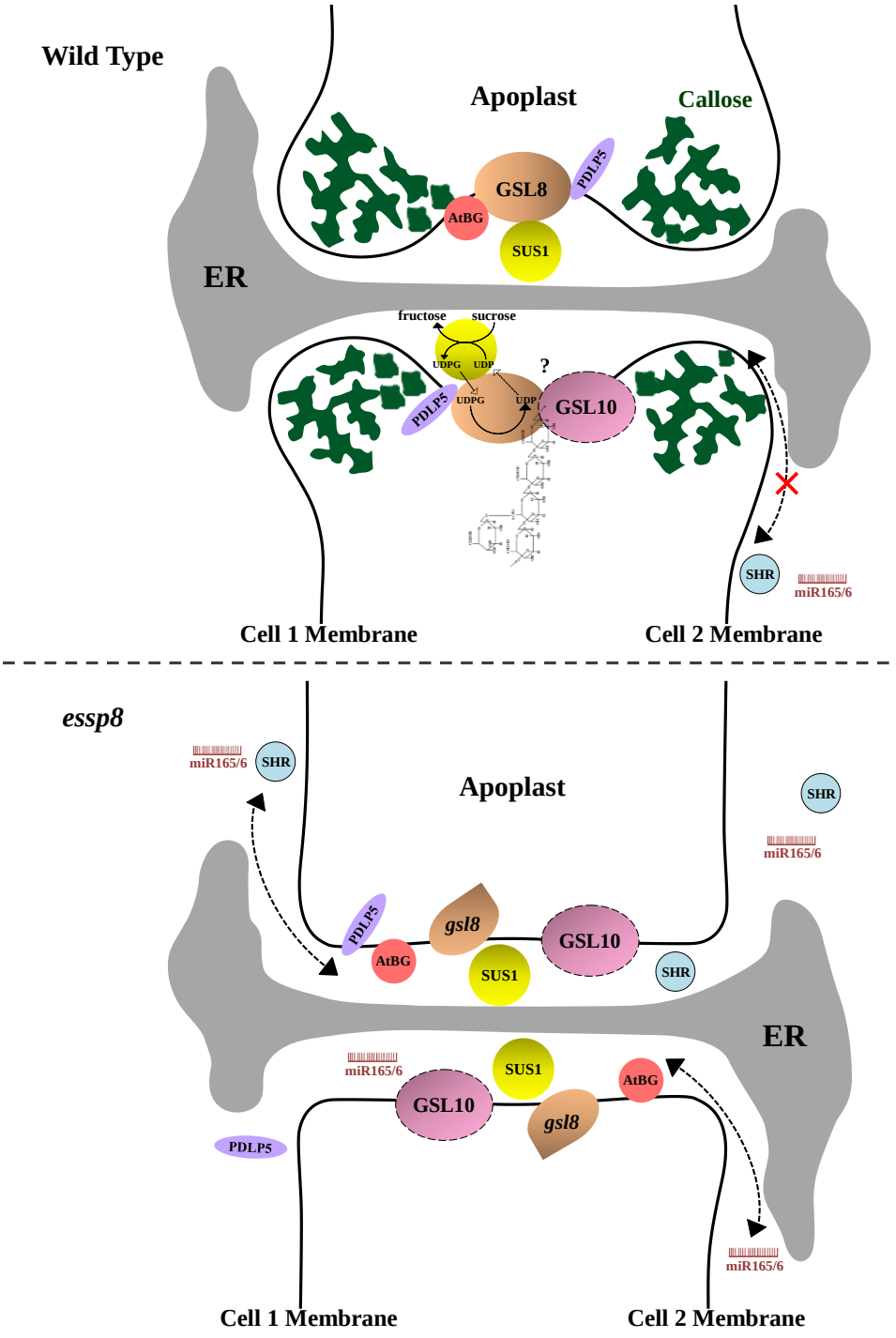

Figure 4.1 A proposed model for GSL8 role in PD regulation.

In wild-type plants, GSL8 negatively regulates PD SEL by forming a CalS complex and induction of callose deposition. Symplastic movement of mobile factors is blocked in the WT. Truncation of GSL8 in *essp8* mutant results in lack of a functional CalS complex at the PD and callose deposition. Absence of callose at the PD in *essp8* induces ectopic movement of mobile factors to adjacent cell layers and dysregulation of intercellular signaling.

PERSPECTIVES

The work presented in this thesis provides novel insight into the role of GLUCAN SYNTHASE-LIKE 8 during early seedling development in Arabidopsis. These new findings raise more questions for future investigation using the materials generated in this study.

Regarding the critical role of GSL8 in cytokinesis and cell plate formation, it remains to be further studied if GSL8 is solely required for callose biosynthesis at the cell plate.

Despite a clear role of callose accumulation in PD regulation, the molecular mechanism(s) underlying this regulation and how the identified players are linked to callose homeostasis have remained elusive. Identifying other interacting partners of GSL8, putative components of the callose synthase complex, would further extend our knowledge of this regulatory network. Additionally, the interaction of currently identified interactors should be reconfirmed using another protein-protein interaction method, e.g. membrane yeast two-hybrid (MYTH) system.

Vaten et al. (2011) previously reported the association of GSL12 with PD and its role in PD regulation. Therefore, it needs to be further investigated how GSL8 and GSL12 contribute to the PD regulation, and if there is any functional overlap. Additionally, the assumption of GSL8-GSL10 heterodimeric complex can be further studied by testing their subcellular localizations to find out whether they are similarly-localized.

No experimental evidence is available regarding GSL8 localization. Therefore, studying the subcellular localization of GSL8, as well as the other members of the GSL family in Arabidopsis, would provide a better understanding of their tissue-specific and subcellular localization/distribution, and elucidate if GSL8 and GSL12 are the only important regulators of plasmodesmata within the GSL family. The ability to characterize the specific roles of GSL8 and GSL12 at the PD, and understand whether they are independently required for PD regulation will also be important in this context. Furthermore, it is worth exploring the possibility of PD-associated GSLs being incorporated into one complex.

The observation that AtBG_PPAP and PDLP5 interact with GSL8, and the likelihood of GSL8 requirement for PDLP5 localization opens up the questions: which specific domain(s) in GSL8 are required for this interaction, if the interactions are only specific to GSL8 and/or other PD-associated GSLs, and whether AtBG_PPAP and PDLP5 are also components of the hypothetical PD-regulating complex?

To provide further evidence for the observed impairment of SHR and miR165/6 movement in *essp8* mutant, a quantification of their target transcripts, *SCR* and *HD-ZIP III* genes, respectively, should be informative. These experiments would address the question of whether ectopic localization of these non-cell autonomous factors indeed affects the expression of their downstream targets. Finally, genome-wide expression analysis can be used to find out the global effect of *gsl8* mutation on gene expression.

Many additional experiments could be listed here. The overall challenge, however, will be to gain sufficient resolution on PD cell-to-cell communication, and how it is tightly regulated in response to both internal and external cues. There is still a lot more to learn in order for us to draw a detailed picture of PD and understand the precise mechanism(s) through which GSL8 contributes to PD regulation and selective transport properties.

BIBLIOGRAPGHY

Altmann, T., Schmidt, R., and Willmitzer, L. (1992). Establishment of a gene tagging system in Arabidopsis thaliana based on the maize transposable element Ac. Theoretical and Applied Genetics **84,** 371-383.

Amari, K., Boutant, E., Hofmann, C., Schmitt-Keichinger, C., Fernandez-Calvino, L., Didier, P., Lerich, A., Mutterer, J., Thomas, C.L., and Heinlein, M. (2010). A family of plasmodesmal proteins with receptor-like properties for plant viral movement proteins. PLoS Pathogens **6,** e1001119.

Amor, Y., Haigler, C.H., Johnson, S., Wainscott, M., and Delmer, D.P. (1995). A membrane-associated form of sucrose synthase and its potential role in synthesis of cellulose and callose in plants. Proceedings of the National Academy of Sciences **92,** 9353-9357.

Andrawis, A., Solomon, M., and Delmer, D.P. (1993). Cotton fiber annexins: a potential role in the regulation of callose synthase. The Plant Journal **3,** 763-772.

Aspinall, G.O., and Kessler, G. (1957). The structure of callose from the grape vine. Chemistry & Industry**,** 1296-1296.

Assaad, F.F. (2001). Plant cytokinesis. Exploring the links. Plant Physiology **126,** 509-516.

Austin, R.S., Vidaurre, D., Stamatiou, G., Breit, R., Provart, N.J., Bonetta, D., Zhang, J., Fung, P., Gong, Y., and Wang, P.W. (2011). Next-generation mapping of Arabidopsis genes. The Plant Journal **67,** 715-725.

Bachman, E.S., and McClay, D.R. (1996). Molecular cloning of the first metazoan beta-1,3 glucanase from eggs of the sea urchin *Strongylocentrotus purpuratus*. Proceedings of the National Academy of Sciences **93,** 6808-6813.

Baima, S., Nobili, F., Sessa, G., Lucchetti, S., Ruberti, I., and Morelli, G. (1995). The expression of the *Athb-8* homeobox gene is restricted to provascular cells in *Arabidopsis thaliana*. Development **121,** 4171-4182.

Baroja-Fernández, E., Muñoz, F.J., Li, J., Bahaji, A., Almagro, G., Montero, M., Etxeberria, E., Hidalgo, M., Sesma, M.T., and Pozueta-Romero, J. (2012). Sucrose synthase activity in the *sus1/sus2/sus3/sus4* Arabidopsis mutant is sufficient to support normal cellulose and starch production. Proceedings of the National Academy of Sciences **109,** 321-326.

Barratt, D.P., Kölling, K., Graf, A., Pike, M., Calder, G., Findlay, K., Zeeman, S.C., and Smith, A.M. (2011). Callose synthase GSL7 is necessary for normal phloem transport and inflorescence growth in Arabidopsis. Plant Physiology **155,** 328-341.

Beauvais, A., Bruneau, J., Mol, P., Buitrago, M., Legrand, R., and Latge, J. (2001). Glucan synthase complex of *Aspergillus fumigatus*. Journal of Bacteriology **183,** 2273-2279.

Becker, J.D., Boavida, L.C., Carneiro, J., Haury, M., and Feijó, J.A. (2003). Transcriptional profiling of Arabidopsis tissues reveals the unique characteristics of the pollen transcriptome. Plant Physiology **133,** 713-725.

Benfey, P.N., Linstead, P.J., Roberts, K., Schiefelbein, J.W., Hauser, M.-T., and Aeschbacher, R.A. (1993). Root development in Arabidopsis: four mutants with dramatically altered root morphogenesis. Development **119,** 57-70.

Benitez-Alfonso, Y., Faulkner, C., Pendle, A., Miyashima, S., Helariutta, Y., and Maule, A. (2013). Symplastic intercellular connectivity regulates lateral root patterning. Developmental Cell **26,** 136-147.

Benitez-Alfonso, Y., Cilia, M., San Roman, A., Thomas, C., Maule, A., Hearn, S., and Jackson, D. (2009). Control of Arabidopsis meristem development by thioredoxin-dependent regulation of intercellular transport. Proceedings of the National Academy of Sciences **106,** 3615-3620.

Bernard, M., and Latgé, J.-P. (2001). *Aspergillus fumigatus* cell wall: composition and biosynthesis. Medical Mycology **39,** 9-17.

Bertani, G. (1951). Studies on lysogenesis I.: The mode of phage liberation by lysogenic *Escherichia coli*. Journal of Bacteriology **62,** 293.

Bouyer, D., Geier, F., Kragler, F., Schnittger, A., Pesch, M., Wester, K., Balkunde, R., Timmer, J., Fleck, C., and Hülskamp, M. (2008). Two-dimensional patterning by a trapping/depletion mechanism: the role of TTG1 and GL3 in Arabidopsis trichome formation. PLoS Biology **6,** e141.

Bowles, D.J. (1990). Defense-related proteins in higher plants. Annual Review of Biochemistry **59,** 873-907.

Bowman, S.M., and Free, S.J. (2006). The structure and synthesis of the fungal cell wall. Bioessays **28,** 799-808.

Brand, U., Grünewald, M., Hobe, M., and Simon, R. (2002). Regulation of *CLV3* expression by two homeobox genes in Arabidopsis. Plant Physiology **129,** 565-575.

Bratzel, F., López-Torrejón, G., Koch, M., Del Pozo, J.C., and Calonje, M. (2010). Keeping cell identity in Arabidopsis requires PRC1 RING-finger homologs that catalyze H2A monoubiquitination. Current Biology **20,** 1853-1859.

Brecknock, S., Dibbayawan, T.P., Vesk, M., Vesk, P.A., Faulkner, C., Barton, D.A., and Overall, R.L. (2011). High resolution scanning electron microscopy of plasmodesmata. Planta **234,** 749-758.

Brownfield, L., Doblin, M., Fincher, G.B., and Bacic, A. (2009). Biochemical and molecular properties of biosynthetic enzymes for (1,3)-beta-glucans in embyrophytes, chlorophytes and rhodophytes. Chemistry, Biochemistry and Biology of (1,3)-beta-glucans and Related Polysaccharides**,** 283-326.

Brownfield, L., Wilson, S., Newbigin, E., Bacic, A., and Read, S. (2008). Molecular control of the glucan synthase-like protein NaGSL1 and callose synthesis during growth of *Nicotiana alata* pollen tubes. Journal of Biochemistry **414,** 43-52.

Brownfield, L., Ford, K., Doblin, M.S., Newbigin, E., Read, S., and Bacic, A. (2007). Proteomic and biochemical evidence links the callose synthase in *Nicotiana alata* pollen tubes to the product of the NaGSL1 gene. The Plant Journal **52,** 147-156.

Brunkard, J.O., Runkel, A.M., and Zambryski, P.C. (2013). Plasmodesmata dynamics are coordinated by intracellular signaling pathways. Current Opinion in Plant Biology **16,** 614-620.

Bryan, W.H., and Newcomb, K. (1954). Stimulation of pectin methylesterase activity of cultured tobacco pith by indole acetic acid. Physiologia Plantarum **7,** 290-297.

Burch-Smith, T.M., and Zambryski, P.C. (2012). Plasmodesmata paradigm shift: regulation from without versus within. Annual Review of Plant Biology **63,** 239-260.

Burch-Smith, T.M., Cui, Y., and Zambryski, P.C. (2012). Reduced levels of class 1 reversibly glycosylated polypeptide increase intercellular transport via plasmodesmata. Plant Signaling & Behavior **7,** 62-67.

Burch-Smith, T.M., Stonebloom, S., Xu, M., and Zambryski, P.C. (2011). Plasmodesmata during development: re-examination of the importance of primary, secondary, and branched plasmodesmata structure versus function. Protoplasma **248,** 61-74.

Burton, R.A., Gidley, M.J., and Fincher, G.B. (2010). Heterogeneity in the chemistry, structure and function of plant cell walls. Nature Chemical Biology **6,** 724-732.

Calonge, T.M., Arellano, M., Coll, P.M., and Perez, P. (2003). Rga5p is a specific Rho1p GTPase-activating protein that regulates cell integrity in *Schizosaccharomyces pombe*. Molecular Microbiology **47,** 507-518.

Caño-Delgado, A.I., Metzlaff, K., and Bevan, M.W. (2000). The *eli1* mutation reveals a link between cell expansion and secondary cell wall formation in *Arabidopsis thaliana*. Development **127,** 3395-3405.

Carella, P., Isaacs, M., and Cameron, R. (2015). Plasmodesmata-located protein overexpression negatively impacts the manifestation of systemic acquired resistance and the long-distance movement of Defective in Induced Resistance 1 in Arabidopsis. Plant Biology **17,** 395-401.

Carlsbecker, A., Lee, J.-Y., Roberts, C.J., Dettmer, J., Lehesranta, S., Zhou, J., Lindgren, O., Moreno-Risueno, M.A., Vatén, A., and Thitamadee, S. (2010). Cell signalling by microRNA165/6 directs gene dose-dependent root cell fate. Nature **465,** 316-321.

Castedo, M., Perfettini, J.-L., Roumier, T., Andreau, K., Medema, R., and Kroemer, G. (2004). Cell death by mitotic catastrophe: a molecular definition. Oncogene **23,** 2825-2837.

Castrillon, D.H., and Wasserman, S.A. (1994). Diaphanous is required for cytokinesis in Drosophila and shares domains of similarity with the products of the limb deformity gene. Development **120,** 3367-3377.

Chen, X.-Y., and Kim, J.-Y. (2009). Callose synthesis in higher plants. Plant Signaling & Behavior **4,** 489-492.

Chen, X.-Y., Liu, L., Lee, E., Han, X., Rim, Y., Chu, H., Kim, S.-W., Sack, F., and Kim, J.-Y. (2009). The Arabidopsis callose synthase gene *GSL8* is required for cytokinesis and cell patterning. Plant Physiology **150,** 105-113.

Chitwood, D.H., Nogueira, F.T., Howell, M.D., Montgomery, T.A., Carrington, J.C., and Timmermans, M.C. (2009). Pattern formation via small RNA mobility. Genes & Development **23,** 549-554.

Corbesier, L., Vincent, C., Jang, S., Fornara, F., Fan, Q., Searle, I., Giakountis, A., Farrona, S., Gissot, L., and Turnbull, C. (2007). FT protein movement contributes to long-distance signaling in floral induction of Arabidopsis. Science **316,** 1030-1033.

Crawford, K.M., and Zambryski, P.C. (2000). Subcellular localization determines the availability of non-targeted proteins to plasmodesmatal transport. Current Biology **10,** 1032-1040.

Cui, H., Levesque, M.P., Vernoux, T., Jung, J.W., Paquette, A.J., Gallagher, K.L., Wang, J.Y., Blilou, I., Scheres, B., and Benfey, P.N. (2007). An evolutionarily conserved mechanism delimiting SHR movement defines a single layer of endodermis in plants. Science **316,** 421-425.

Cui, X., Shin, H., Song, C., Laosinchai, W., Amano, Y., and Brown, M.R. (2001). A putative plant homolog of the yeast β-1,3-glucan synthase subunit FKS1 from cotton (*Gossypium hirsutum* L.) fibers. Planta **213,** 223-230.

Curtis, M.D., and Grossniklaus, U. (2003). A gateway cloning vector set for high-throughput functional analysis of genes *in planta*. Plant Physiology **133,** 462-469.

Czechowski, T., Stitt, M., Altmann, T., Udvardi, M.K., and Scheible, W.-R. (2005). Genome-wide identification and testing of superior reference genes for transcript normalization in Arabidopsis. Plant Physiology **139,** 5-17.

D'Amato, F. (1984). Role of Polyploidy in Reproductive Organs and Tissues. In Embryology of Angiosperms (Springer Berlin Heidelberg), pp. 519-566.

Daum, G., Medzihradszky, A., Suzaki, T., and Lohmann, J.U. (2014). A mechanistic framework for noncell autonomous stem cell induction in Arabidopsis. Proceedings of the National Academy of Sciences **111,** 14619-14624.

De Muyt, A., Pereira, L., Vezon, D., Chelysheva, L., Gendrot, G., Chambon, A., Lainé-Choinard, S., Pelletier, G., Mercier, R., and Nogué, F. (2009). A high throughput genetic screen identifies new early meiotic recombination functions in *Arabidopsis thaliana*. PLoS Genetics **5,** e1000654.

De Storme, N., and Geelen, D. (2013). Pre-meiotic endomitosis in the cytokinesis-defective tomato mutant *pmcd1* generates tetraploid meiocytes and diploid gametes. Journal of Experimental Botany **64,** 2345-2358.

De Storme, N., and Geelen, D. (2014). Callose homeostasis at plasmodesmata: molecular regulators and developmental relevance. Frontiers in Plant Science **5,** 1-23.

De Storme, N., Copenhaver, G.P., and Geelen, D. (2012). Production of diploid male gametes in Arabidopsis by cold-induced destabilization of postmeiotic radial microtubule arrays. Plant Physiology **160,** 1808-1826.

De Storme, N., De Schrijver, J., Van Criekinge, W., Wewer, V., Dörmann, P., and Geelen, D. (2013). GLUCAN SYNTHASE-LIKE8 and STEROL METHYLTRANSFERASE2 are required for ploidy consistency of the sexual reproduction system in Arabidopsis. The Plant Cell **25,** 387-403.

Dhugga, K.S. (2012). Biosynthesis of non-cellulosic polysaccharides of plant cell walls. Phytochemistry **74,** 8-19.

Di Laurenzio, L., Wysocka-Diller, J., Malamy, J.E., Pysh, L., Helariutta, Y., Freshour, G., Hahn, M.G., Feldmann, K.A., and Benfey, P.N. (1996). The *SCARECROW* gene regulates an asymmetric cell division that is essential for generating the radial organization of the Arabidopsis root. Cell **86,** 423-433.

Digiuni, S., Schellmann, S., Geier, F., Greese, B., Pesch, M., Wester, K., Dartan, B., Mach, V., Srinivas, B.P., and Timmer, J. (2008). A competitive complex formation mechanism underlies trichome patterning on Arabidopsis leaves. Molecular Systems Biology **4,** 1-11.

Doblin, M.S., De Melis, L., Newbigin, E., Bacic, A., and Read, S.M. (2001). Pollen tubes of *Nicotiana alata* express two genes from different β-glucan synthase families. Plant Physiology **125,** 2040-2052.

Doelling, J.H., Yan, N., Kurepa, J., Walker, J., and Vierstra, R.D. (2001). The ubiquitin-specific protease UBP14 is essential for early embryo development in *Arabidopsis thaliana*. The Plant Journal **27,** 393-405.

Dolan, L., Janmaat, K., Willemsen, V., Linstead, P., Poethig, S., Roberts, K., and Scheres, B. (1993). Cellular organisation of the *Arabidopsis thaliana* root. Development **119,** 71-84.

Dong, X., Hong, Z., Sivaramakrishnan, M., Mahfouz, M., and Verma, D.P.S. (2005). Callose synthase (CALS5) is required for exine formation during microgametogenesis and for pollen viability in Arabidopsis. The Plant Journal **42,** 315-328.

Dong, X., Hong, Z., Chatterjee, J., Kim, S., and Verma, D.P.S. (2008). Expression of callose synthase genes and its connection with *Npr1* signaling pathway during pathogen infection. Planta **229,** 87-98.

Douglas, C. (2001). Fungal β (1,3)-D-glucan synthesis. Medical Mycology **39,** 55-66.

Douglas, C.M., Foor, F., Marrinan, J.A., Morin, N., Nielsen, J.B., Dahl, A.M., Mazur, P., Baginsky, W., Li, W., and El-Sherbeini, M. (1994). The *Saccharomyces cerevisiae FKS1* (*ETG1*) gene encodes an integral membrane protein which is a subunit of 1,3-beta-D-glucan synthase. Proceedings of the National Academy of Sciences **91,** 12907-12911.

Du, Q., and Wang, H. (2015). The role of HD-ZIP III transcription factors and miR165/166 in vascular development and secondary cell wall formation. Plant Signaling & Behavior**,** e1078955.

Dunoyer, P., Himber, C., and Voinnet, O. (2005). DICER-LIKE 4 is required for RNA interference and produces the 21-nucleotide small interfering RNA component of the plant cell-to-cell silencing signal. Nature Genetics **37,** 1356-1360.

Dunoyer, P., Himber, C., Ruiz-Ferrer, V., Alioua, A., and Voinnet, O. (2007). Intra- and intercellular RNA interference in *Arabidopsis thaliana* requires components of the microRNA and heterochromatic silencing pathways. Nature Genetics **39,** 848-856.

Earley, K.W., Haag, J.R., Pontes, O., Opper, K., Juehne, T., Song, K., and Pikaard, C.S. (2006). Gateway-compatible vectors for plant functional genomics and proteomics. The Plant Journal **45,** 616-629.

Edgar, B.A., and Orr-Weaver, T.L. (2001). Endoreplication cell cycles: more for less. Cell **105,** 297-306.

Ellinger, D., Naumann, M., Falter, C., Zwikowics, C., Jamrow, T., Manisseri, C., Somerville, S.C., and Voigt, C.A. (2013). Elevated early callose deposition results in complete penetration resistance to powdery mildew in Arabidopsis. Plant Physiology **161,** 1433-1444.

Ellinger, D., Glöckner, A., Koch, J., Naumann, M., Stürtz, V., Schütt, K., Manisseri, C., Somerville, S.C., and Voigt, C.A. (2014). Interaction of the Arabidopsis GTPase RabA4c with its effector PMR4 results in complete penetration resistance to powdery mildew. The Plant Cell **26,** 3185-3200.

Elortza, F., Nühse, T.S., Foster, L.J., Stensballe, A., Peck, S.C., and Jensen, O.N. (2003). Proteomic analysis of glycosylphosphatidylinositol-anchored membrane proteins. Molecular & Cellular Proteomics **2,** 1261-1270.

Emery, J.F., Floyd, S.K., Alvarez, J., Eshed, Y., Hawker, N.P., Izhaki, A., Baum, S.F., and Bowman, J.L. (2003). Radial patterning of Arabidopsis shoots by class III HD-ZIP and KANADI genes. Current Biology **13,** 1768-1774.

Enns, L.C., Kanaoka, M.M., Torii, K.U., Comai, L., Okada, K., and Cleland, R.E. (2005). Two callose synthases, GSL1 and GSL5, play an essential and redundant role in plant and pollen development and in fertility. Plant Molecular Biology **58,** 333-349.

Etxeberria, E., and Gonzalez, P. (2003). Evidence for a tonoplast-associated form of sucrose synthase and its potential involvement in sucrose mobilization from the vacuole. Journal of Experimental Botany **54,** 1407-1414.

Falbel, T.G., Koch, L.M., Nadeau, J.A., Segui-Simarro, J.M., Sack, F.D., and Bednarek, S.Y. (2003). SCD1 is required for cell cytokinesis and polarized cell expansion in *Arabidopsis thaliana*. Development **130,** 4011-4024.

Faulkner, C. (2013). Receptor-mediated signaling at plasmodesmata. Frontiers in Plant Science **4,** 1-6.

Faulkner, C., Akman, O.E., Bell, K., Jeffree, C., and Oparka, K. (2008). Peeking into pit fields: a multiple twinning model of secondary plasmodesmata formation in tobacco. The Plant Cell **20,** 1504-1518.

Faulkner, C., Petutschnig, E., Benitez-Alfonso, Y., Beck, M., Robatzek, S., Lipka, V., and Maule, A.J. (2013). LYM2-dependent chitin perception limits molecular flux via plasmodesmata. Proceedings of the National Academy of Sciences **110,** 9166-9170.

Fernandez-Calvino, L., Faulkner, C., Walshaw, J., Saalbach, G., Bayer, E., Benitez-Alfonso, Y., and Maule, A. (2011). Arabidopsis plasmodesmal proteome. PLoS One **6,** e18880.

Fitzgibbon, J., Beck, M., Zhou, J., Faulkner, C., Robatzek, S., and Oparka, K. (2013). A developmental framework for complex plasmodesmata formation revealed by large-scale imaging of the Arabidopsis leaf epidermis. The Plant Cell **25,** 57-70.

Fletcher, J.C., Brand, U., Running, M.P., Simon, R., and Meyerowitz, E.M. (1999). Signaling of cell fate decisions by CLAVATA3 in Arabidopsis shoot meristems. Science **283,** 1911-1914.

Fontaine, T., Simenel, C., Dubreucq, G., Adam, O., Delepierre, M., Lemoine, J., Vorgias, C.E., Diaquin, M., and Latgé, J.-P. (2000). Molecular organization of the alkali-insoluble fraction of *Aspergillus fumigatus* cell wall. Journal of Biological Chemistry **275,** 27594-27607.

Franceschini, A., Szklarczyk, D., Frankild, S., Kuhn, M., Simonovic, M., Roth, A., Lin, J., Minguez, P., Bork, P., and von Mering, C. (2013). STRING v9. 1: protein-protein interaction networks, with increased coverage and integration. Nucleic Acids Research **41,** D808-D815.

Gallagher, K.L., and Benfey, P.N. (2009). Both the conserved GRAS domain and nuclear localization are required for SHORT-ROOT movement. The Plant Journal **57,** 785-797.

Gallagher, K.L., Paquette, A.J., Nakajima, K., and Benfey, P.N. (2004). Mechanisms regulating SHORT-ROOT intercellular movement. Current Biology **14,** 1847-1851.

Gapper, C., and Dolan, L. (2006). Control of plant development by reactive oxygen species. Plant Physiology **141,** 341-345.

Gardiner, J.C., Taylor, N.G., and Turner, S.R. (2003). Control of cellulose synthase complex localization in developing xylem. The Plant Cell **15,** 1740-1748.

Gaudioso-Pedraza, R., and Benitez-Alfonso, Y. (2014). A phylogenetic approach to study the origin and evolution of plasmodesmata-localized glycosyl hydrolases family 17. Frontiers in Plant Science **5,** 1-14.

Green, K.A., Prigge, M.J., Katzman, R.B., and Clark, S.E. (2005). CORONA, a member of the class III homeodomain leucine zipper gene family in Arabidopsis, regulates stem cell specification and organogenesis. The Plant Cell **17,** 691-704.

Grün, C.H., Hochstenbach, F., Humbel, B.M., Verkleij, A.J., Sietsma, J.H., Klis, F.M., Kamerling, J.P., and Vliegenthart, J.F. (2005). The structure of cell wall α-glucan from fission yeast. Glycobiology **15,** 245-257.

Guseman, J.M., Lee, J.S., Bogenschutz, N.L., Peterson, K.M., Virata, R.E., Xie, B., Kanaoka, M.M., Hong, Z., and Torii, K.U. (2010). Dysregulation of cell-to-cell

connectivity and stomatal patterning by loss-of-function mutation in Arabidopsis *CHORUS* (*GLUCAN SYNTHASE-LIKE 8*). Development **137,** 1731-1741.

Hake, S., and Freeling, M. (1986). Analysis of genetic mosaics shows that the extra epidermal cell divisions in *knotted* mutant maize plants are induced by adjacent mesophyll cells. Nature **320,** 621-623.

Han, X., Kumar, D., Chen, H., Wu, S., and Kim, J.-Y. (2014a). Transcription factor-mediated cell-to-cell signalling in plants. Journal of Experimental Botany **65,** 1737-1749.

Han, X., Hyun, T.K., Zhang, M., Kumar, R., Koh, E.-j., Kang, B.-H., Lucas, W.J., and Kim, J.-Y. (2014b). Auxin-callose-mediated plasmodesmal gating is essential for tropic auxin gradient formation and signaling. Developmental Cell **28,** 132-146.

Hardin, S.C., Winter, H., and Huber, S.C. (2004). Phosphorylation of the amino terminus of maize Sucrose Synthase in relation to membrane association and enzyme activity. Plant Physiology **134,** 1427-1438.

Hartley, J.L., Temple, G.F., and Brasch, M.A. (2000). DNA cloning using *in vitro* site-specific recombination. Genome Research **10,** 1788-1795.

Hatzfeld, J., and Buttin, G. (1975). Temperature-sensitive cell cycle mutants: a Chinese hamster cell line with a reversible block in cytokinesis. Cell **5,** 123-129.

Hayashi, T., Read, S., Bussell, J., Thelen, M., Lin, F.-C., Brown, R., and Delmer, D. (1987). UDP-glucose: (1→3)-β-glucan synthases from mung bean and cotton: Differential effects of Ca^{2+} and Mg^{2+} on enzyme properties and on macromolecular structure of the glucan product. Plant Physiology **83,** 1054-1062.

Heinlein, M. (2015). Plant virus replication and movement. Virology **479,** 657-671.

Helariutta, Y., Fukaki, H., Wysocka-Diller, J., Nakajima, K., Jung, J., Sena, G., Hauser, M.-T., and Benfey, P.N. (2000). The *SHORT-ROOT* gene controls radial patterning of the Arabidopsis root through radial signaling. Cell **101,** 555-567.

Hirai, M.Y., Fujiwara, T., Goto, K., Komeda, Y., Chino, M., and Naito, S. (1994). Differential regulation of soybean seed storage protein gene promoter-GUS fusions by exogenously applied methionine in transgenic *Arabidopsis thaliana*. Plant & Cell Physiology **35,** 927-934.

Hirakawa, Y., Kondo, Y., and Fukuda, H. (2011). Establishment and maintenance of vascular cell communities through local signaling. Current Opinion in Plant Biology **14,** 17-23.

Hong, Z., Delauney, A.J., and Verma, D.P.S. (2001a). A cell plate–specific callose synthase and its interaction with phragmoplastin. The Plant Cell **13,** 755-768.

Hong, Z., Zhang, Z., Olson, J.M., and Verma, D.P.S. (2001b). A novel UDP-glucose transferase is part of the callose synthase complex and interacts with phragmoplastin at the forming cell plate. The Plant Cell **13,** 769-779.

Hooper, C.M., Tanz, S.K., Castleden, I.R., Vacher, M.A., Small, I.D., and Millar, A.H. (2014). SUBAcon: a consensus algorithm for unifying the subcellular localization data of the Arabidopsis proteome. Bioinformatics **30,** 3356-3364.

Huang, L., Chen, X.-Y., Rim, Y., Han, X., Cho, W.K., Kim, S.-W., and Kim, J.-Y. (2009). Arabidopsis glucan synthase-like 10 functions in male gametogenesis. Journal of Plant Physiology **166,** 344-352.

Ishihara, S., Hirata, A., Nogami, S., Beauvais, A., Latge, J.-P., and Ohya, Y. (2007). Homologous subunits of 1,3-beta-glucan synthase are important for spore wall assembly in *Saccharomyces cerevisiae*. Eukaryotic Cell **6,** 143-156.

Jach, G., Görnhardt, B., Mundy, J., Logemann, J., Pinsdorf, E., Leah, R., Schell, J., and Maas, C. (1995). Enhanced quantitative resistance against fungal disease by combinatorial expression of different barley antifungal proteins in transgenic tobacco. The Plant Journal **8,** 97-109.

Jacobs, A.K., Lipka, V., Burton, R.A., Panstruga, R., Strizhov, N., Schulze-Lefert, P., and Fincher, G.B. (2003). An Arabidopsis callose synthase, GSL5, is required for wound and papillary callose formation. The Plant Cell **15,** 2503-2513.

Jares-Erijman, E.A., and Jovin, T.M. (2006). Imaging molecular interactions in living cells by FRET microscopy. Current Opinion in Chemical Biology **10,** 409-416.

Jo, Y., Cho, W.K., Rim, Y., Moon, J., Chen, X.-Y., Chu, H., Kim, C.Y., Park, Z.-Y., Lucas, W.J., and Kim, J.-Y. (2011). Plasmodesmal receptor-like kinases identified through analysis of rice cell wall extracted proteins. Protoplasma **248,** 191-203.

Joubès, J., and Chevalier, C. (2000). Endoreduplication in Higher Plants. In The Plant Cell Cycle (Springer Netherlands), pp. 191-201.

Juarez, M.T., Kui, J.S., Thomas, J., Heller, B.A., and Timmermans, M.C. (2004). microRNA-mediated repression of rolled *leaf1* specifies maize leaf polarity. Nature **428,** 84-88.

Jung, J.-H., and Park, C.-M. (2007). *MIR166/165* genes exhibit dynamic expression patterns in regulating shoot apical meristem and floral development in Arabidopsis. Planta **225,** 1327-1338.

Kakimoto, T., and Shibaoka, H. (1992). Synthesis of polysaccharides in phragmoplasts isolated from tobacco BY-2 cells. Plant & Cell Physiology **33,** 353-361.

Käll, L., Krogh, A., and Sonnhammer, E.L. (2007). Advantages of combined transmembrane topology and signal peptide prediction—the Phobius web server. Nucleic Acids Research **35,** W429-W432.

Källberg, M., Wang, H., Wang, S., Peng, J., Wang, Z., Lu, H., and Xu, J. (2012). Template-based protein structure modeling using the RaptorX web server. Nature Protocols **7,** 1511-1522.

Kaminski, C.F., Rees, E.J., and Schierle, G.S.K. (2014). A Quantitative Protocol for Intensity-Based Live Cell FRET Imaging. In Fluorescence Spectroscopy and Microscopy (Springer New York), pp. 445-454.

Kankanala, P., Czymmek, K., and Valent, B. (2007). Roles for rice membrane dynamics and plasmodesmata during biotrophic invasion by the blast fungus. The Plant Cell **19,** 706-724.

Kapteyn, J.C., Van Den Ende, H., and Klis, F.M. (1999). The contribution of cell wall proteins to the organization of the yeast cell wall. Biochimica et Biophysica Acta (BBA)-General Subjects **1426,** 373-383.

Karess, R.E., Chang, X.-j., Edwards, K.A., Kulkarni, S., Aguilera, I., and Kiehart, D.P. (1991). The regulatory light chain of nonmuscle myosin is encoded by spaghetti-squash, a gene required for cytokinesis in Drosophila. Cell **65,** 1177-1189.

Kauffmann, S., Legrand, M., Geoffroy, P., and Fritig, B. (1987). Biological function of 'pathogenesis-related' proteins: four PR proteins of tobacco have 1,3-β-glucanase activity. The EMBO Journal **6,** 3209-3212.

Kelly, R., Register, E., Hsu, M.-J., Kurtz, M., and Nielsen, J. (1996). Isolation of a gene involved in 1,3-beta-glucan synthesis in *Aspergillus nidulans* and purification of the corresponding protein. Journal of Bacteriology **178,** 4381-4391.

Kempers, R., and van Bel, A.J. (1997). Symplasmic connections between sieve element and companion cell in the stem phloem of *Vicia faba* L. have a molecular exclusion limit of at least 10 kDa. Planta **201,** 195-201.

Kim, J.-Y., Yuan, Z., and Jackson, D. (2003). Developmental regulation and significance of KNOX protein trafficking in Arabidopsis. Development **130,** 4351-4362.

Kim, Y., Schumaker, K.S., and Zhu, J.-K. (2006). EMS Mutagenesis of Arabidopsis. In Arabidopsis Protocols (Humana Press: Springer), pp. 101-103.

Kitagawa, M., Paultre, D., and Rademaker, H. (2015). Intercellular communication via plasmodesmata. New Phytologist **205,** 970-972.

Klis, F., De Groot, P., and Hellingwerf, K. (2001). Molecular organization of the cell wall of *Candida albicans*. Medical Mycology **39,** 1-8.

Knauer, S., Holt, A.L., Rubio-Somoza, I., Tucker, E.J., Hinze, A., Pisch, M., Javelle, M., Timmermans, M.C., Tucker, M.R., and Laux, T. (2013). A protodermal miR394 signal defines a region of stem cell competence in the Arabidopsis shoot meristem. Developmental Cell **24,** 125-132.

Knox, J.P., and Benitez-Alfonso, Y. (2014). Roles and regulation of plant cell walls surrounding plasmodesmata. Current Opinion in Plant Biology **22,** 93-100.

Koizumi, K., Wu, S., MacRae-Crerar, A., and Gallagher, K.L. (2011). An essential protein that interacts with endosomes and promotes movement of the SHORT-ROOT transcription factor. Current Biology **21,** 1559-1564.

Koizumi, K., Hayashi, T., Wu, S., and Gallagher, K.L. (2012). The SHORT-ROOT protein acts as a mobile, dose-dependent signal in patterning the ground tissue. Proceedings of the National Academy of Sciences **109,** 13010-13015.

Kollár, R., Reinhold, B.B., Petráková, E., Yeh, H.J., Ashwell, G., Drgonová, J., Kapteyn, J.C., Klis, F.M., and Cabib, E. (1997). Architecture of the yeast cell wall β (1→6)-glucan interconnects mannoprotein, β (1→3)-glucan, and chitin. Journal of Biological Chemistry **272,** 17762-17775.

Komina, O., Zhou, Y., Sarath, G., and Chollet, R. (2002). *In vivo* and *in vitro* phosphorylation of membrane and soluble forms of soybean nodule Sucrose Synthase. Plant Physiology **129,** 1664-1673.

Koncz, C., and Schell, J. (1986). The promoter of TL-DNA gene 5 controls the tissue-specific expression of chimaeric genes carried by a novel type of *Agrobacterium* binary vector. Molecular & General Genetics **204,** 383-396.

Kong, D., Karve, R., Willet, A., Chen, M.-K., Oden, J., and Shpak, E.D. (2012). Regulation of plasmodesmatal permeability and stomatal patterning by the glycosyltransferase-like protein KOBITO1. Plant Physiology **159,** 156-168.

Kopischke, M., Westphal, L., Schneeberger, K., Clark, R., Ossowski, S., Wewer, V., Fuchs, R., Landtag, J., Hause, G., and Dörmann, P. (2013). Impaired sterol ester synthesis alters the response of *Arabidopsis thaliana* to *Phytophthora infestans*. The Plant Journal **73,** 456-468.

Kurata, T., Okada, K., and Wada, T. (2005a). Intercellular movement of transcription factors. Current Opinion in Plant Biology **8,** 600-605.

Kurata, T., Ishida, T., Kawabata-Awai, C., Noguchi, M., Hattori, S., Sano, R., Nagasaka, R., Tominaga, R., Koshino-Kimura, Y., and Kato, T. (2005b). Cell-to-cell movement of the CAPRICE protein in Arabidopsis root epidermal cell differentiation. Development **132,** 5387-5398.

Lakowicz, J.R. (2006). Plasmonics in biology and plasmon-controlled fluorescence. Plasmonics **1,** 5-33.

Lampard, G.R., MacAlister, C.A., and Bergmann, D.C. (2008). Arabidopsis stomatal initiation is controlled by MAPK-mediated regulation of the bHLH SPEECHLESS. Science **322,** 1113-1116.

Laux, T., Mayer, K., Berger, J., and Jurgens, G. (1996). The *WUSCHEL* gene is required for shoot and floral meristem integrity in Arabidopsis. Development **122,** 87-96.

Lee, H.O., Davidson, J.M., and Duronio, R.J. (2009). Endoreplication: polyploidy with purpose. Genes & Development **23,** 2461-2477.

Lee, J.-Y., Colinas, J., Wang, J.Y., Mace, D., Ohler, U., and Benfey, P.N. (2006). Transcriptional and posttranscriptional regulation of transcription factor expression in Arabidopsis roots. Proceedings of the National Academy of Sciences **103,** 6055-6060.

Lee, J.-Y., Wang, X., Cui, W., Sager, R., Modla, S., Czymmek, K., Zybaliov, B., van Wijk, K., Zhang, C., and Lu, H. (2011). A plasmodesmata-localized protein mediates crosstalk between cell-to-cell communication and innate immunity in *Arabidopsis*. The Plant Cell **23,** 3353-3373.

Lee, M.W., Jelenska, J., and Greenberg, J.T. (2008). Arabidopsis proteins important for modulating defense responses to *Pseudomonas syringae* that secrete HopW1-1. The Plant Journal **54,** 452-465.

Lermontova, I., Schubert, V., Fuchs, J., Klatte, S., Macas, J., and Schubert, I. (2006). Loading of Arabidopsis centromeric histone CENH3 occurs mainly during G2 and requires the presence of the histone fold domain. The Plant Cell **18,** 2443-2451.

Lerouxel, O., Cavalier, D.M., Liepman, A.H., and Keegstra, K. (2006). Biosynthesis of plant cell wall polysaccharides — a complex process. Current Opinion in Plant Biology **9,** 621-630.

Lessard, P.A., Allen, R.D., Fujiwara, T., and Beachy, R.N. (1993). Upstream regulatory sequences from two β-conglycinin genes. Plant Molecular Biology **22,** 873-885.

Levesque, M.P., Vernoux, T., Busch, W., Cui, H., Wang, J.Y., Blilou, I., Hassan, H., Nakajima, K., Matsumoto, N., and Lohmann, J.U. (2006). Whole-genome

analysis of the SHORT-ROOT developmental pathway in Arabidopsis. PLoS Biology **4,** e249.

Levy, A., Guenoune-Gelbart, D., and Epel, B.L. (2006). Plasmodesmal gate keepers for intercellular communication. The Plant Journal **49,** 669-682.

Levy, A., Erlanger, M., Rosenthal, M., and Epel, B.L. (2007). A plasmodesmata-associated β-1,3-glucanase in Arabidopsis. The Plant Journal **49,** 669-682.

Li, C., Chen, C., Gao, L., Yang, S., Nguyen, V., Shi, X., Siminovitch, K., Kohalmi, S.E., Huang, S., and Wu, K. (2015). The Arabidopsis SWI2/SNF2 chromatin Remodeler BRAHMA regulates polycomb function during vegetative development and directly activates the flowering repressor gene *SVP*. PLoS Genetics **11,** e1004944.

Li, H., Bacic, A., and Read, S.M. (1997). Activation of pollen tube callose synthase by detergents (evidence for different mechanisms of action). Plant Physiology **114,** 1255-1265.

Li, H., Bacic, A., and Read, S.M. (1999a). Role of a callose synthase zymogen in regulating wall deposition in pollen tubes of *Nicotiana alata*. Planta **208,** 528-538.

Li, H., Lin, Y., Heath, R.M., Zhu, M.X., and Yang, Z. (1999b). Control of pollen tube tip growth by a Rop GTPase–dependent pathway that leads to tip-localized calcium influx. The Plant Cell **11,** 1731-1742.

Lin, S.-I., Chiang, S.-F., Lin, W.-Y., Chen, J.-W., Tseng, C.-Y., Wu, P.-C., and Chiou, T.-J. (2008). Regulatory network of microRNA399 and *PHO2* by systemic signaling. Plant Physiology **147,** 732-746.

Liu, Q., Yao, X., Pi, L., Wang, H., Cui, X., and Huang, H. (2009). The *ARGONAUTE10* gene modulates shoot apical meristem maintenance and establishment of leaf polarity by repressing miR165/166 in Arabidopsis. The Plant Journal **58,** 27-40.

Liu, Z., Running, M.P., and Meyerowitz, E.M. (1997). TSO1 functions in cell division during Arabidopsis flower development. Development **124,** 665-672.

Long, Y., Scheres, B., and Blilou, I. (2015). The logic of communication: roles for mobile transcription factors in plants. Journal of Experimental Botany **66,** 1133-1144.

Lordier, L., Jalil, A., Aurade, F., Larbret, F., Larghero, J., Debili, N., Vainchenker, W., and Chang, Y. (2008). Megakaryocyte endomitosis is a failure of late cytokinesis related to defects in the contractile ring and Rho/Rock signaling. Blood **112,** 3164-3174.

Lu, Q., Tang, X.R., Tian, G., Wang, F., Liu, K.D., Nguyen, V., Kohalmi, S.E., Keller, W.A., Tsang, E.W.T., Harada, J.J., Rothstein, S.J., and Cui, Y.H. (2010). Arabidopsis homolog of the yeast TREX-2 mRNA export complex: components and anchoring nucleoporin. The Plant Journal **61,** 259-270.

Lucas, W.J. (2006). Plant viral movement proteins: agents for cell-to-cell trafficking of viral genomes. Virology **344,** 169-184.

Lucas, W.J., and Lee, J.-Y. (2004). Plasmodesmata as a supracellular control network in plants. Nature Reviews Molecular Cell Biology **5,** 712-726.

Lucas, W.J., Ham, B.-K., and Kim, J.-Y. (2009). Plasmodesmata–bridging the gap between neighboring plant cells. Trends in Cell Biology **19,** 495-503.

Lucas, W.J., Bouché-Pillon, S., Jackson, D.P., Nguyen, L., Baker, L., Ding, B., and Hake, S. (1995). Selective trafficking of KNOTTED1 homeodomain protein and its mRNA through plasmodesmata. Science **270,** 1980-1983.

Lukowitz, W., Mayer, U., and Jürgens, G. (1996). Cytokinesis in the Arabidopsis embryo involves the syntaxin-related *KNOLLE* gene product. Cell **84,** 61-71.

Lukowitz, W., Gillmor, C.S., and Scheible, W.-R. (2000). Positional cloning in Arabidopsis. Why it feels good to have a genome initiative working for you. Plant Physiology **123,** 795-806.

Maeda, H., Song, W., Sage, T., and DellaPenna, D. (2014). Role of callose synthases in transfer cell wall development in tocopherol deficient Arabidopsis mutants. Frontiers in Plant Science **5 (46),** 1-15.

Mähönen, A.P., ten Tusscher, K., Siligato, R., Smetana, O., Díaz-Triviño, S., Salojärvi, J., Wachsman, G., Prasad, K., Heidstra, R., and Scheres, B. (2014). PLETHORA gradient formation mechanism separates auxin responses. Nature **515,** 125-129.

Manners, D.J., Masson, A.J., and Patterson, J.C. (1973). The structure of a beta-(1->3)-D-glucan from yeast cell walls. Journal of Biochemistry **135,** 19-30.

Matsuzaki, Y., Ogawa-Ohnishi, M., Mori, A., and Matsubayashi, Y. (2010). Secreted peptide signals required for maintenance of root stem cell niche in Arabidopsis. Science **329,** 1065-1067.

Maule, A., Faulkner, C., and Benitez-Alfonso, Y. (2012). Plasmodesmata "in communicado". Frontiers in Plant Science **3,** 1-5.

Maule, A., Gaudioso-Pedraza, R., and Benitez-Alfonso, Y. (2013). Callose deposition and symplastic connectivity are regulated prior to lateral root emergence. Communicative & Integrative Biology **6,** e26531.

Maule, A.J. (2008). Plasmodesmata: structure, function and biogenesis. Current Opinion in Plant Biology **11,** 680-686.

Maule, A.J., Benitez-Alfonso, Y., and Faulkner, C. (2011). Plasmodesmata–membrane tunnels with attitude. Current Opinion in Plant Biology **14,** 683-690.

Mazur, P., Morin, N., Baginsky, W., El-Sherbeini, M., Clemas, J.A., Nielsen, J.B., and Foor, F. (1995). Differential expression and function of two homologous subunits of yeast 1,3-beta-D-glucan synthase. Molecular and Cellular Biology **15,** 5671-5681.

McCall, K. (2004). Eggs over easy: cell death in the Drosophila ovary. Developmental Biology **274,** 3-14.

McConnell, J.R., Emery, J., Eshed, Y., Bao, N., Bowman, J., and Barton, M.K. (2001). Role of PHABULOSA and PHAVOLUTA in determining radial patterning in shoots. Nature **411,** 709-713.

McMichael, C.M., Reynolds, G.D., Koch, L.M., Wang, C., Jiang, N., Nadeau, J., Sack, F.D., Gelderman, M.B., Pan, J., and Bednarek, S.Y. (2013). Mediation of clathrin-dependent trafficking during cytokinesis and cell expansion by Arabidopsis STOMATAL CYTOKINESIS DEFECIVE proteins. The Plant Cell **25,** 3910-3925.

Miyashima, S., and Nakajima, K. (2011). The root endodermis: A hub of developmental signals and nutrient flow. Plant Signaling & Behavior **6,** 1954-1958.

Miyashima, S., Koi, S., Hashimoto, T., and Nakajima, K. (2011). Non-cell-autonomous microRNA165 acts in a dose-dependent manner to regulate multiple differentiation status in the Arabidopsis root. Development **138,** 2303-2313.

Mohnen, D. (2008). Pectin structure and biosynthesis. Current Opinion in Plant Biology **11,** 266-277.

Murashige, T., and Skoog, F. (1962). A revised medium for rapid growth and bio assays with tobacco tissue cultures. Physiologia Plantarum **15,** 473-497.

Nagel, R., Elliott, A., Masel, A., Birch, R., and Manners, J. (1990). Electroporation of binary Ti plasmid vector into *Agrobacterium tumefaciens* and *Agrobacterium rhizogenes*. FEMS Microbiology Letters **67,** 325-328.

Nakajima, K., Sena, G., Nawy, T., and Benfey, P.N. (2001). Intercellular movement of the putative transcription factor SHR in root patterning. Nature **413,** 307-311.

Neufeld, T.P., and Rubin, G.M. (1994). The Drosophila peanut gene is required for cytokinesis and encodes a protein similar to yeast putative bud neck filament proteins. Cell **77,** 371-379.

Nishimura, M.T., Stein, M., Hou, B.-H., Vogel, J.P., Edwards, H., and Somerville, S.C. (2003). Loss of a callose synthase results in salicylic acid-dependent disease resistance. Science **301,** 969-972.

Nogueira, F., Chitwood, D.H., Madi, S., Ohtsu, K., Schnable, P.S., Scanlon, M.J., and Timmermans, M. (2009). Regulation of small RNA accumulation in the maize shoot apex. PLoS Genetics **5,** e1000320.

Ochando, I., Jover-Gil, S., Ripoll, J.J., Candela, H., Vera, A., Ponce, M.R., Martínez-Laborda, A., and Micol, J.L. (2006). Mutations in the microRNA complementarity site of the *INCURVATA4* gene perturb meristem function and adaxialize lateral organs in Arabidopsis. Plant Physiology **141,** 607-619.

Oparka, K.J. (2004). Getting the message across: how do plant cells exchange macromolecular complexes? Trends in Plant Science **9,** 33-41.

Oparka, K.J., and Cruz, S.S. (2000). The great escape: phloem transport and unloading of macromolecules 1. Annual Review of Plant Biology **51,** 323-347.

Østergaard, L., Petersen, M., Mattsson, O., and Mundy, J. (2002). An Arabidopsis callose synthase. Plant Molecular Biology **49,** 559-566.

Pagant, S., Bichet, A., Sugimoto, K., Lerouxel, O., Desprez, T., McCann, M., Lerouge, P., Vernhettes, S., and Höfte, H. (2002). KOBITO1 encodes a novel plasma membrane protein necessary for normal synthesis of cellulose during cell expansion in Arabidopsis. The Plant Cell **14,** 2001-2013.

Pampalona, J., Frías, C., Genescà, A., and Tusell, L. (2012). Progressive telomere dysfunction causes cytokinesis failure and leads to the accumulation of polyploid cells. PLoS Genetics **8,** e1002679.

Park, B.-C., Park, Y.-H., Yi, S., Choi, Y.K., Kang, E.-H., and Park, H.-M. (2014). Transcriptional regulation of *fksA*, a β-1,3-glucan synthase gene, by the APSES protein StuA during *Aspergillus nidulans* development. Journal of Microbiology **52,** 940-947.

Pesch, M., and Hülskamp, M. (2009). One, two, three… models for trichome patterning in Arabidopsis? Current Opinion in Plant Biology **12,** 587-592.

Piršelová, B., and Matušíková, I. (2013). Callose: the plant cell wall polysaccharide with multiple biological functions. Acta Physiologiae Plantarum **35,** 635-644.

Prigge, M.J., Otsuga, D., Alonso, J.M., Ecker, J.R., Drews, G.N., and Clark, S.E. (2005). Class III homeodomain-leucine zipper gene family members have overlapping, antagonistic, and distinct roles in Arabidopsis development. The Plant Cell **17,** 61-76.

Pritchett, T., Tanner, E., and McCall, K. (2009). Cracking open cell death in the Drosophila ovary. Apoptosis **14,** 969-979.

Qadota, H., Python, C.P., Inoue, S.B., Arisawa, M., Anraku, Y., Zheng, Y., Watanabe, T., Levin, D.E., and Ohya, Y. (1996). Identification of yeast Rho1p GTPase as a regulatory subunit of 1,3-β-glucan synthase. Science **272,** 279-281.

Radford, J., Vesk, M., and Overall, R. (1998). Callose deposition at plasmodesmata. Protoplasma **201,** 30-37.

Richmond, T.A., and Somerville, C.R. (2001). Integrative Approaches to Determining Csl Function. In Plant Cell Walls (Springer Netherlands), pp. 131-143.

Rieu, I., and Laux, T. (2009). Signaling pathways maintaining stem cells at the plant shoot apex. Seminars in Cell & Developmental Biology **20,** 1083-1088.

Rinne, P., and van der Schoot, C. (1998). Symplasmic fields in the tunica of the shoot apical meristem coordinate morphogenetic events. Development **125,** 1477-1485.

Rinne, P.L., Kaikuranta, P.M., and Van Der Schoot, C. (2001). The shoot apical meristem restores its symplasmic organization during chilling-induced release from dormancy. The Plant Journal **26,** 249-264.

Rinne, P.L., Welling, A., Vahala, J., Ripel, L., Ruonala, R., Kangasjärvi, J., and van der Schoot, C. (2011a). Chilling of dormant buds hyperinduces FLOWERING LOCUS T and recruits GA-inducible 1, 3-β-glucanases to reopen signal conduits and release dormancy in Populus. The Plant Cell **23,** 130-146.

Rinne, P.L., Welling, A., Vahala, J., Ripel, L., Ruonala, R., Kangasjärvi, J., and van der Schoot, C. (2011b). Chilling of dormant buds hyperinduces FLOWERING LOCUS T and recruits GA-inducible 1,3-β-glucanases to reopen signal conduits and release dormancy in Populus. The Plant Cell **23,** 130-146.

Roldán, M., Gómez-Mena, C., Ruiz-García, L., Salinas, J., and Martínez-Zapater, J.M. (1999). Sucrose availability on the aerial part of the plant promotes morphogenesis and flowering of Arabidopsis in the dark. The Plant Journal **20,** 581-590.

Röper, W., and Röper, S. (1977). Centripetal wall formation in roots of *Vicia faba* after caffeine treatment. Protoplasma **93,** 89-100.

Ruan, Y.-L., Xu, S.-M., White, R., and Furbank, R.T. (2004). Genotypic and developmental evidence for the role of plasmodesmatal regulation in cotton fiber elongation mediated by callose turnover. Plant Physiology **136,** 4104-4113.

Rutschow, H.L., Baskin, T.I., and Kramer, E.M. (2011). Regulation of solute flux through plasmodesmata in the root meristem. Plant Physiology **155,** 1817-1826.

Sabatini, S., Beis, D., Wolkenfelt, H., Murfett, J., Guilfoyle, T., Malamy, J., Benfey, P., Leyser, O., Bechtold, N., and Weisbeek, P. (1999). An auxin-dependent distal organizer of pattern and polarity in the Arabidopsis root. Cell **99,** 463-472.

Sagi, G., Katz, A., Guenoune-Gelbart, D., and Epel, B.L. (2005). Class 1 reversibly glycosylated polypeptides are plasmodesmal-associated proteins delivered to plasmodesmata via the Golgi apparatus. The Plant Cell **17,** 1788-1800.

Samuels, A.L., Giddings, T.H., and Staehelin, L.A. (1995). Cytokinesis in tobacco BY-2 and root tip cells: a new model of cell plate formation in higher plants. The Journal of Cell Biology **130,** 1345-1357.

Sato, S., Kato, T., Kakegawa, K., Ishii, T., Liu, Y.-G., Awano, T., Takabe, K., Nishiyama, Y., Kuga, S., and Sato, S. (2001). Role of the putative membrane-bound endo-1,4-β-glucanase KORRIGAN in cell elongation and cellulose synthesis in *Arabidopsis thaliana*. Plant & Cell Physiology **42,** 251-263.

Scheres, B., Di Laurenzio, L., Willemsen, V., Hauser, M.-T., Janmaat, K., Weisbeek, P., and Benfey, P.N. (1995). Mutations affecting the radial organisation of the Arabidopsis root display specific defects throughout the embryonic axis. Development **121,** 53-62.

Scherp, P., Grotha, R., and Kutschera, U. (2001). Occurrence and phylogenetic significance of cytokinesis-related callose in green algae, bryophytes, ferns and seed plants. Plant Cell Reports **20,** 143-149.

Schlereth, A., Möller, B., Liu, W., Kientz, M., Flipse, J., Rademacher, E.H., Schmid, M., Jürgens, G., and Weijers, D. (2010). MONOPTEROS controls embryonic root initiation by regulating a mobile transcription factor. Nature **464,** 913-916.

Schmid, M., Davison, T.S., Henz, S.R., Pape, U.J., Demar, M., Vingron, M., Schölkopf, B., Weigel, D., and Lohmann, J.U. (2005). A gene expression map of *Arabidopsis thaliana* development. Nature Genetics **37,** 501-506.

Schwab, R., Ossowski, S., Riester, M., Warthmann, N., and Weigel, D. (2006). Highly specific gene silencing by artificial microRNAs in Arabidopsis. The Plant Cell **18,** 1121-1133.

Sela-Buurlage, M.B., Ponstein, A.S., Bres-Vloemans, S.A., Melchers, L.S., van den Elzen, P.J., and Cornelissen, B.J. (1993). Only specific tobacco (*Nicotiana tabacum*) chitinases and beta-1,3-glucanases exhibit antifungal activity. Plant Physiology **101,** 857-863.

Serres, M.P., Kossatz, U., Chi, Y., Roberts, J.M., Malek, N.P., and Besson, A. (2012). p27Kip1 controls cytokinesis via the regulation of citron kinase activation. The Journal of Clinical Investigation **122,** 844.

Sessions, A., Yanofsky, M.F., and Weigel, D. (2000). Cell-cell signaling and movement by the floral transcription factors LEAFY and APETALA1. Science **289,** 779-781.

Sevilem, I., Miyashima, S., and Helariutta, Y. (2013). Cell-to-cell communication via plasmodesmata in vascular plants. Cell Adhesion and Migration **7,** 27-32.

Shematek, E.M., Braatz, J.A., and Cabib, E. (1980). Biosynthesis of the yeast cell wall. Journal of Biological Chemistry **255,** 888-894.

Shin, H., and Brown, R.M. (1999). GTPase activity and biochemical characterization of a recombinant cotton fiber annexin. Plant Physiology **119,** 925-934.

Simossis, V.A., and Heringa, J. (2005). PRALINE: a multiple sequence alignment toolbox that integrates homology-extended and secondary structure information. Nucleic Acids Research **33,** W289-W294.

Simpson, C., Thomas, C., Findlay, K., Bayer, E., and Maule, A.J. (2009). An Arabidopsis GPI-anchor plasmodesmal neck protein with callose binding activity and potential to regulate cell-to-cell trafficking. The Plant Cell **21,** 581-594.

Sivaguru, M., Fujiwara, T., Šamaj, J., Baluška, F., Yang, Z., Osawa, H., Maeda, T., Mori, T., Volkmann, D., and Matsumoto, H. (2000). Aluminum-induced 1→3-β-d-glucan inhibits cell-to-cell trafficking of molecules through plasmodesmata. A new mechanism of aluminum toxicity in plants. Plant Physiology **124,** 991-1006.

Smith, Z.R., and Long, J.A. (2010). Control of Arabidopsis apical–basal embryo polarity by antagonistic transcription factors. Nature **464,** 423-426.

Söllner, R., Glässer, G., Wanner, G., Somerville, C.R., Jürgens, G., and Assaad, F.F. (2002). Cytokinesis-defective mutants of Arabidopsis. Plant Physiology **129,** 678-690.

Sparkes, I.A., Runions, J., Kearns, A., and Hawes, C. (2006). Rapid, transient expression of fluorescent fusion proteins in tobacco plants and generation of stably transformed plants. Nature Protocols **1,** 2019-2025.

Spielman, M., Preuss, D., Li, F.-L., Browne, W.E., Scott, R.J., and Dickinson, H.G. (1997). TETRASPORE is required for male meiotic cytokinesis in *Arabidopsis thaliana*. Development **124,** 2645-2657.

Spradling, A.C., Nystul, T., Lighthouse, D., Morris, L., Fox, D., Cox, R., Tootle, T., Frederick, R., and Skora, A. (2008). Stem cells and their niches: Integrated units that maintain Drosophila tissues. Cold Spring Harbor Symposia on Quantitative Biology **73,** 49-57.

Stahl, Y., and Simon, R. (2013). Gated communities: apoplastic and symplastic signals converge at plasmodesmata to control cell fates. Journal of Experimental Botany **64,** 5237-5241.

Stahl, Y., Wink, R.H., Ingram, G.C., and Simon, R. (2009). A signaling module controlling the stem cell niche in Arabidopsis root meristems. Current Biology **19,** 909-914.

Stahl, Y., Grabowski, S., Bleckmann, A., Kühnemuth, R., Weidtkamp-Peters, S., Pinto, K.G., Kirschner, G.K., Schmid, J.B., Wink, R.H., and Hülsewede, A. (2013). Moderation of Arabidopsis root stemness by CLAVATA1 and ARABIDOPSIS CRINKLY4 receptor kinase complexes. Current Biology **23,** 362-371.

Stintzi, A., Heitz, T., Prasad, V., Wiedemann-Merdinoglu, S., Kauffmann, S., Geoffroy, P., Legrand, M., and Fritig, B. (1993). Plant 'pathogenesis-related' proteins and their role in defense against pathogens. Biochimie **75,** 687-706.

Strompen, G., El Kasmi, F., Richter, S., Lukowitz, W., Assaad, F.F., Jürgens, G., and Mayer, U. (2002). The Arabidopsis *HINKEL* gene encodes a kinesin-related protein involved in cytokinesis and is expressed in a cell cycle-dependent manner. Current Biology **12,** 153-158.

Subbaiah, C.C., Palaniappan, A., Duncan, K., Rhoads, D.M., Huber, S.C., and Sachs, M.M. (2006). Mitochondrial localization and putative signaling function of sucrose synthase in maize. Journal of Biological Chemistry **281,** 15625-15635.

Sugimoto-Shirasu, K., and Roberts, K. (2003). "Big it up": endoreduplication and cell-size control in plants. Current Opinion in Plant Biology **6,** 544-553.

Sun, L., Gurnon, J.R., Adams, B.J., Graves, M.V., and Van Etten, J.L. (2000). Characterization of a β-1,3-glucanase encoded by chlorella virus PBCV-1. Virology **276,** 27-36.

Suzuki, T., Fujikura, K., Higashiyama, T., and Takata, K. (1997). DNA staining for fluorescence and laser confocal microscopy. Journal of Histochemistry & Cytochemistry **45,** 49-53.

Takahashi, F., Sato-Nara, K., Kobayashi, K., Suzuki, M., and Suzuki, H. (2003). Sugar-induced adventitious roots in Arabidopsis seedlings. Journal of Plant Research **116,** 83-91.

Talbert, P.B., Adler, H.T., Parks, D.W., and Comai, L. (1995). The *REVOLUTA* gene is necessary for apical meristem development and for limiting cell divisions in the leaves and stems of *Arabidopsis thaliana*. Development **121,** 2723-2735.

Tamura, K., Stecher, G., Peterson, D., Filipski, A., and Kumar, S. (2013). MEGA6: molecular evolutionary genetics analysis version 6.0. Molecular Biology & Evolution **30,** 2725-2729.

Tang, X., Hou, A., Babu, M., Nguyen, V., Hurtado, L., Lu, Q., Reyes, J.C., Wang, A., Keller, W.A., and Harada, J.J. (2008). The Arabidopsis BRAHMA chromatin-remodeling ATPase is involved in repression of seed maturation genes in leaves. Plant Physiology **147,** 1143-1157.

Tang, X., Bian, S., Tang, M., Lu, Q., Li, S., Liu, X., Tian, G., Nguyen, V., Tsang, E.W., and Wang, A. (2012a). MicroRNA–mediated repression of the seed maturation program during vegetative development in Arabidopsis. PLoS Genetics **8,** e1003091.

Tang, X., Lim, M.-H., Pelletier, J., Tang, M., Nguyen, V., Keller, W.A., Tsang, E.W.T., Wang, A., Rothstein, S.J., Harada, J.J., and Cui, Y. (2012b). Synergistic repression of the embryonic programme by SET DOMAIN GROUP 8 and EMBRYONIC FLOWER 2 in Arabidopsis seedlings. Journal of Experimental Botany **63,** 1391-1404.

Taylor, N.G., Laurie, S., and Turner, S.R. (2000). Multiple cellulose synthase catalytic subunits are required for cellulose synthesis in Arabidopsis. The Plant Cell **12,** 2529-2539.

Thiele, K., Wanner, G., Kindzierski, V., Jürgens, G., Mayer, U., Pachl, F., and Assaad, F.F. (2009). The timely deposition of callose is essential for cytokinesis in Arabidopsis. The Plant Journal **58,** 13-26.

Thomas, C.L., Bayer, E.M., Ritzenthaler, C., Fernandez-Calvino, L., and Maule, A.J. (2008). Specific targeting of a plasmodesmal protein affecting cell-to-cell communication. PLoS Biology **6,** e7.

Thompson, L.H., and Lindl, P.A. (1976). A CHO-cell mutant with a defect in cytokinesis. Somatic Cell Genetics **2,** 387-400.

Tilsner, J., Taliansky, M.E., and Torrance, L. (2014). Plant virus movement. eLS.

Töller, A., Brownfield, L., Neu, C., Twell, D., and Schulze-Lefert, P. (2008). Dual function of Arabidopsis glucan synthase-like genes GSL8 and GSL10 in male gametophyte development and plant growth. The Plant Journal **54,** 911-923.

Touihri, S., Knöll, C., Stierhof, Y.D., Müller, I., Mayer, U., and Jürgens, G. (2011). Functional anatomy of the Arabidopsis cytokinesis-specific syntaxin KNOLLE. The Plant Journal **68,** 755-764.

Tretter, E.M., Alvarez, J.P., Eshed, Y., and Bowman, J.L. (2008). Activity range of Arabidopsis small RNAs derived from different biogenesis pathways. Plant Physiology **147,** 58-62.

Tsirigos, K.D., Peters, C., Shu, N., Käll, L., and Elofsson, A. (2015). The TOPCONS web server for consensus prediction of membrane protein topology and signal peptides. Nucleic Acids Research **43,** W401-W407.

Tzafrir, I., McElver, J.A., Liu, C.-m., Yang, L.J., Wu, J.Q., Martinez, A., Patton, D.A., and Meinke, D.W. (2002). Diversity of TITAN functions in Arabidopsis seed development. Plant Physiology **128,** 38-51.

Vakifahmetoglu, H., Olsson, M., and Zhivotovsky, B. (2008). Death through a tragedy: mitotic catastrophe. Cell Death & Differentiation **15,** 1153-1162.

Van den Berg, C., Willemsen, V., Hendriks, G., Weisbeek, P., and Scheres, B. (1997). Short-range control of cell differentiation in the Arabidopsis root meristem. Nature **390,** 287-289.

Van Munster, E.B., and Gadella, T.W. (2005). Fluorescence Lifetime Imaging Microscopy (FLIM). In Microscopy Techniques (Springer Berlin Heidelberg), pp. 143-175.

Vatén, A., Dettmer, J., Wu, S., Stierhof, Y.-D., Miyashima, S., Yadav, S.R., Roberts, C.J., Campilho, A., Bulone, V., and Lichtenberger, R. (2011). Callose biosynthesis regulates symplastic trafficking during root development. Developmental Cell **21,** 1144-1155.

Verma, D.P.S. (2001). Cytokinesis and building of the cell plate in plants. Annual Review of Plant Biology **52,** 751-784.

Verma, D.P.S., and Hong, Z. (2001). Plant callose synthase complexes. Plant Molecular Biology **47,** 693-701.

Waizenegger, I., Lukowitz, W., Assaad, F., Schwarz, H., Jürgens, G., and Mayer, U. (2000). The Arabidopsis *KNOLLE* and *KEULE* genes interact to promote vesicle fusion during cytokinesis. Current Biology **10,** 1371-1374.

Wang, X., Sager, R., Cui, W., Zhang, C., Lu, H., and Lee, J.-Y. (2013). Salicylic acid regulates plasmodesmata closure during innate immune responses in Arabidopsis. The Plant Cell **25,** 2315-2329.

Wawrzynska, A., Rodibaugh, N.L., and Innes, R.W. (2010). Synergistic activation of defense responses in Arabidopsis by simultaneous loss of the GSL5 callose synthase and the EDR1 protein kinase. Molecular Plant-Microbe Interactions **23,** 578-584.

Welch, D., Hassan, H., Blilou, I., Immink, R., Heidstra, R., and Scheres, B. (2007). Arabidopsis JACKDAW and MAGPIE zinc finger proteins delimit asymmetric cell division and stabilize tissue boundaries by restricting SHORT-ROOT action. Genes & Development **21,** 2196-2204.

Wester, K., Digiuni, S., Geier, F., Timmer, J., Fleck, C., and Hülskamp, M. (2009). Functional diversity of R3 single-repeat genes in trichome development. Development **136,** 1487-1496.

Winter, H., and Huber, S.C. (2000). Regulation of sucrose metabolism in higher plants: localization and regulation of activity of key enzymes. Critical Reviews in Plant Sciences **19,** 31-67.

Wu, S., and Gallagher, K.L. (2013). Intact microtubules are required for the intercellular movement of the SHORT-ROOT transcription factor. The Plant Journal **74,** 148-159.

Wu, S., and Gallagher, K.L. (2014). The movement of the non-cell-autonomous transcription factor, SHORT-ROOT relies on the endomembrane system. The Plant Journal **80,** 396-409.

Wu, X., Weigel, D., and Wigge, P.A. (2002). Signaling in plants by intercellular RNA and protein movement. Genes & Development **16,** 151-158.

Wu, X., Dinneny, J.R., Crawford, K.M., Rhee, Y., Citovsky, V., Zambryski, P.C., and Weigel, D. (2003). Modes of intercellular transcription factor movement in the Arabidopsis apex. Development **130,** 3735-3745.

Wysocka-Diller, J.W., Helariutta, Y., Fukaki, H., Malamy, J.E., and Benfey, P.N. (2000). Molecular analysis of SCARECROW function reveals a radial patterning mechanism common to root and shoot. Development **127,** 595-603.

Xie, B., and Hong, Z. (2011). Unplugging the callose plug from sieve pores. Plant Signaling & Behavior **6,** 491-493.

Xie, B., Wang, X., Zhu, M., Zhang, Z., and Hong, Z. (2011). CALS7 encodes a callose synthase responsible for callose deposition in the phloem. The Plant Journal **65,** 1-14.

Xie, B., Deng, Y., Kanaoka, M.M., Okada, K., and Hong, Z. (2012). Expression of Arabidopsis callose synthase 5 results in callose accumulation and cell wall permeability alteration. Plant Science **183,** 1-8.

Xu, X.M., and Jackson, D. (2010). Lights at the end of the tunnel: new views of plasmodesmal structure and function. Current Opinion in Plant Biology **13,** 684-692.

Xu, X.M., Wang, J., Xuan, Z., Goldshmidt, A., Borrill, P.G., Hariharan, N., Kim, J.Y., and Jackson, D. (2011). Chaperonins facilitate KNOTTED1 cell-to-cell trafficking and stem cell function. Science **333,** 1141-1144.

Yadav, R.K., Tavakkoli, M., and Reddy, G.V. (2010). WUSCHEL mediates stem cell homeostasis by regulating stem cell number and patterns of cell division and differentiation of stem cell progenitors. Development **137,** 3581-3589.

Yadav, R.K., Perales, M., Gruel, J., Girke, T., Jönsson, H., and Reddy, G.V. (2011). WUSCHEL protein movement mediates stem cell homeostasis in the Arabidopsis shoot apex. Genes & Development **25,** 2025-2030.

Yadav, S.R., Yan, D., Sevilem, I., and Helariutta, Y. (2014). Plasmodesmata-mediated intercellular signaling during plant growth and development. Frontiers in Plant Science **5,** 1-7.

Yang, Y.H., Kang, H.-W., and Ro, H.-S. (2014). Cloning and molecular characterization of β-1,3-glucan synthase from *Sparassis crispa*. Mycobiology **42,** 167-173.

Yu, C.-H., Guo, G.-Q., Nie, X.-W., and Zheng, G.-C. (2004). Cytochemical localization of pectinase activity in pollen mother cells of tobacco during meiotic prophase and its relation to the formation of secondary plasmodesmata and cytoplasmic channels. Acta Botanica Sinica **46,** 1443-1453.

Zavaliev, R., Sagi, G., Gera, A., and Epel, B.L. (2010). The constitutive expression of Arabidopsis plasmodesmal-associated class 1 reversibly glycosylated polypeptide impairs plant development and virus spread. Journal of Experimental Botany **61,** 131-142.

Zavaliev, R., Ueki, S., Epel, B.L., and Citovsky, V. (2011). Biology of callose (β-1, 3-glucan) turnover at plasmodesmata. Protoplasma **248,** 117-130.

Zavaliev, R., Levy, A., Gera, A., and Epel, B.L. (2013). Subcellular dynamics and role of Arabidopsis β-1,3-glucanases in cell-to-cell movement of tobamoviruses. Molecular Plant-Microbe Interactions **26,** 1016-1030.

Zhang, X., Henriques, R., Lin, S.-S., Niu, Q.-W., and Chua, N.-H. (2006). *Agrobacterium*-mediated transformation of *Arabidopsis thaliana* using the floral dip method. Nature Protocols **1,** 641-646.

Zheng, Y., Anderson, S., Zhang, Y., and Garavito, R.M. (2011). The structure of Sucrose Synthase-1 from *Arabidopsis thaliana* and its functional implications. Journal of Biological Chemistry **286,** 36108-36118.

Zhou, G.-K., Kubo, M., Zhong, R., Demura, T., and Ye, Z.-H. (2007). Overexpression of miR165 affects apical meristem formation, organ polarity establishment and vascular development in Arabidopsis. Plant and Cell Physiology **48,** 391-404.

Zimmermann, P., Hirsch-Hoffmann, M., Hennig, L., and Gruissem, W. (2004). GENEVESTIGATOR. Arabidopsis microarray database and analysis toolbox. Plant Physiology **136,** 2621-2632.

APPENDICES

Appendix I List of mutant lines and primers used for genotyping

Gene	Mutant	Allele	Primer	Primer Sequence (5'-3')
GSL8	*essp8*	*essp8*	*essp8*-FW	TGCGTTGACCATTGTTAGCTTG
			essp8-Rev	AGGACAAAGTGGGAACGAAGAG
	SALK_111500	*gsl8-1*	GSTD-5-FW	TCTCGAATTAACGTTGTGAATCC
			GSTD-5-Rev	ACGGACATCAAACCAGTTTTG
	SALK_109342	*gsl8-2*	GSTD-7-FW	GCATCACACCAGCCTAAAATC
			GSTD-7-Rev	ATATGCTGCGATGTTTTCACC
	SAIL_21_B02/CS801051	*gsl8-3*	GSTD-9-FW	GAAACCAAGTACCTCCCAAGC
			GSTD-9-Rev	CATCATCCCAGATTCGAAATG
	SALK_098374C	*gsl8-4*	GSTD-1-FW	TGTACAAAGGTGGAGTGGGAG
			GSTD-1-Rev	TCGAGTCTATGAGCTTCCAATG
HINKEL	SALK_056766C	*hinkel*	HNK-2-FW	ACAAATGCTAATCAGATGCCG
			HNK-2-Rev	TTAAGTCTGCACAATGTTGCC
KNOLL	CS1001988/ SK6760	*knolle*	KNL-1-FW	AATGTGATTAGTCAAAATTTTGGG
			KNL-1-Rev	CAAACCCATCTCTGCTTTCAC
SCD1	SALK_039883	*scd1*	SCD-1-FW	GAAGTTCAGAACCACGCAGAC
			SCD-1-Rev	GGGGTGCTTCTTCATTTAAGC
KEULE	SALK_032092C	*keule*	KEUL-FW	ATGAGATTGATGGTCGTGACC
			KEUL-Rev	ATGGGACAGCGAATATTTGTG

Appendix I cont'd

Gene	**Mutant**	**Allele**	**Primer**	**Primer Sequence (5'-3')**
KORRIGAN	CS6390	*korrigan*	KRG-1-FW-1	CGCGGCACAGTTTTAACGAT
			KRG-1-FW-2	GCTAATGTCGGGTGGATGGAA
			KRG-1-Rev	CTCTTCAGACGACCGTAGCC
AtBG_PPAP	SALK_019116/CS25030	*atbg-1*	ATBG-FW	TGATCCCAAGTGAGTAAACCG
			ATBG-Rev	TGCTCACAACCACTCACTACG
GSL10	GABI_038F11	*gsl10-1*	GSL10-1-F	TGTGATAGACTTCCTCAACAGCAT
			GSL10-1-R	GCTCTTCATGTTCCTCTTACCAAT
	GABI_054E08	*gsl10-2*	GSL10-2-F	TTTTTCCATCTAAGAAAAGCCAAC
			GSL10-2-R	TCCAGAAGAAACAGAACCT
	SALK_143945	*gsl10-3*	GSL10-3-F	TTAGGATGAATGTTGCTGTTGG
			GSL10-3-R	TCATCCCTTTCAATCCTCTCC
	SALK_124294	*gsl10-4*	GSL10-4-F	TGTGACGCATGTGCTATCTTC
			GSL10-4-R	GAGCAAACAGCCAAGAAACAG
	SK5250	*gsl10-5*	GSL10-5-F	GACGAGTGCTTTCTGCAAATC
			GSL10-5-R	CCCAAGAATTCTGGTAGGCTC

Appendix II List of primers used for *essp8* rough-mapping

BAC	Primer	Primer Sequence (5'-3')
F17A22	F17A22-FW	ACGAATATTGATTGTCTAAG
	F17A22-Rev	AACCTAAGGGAAGGCTAC
T3D7	T3D7-FW	GGTATCGATTGAGCAAATAA
	T3D7-Rev	ACATGCGTCTGCTTGGAG
F13M22	F13M22-FW	AATATCCTCACGGTAAAATG
	F13M22-Rev	GGTTAAATGAAACAATTTAG
F11F19	F11F19-FW	GTACTGGATGTCAAACTAGA
	F11F19-Rev	ATAGCATGGTGATAAATAAG
F19I3	F19I3-FW	TTGTCTTAAGGGTAGTTATG
	F19I3-Rev	AGGGACTTGACGAAAGAG
F13P17	F13P17-FW	CTGCTGTCAAAAAAGAAGA
	F13P17-Rev	ACCTTATCCAAACAAATGTA
F25I18	F25I18-FW	GCGGTTCTCCTAATGAAG
	F25I18-Rev	TTTCCACGTATACTAGCA

Appendix III List of primers used to generate expression, overexpression and FRET-related constructs

Gene	Primer	Primer Sequence (5'-3')
SHR	SHR-FW	GGGGACAAGTTTGTACAAAAAAGCAGGCTTGAACGGTTCATTTCTGGGGCTA
	SHR-Rev	GGGGACCACTTTGTACAAGAAAGCTGGGTCCGTTGGCCGCCACGCACTA
PDLP5	PDLP5-OE-FW	GGGGACAAGTTTGTACAAAAAAGCAGGCTTGATGATCAAGACAAAGACGA
	PDLP5-OE-Rev	GGGGACCACTTTGTACAAGAAAGCTGGGTCTTTACACCATTTCTCATCTTG
GSL8	GSL8-FW	GGGGACAAGTTTGTACAAAAAAGCAGGCTTGATGGCTAGGGTTTATAGTA
	GSL8-Rev	GGGGACCACTTTGTACAAGAAAGCTGGGTCGGTCTCAACATTAGCTCTG
	GSL8-M.Rev	GGGGACCACTTTGTACAAGAAAGCTGGGTCTAACCTTTTCACAACAGGA
SCD1	SCD1-FW	GGGGACAAGTTTGTACAAAAAAGCAGGCTTGATGGGACGGATCTTCGAGTA
	SCD1-Rev	GGGGACCACTTTGTACAAGAAAGCTGGGTCGATGTTGATGGTGGCATCCC
AtBG_PPAP	AtBGPPAP-FW	GGGGACAAGTTTGTACAAAAAAGCAGGCTTGATGGCTTCTTCTTCTCTGCA
	AtBGPPAP-Rev	GGGGACCACTTTGTACAAGAAAGCTGGGTCCAACCGAAGCTTGATGATG
SUS1	SUS1-FW	GGGGACAAGTTTGTACAAAAAAGCAGGCTTGATGGCAAACGCTGAACGTAT
	SUS1-Rev	GGGGACCACTTTGTACAAGAAAGCTGGGTCATCATCTTGTGCAAGAGGAAC
ROP4	ROP4-FW	GGGGACAAGTTTGTACAAAAAAGCAGGCTTGATGAGTGCTTCGAGGTTTATAA
	ROP4-Rev	GGGGACCACTTTGTACAAGAAAGCTGGGTCCAAGAACACGCAGCGGTT
UDPG	UDPG-FW	GGGGACAAGTTTGTACAAAAAAGCAGGCTTGATGGGGAAAAGAGGAAGG
	UDPG-Rev	GGGGACCACTTTGTACAAGAAAGCTGGGTCTGAATCTGCAATTTGAGACAC

Appendix IV T-DNA insertions-specific primers used for genotyping

T-DNA	**Primer**	**Primer Sequence (5'-3')**
SALK T-DNA	LBb1.3	ATTTTGCCGATTTCGGAAC
SAIL T-DNA	LB3	TAGCATCTGAATTTCATAACCAATCTCGATACAC
SK T-DNA	pSKTAIL-L3	ATACGACGGATCGTAATTTGTCG
GABI T-DNA	GABI-8474	ATAATAACGCTGCGGACATCTACATTTT

Appendix V List of primers used for qRT-PCR

Gene	**Primer**	**Primer Sequence (5'-3')**
GAPDH	qGAPDH-FW	CTTGGAAGGAGCTAGGAATTGACA
	qGAPDH-Rev	ATGTGTTTCCCTGCACCTTCTC
CLAVATA3	qCLV3-FW	GATGCTTCTGATCTCACTCAAGC
	qCLV3-Rev	TCAGGTCCCGAAGGAACAGT

Appendix VI List of Arabidopsis GSLs accession numbers

Gene	Accession Gene ID
AtGSL1	AT4G04970
AtGSL2	AT2G13680
AtGSL3	AT2G51960
AtGSL4	AT3G14570
AtGSL5	AT4G03550
AtGSL6	AT1G05570
AtGSL7	AT1G06490
AtGSL8	AT2G36850
AtGSL9	AT5G36870
AtGSL10	AT3G07160
AtGSL11	AT3G59100
AtGSL12	AT5G13000

Appendix VII Alignment of the Arabidopsis GSL family amino acid sequence

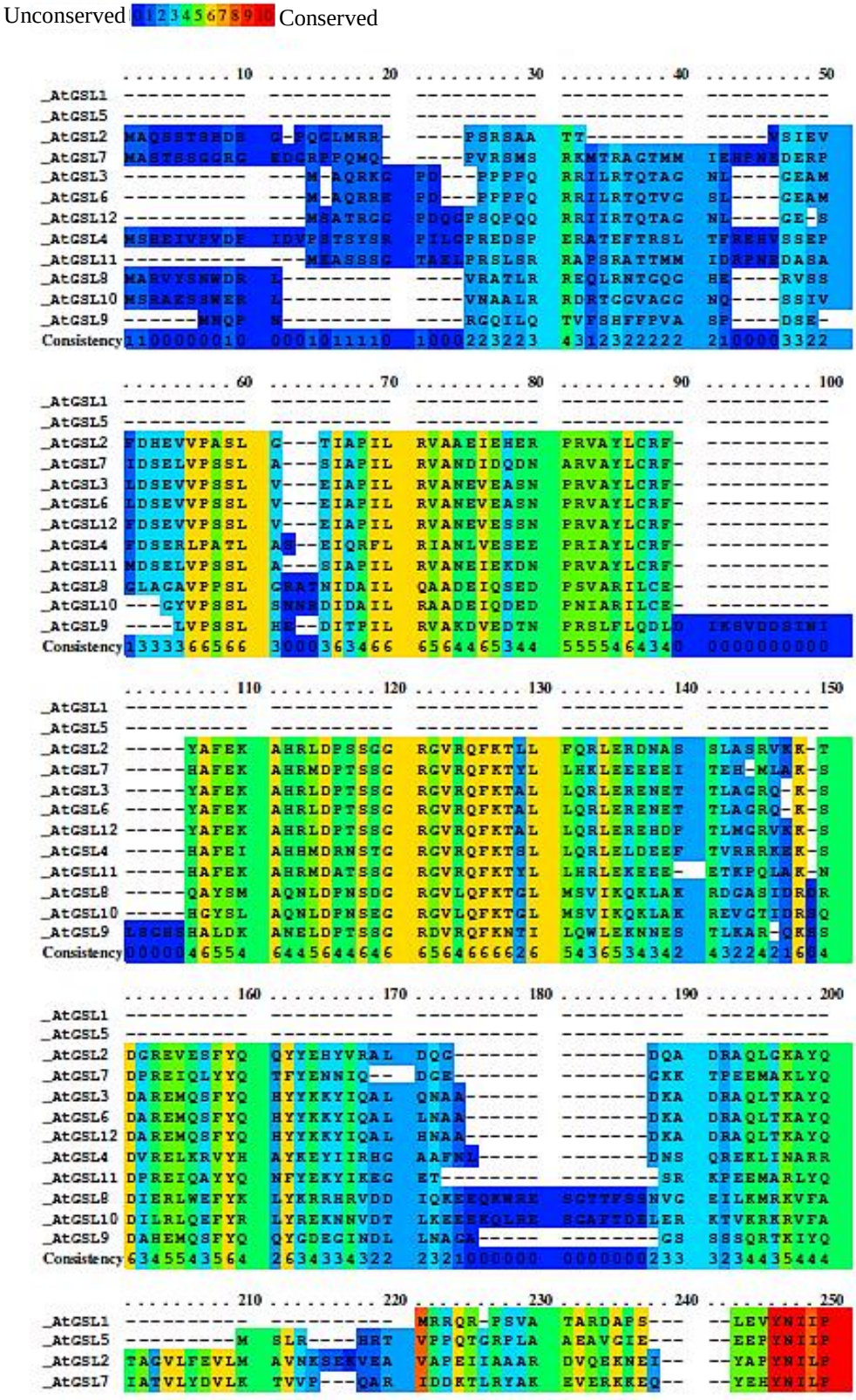

Appendix VII cont'd

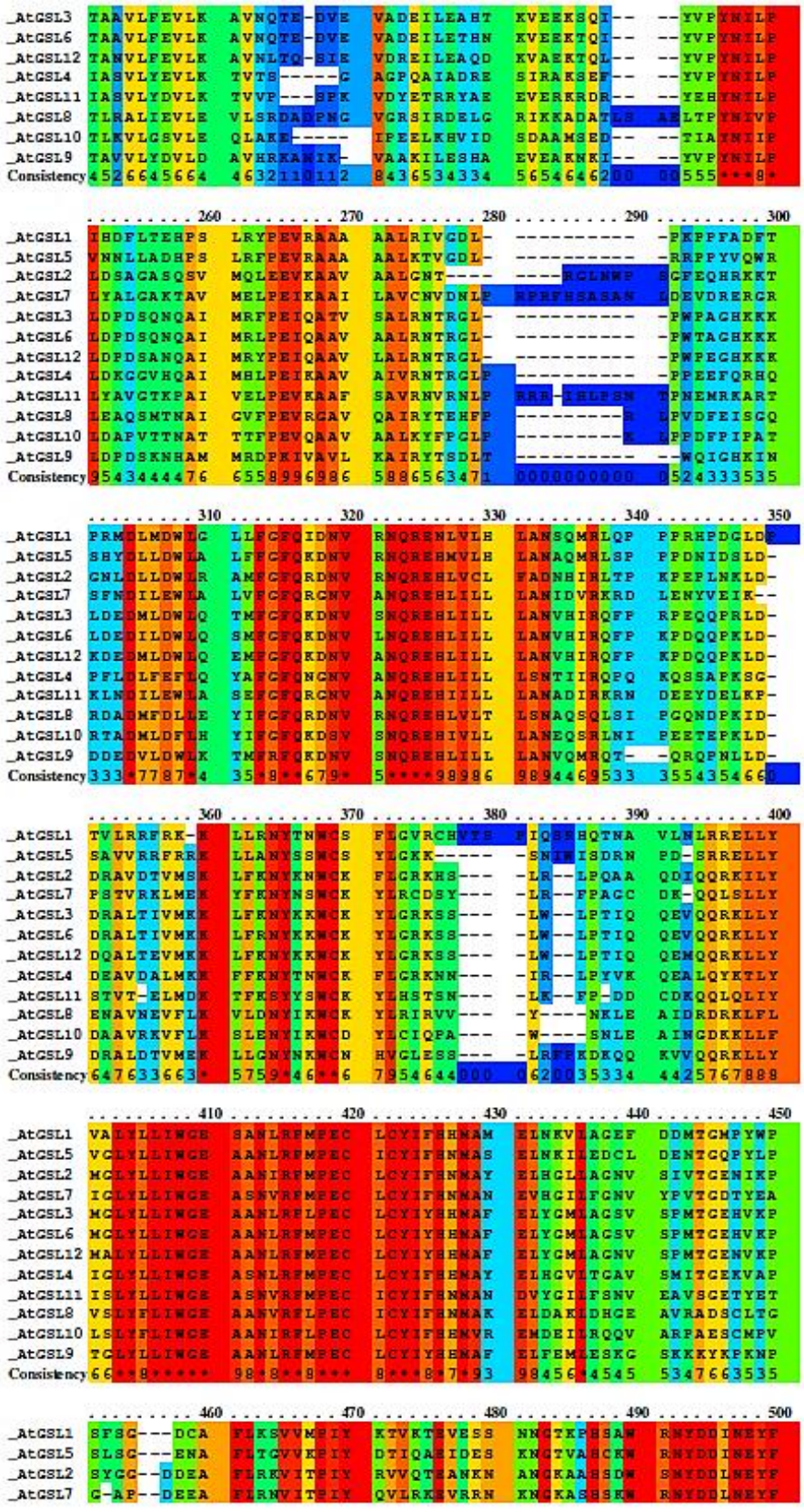

Appendix VII cont'd

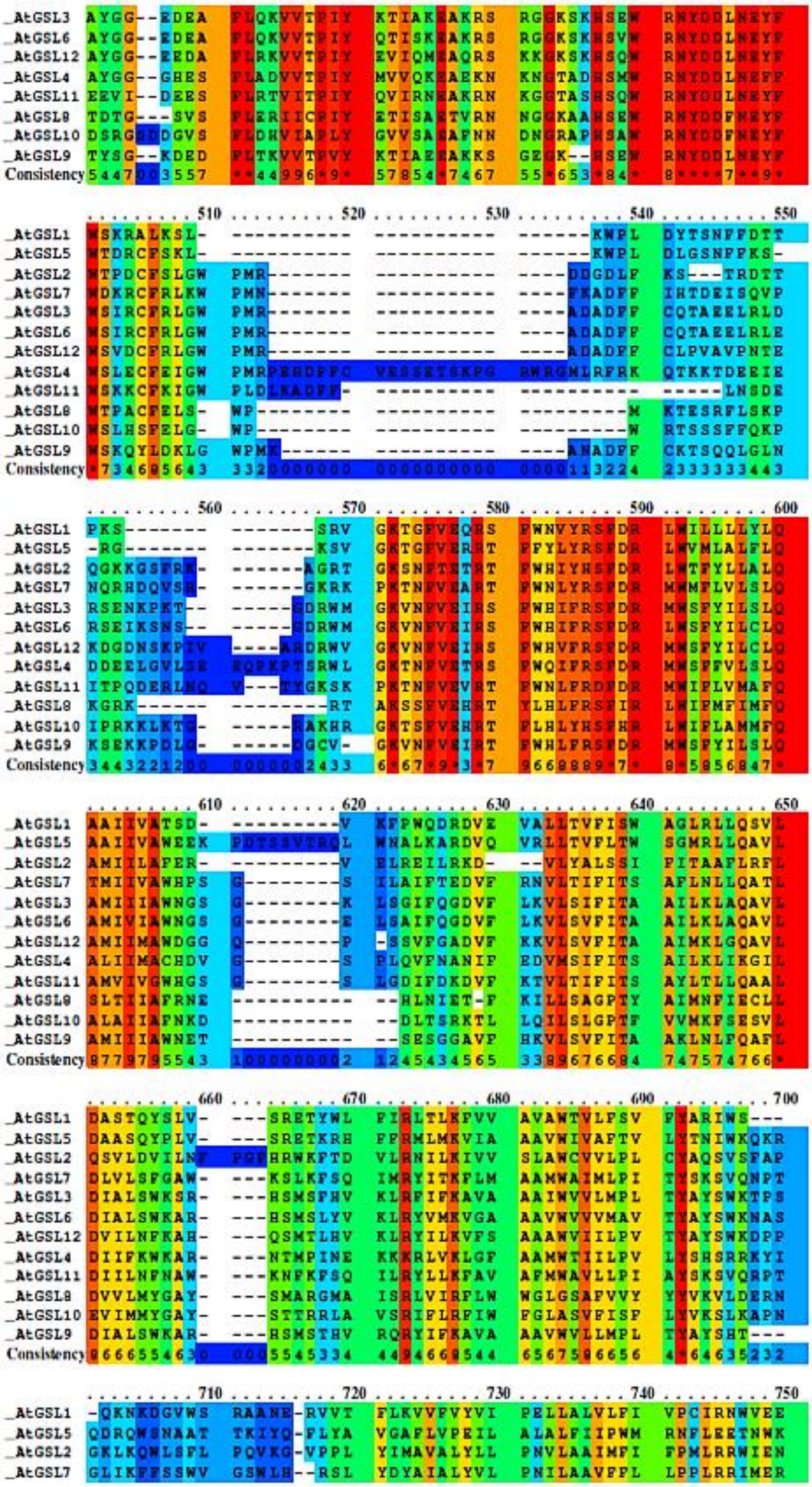

Appendix VII cont'd

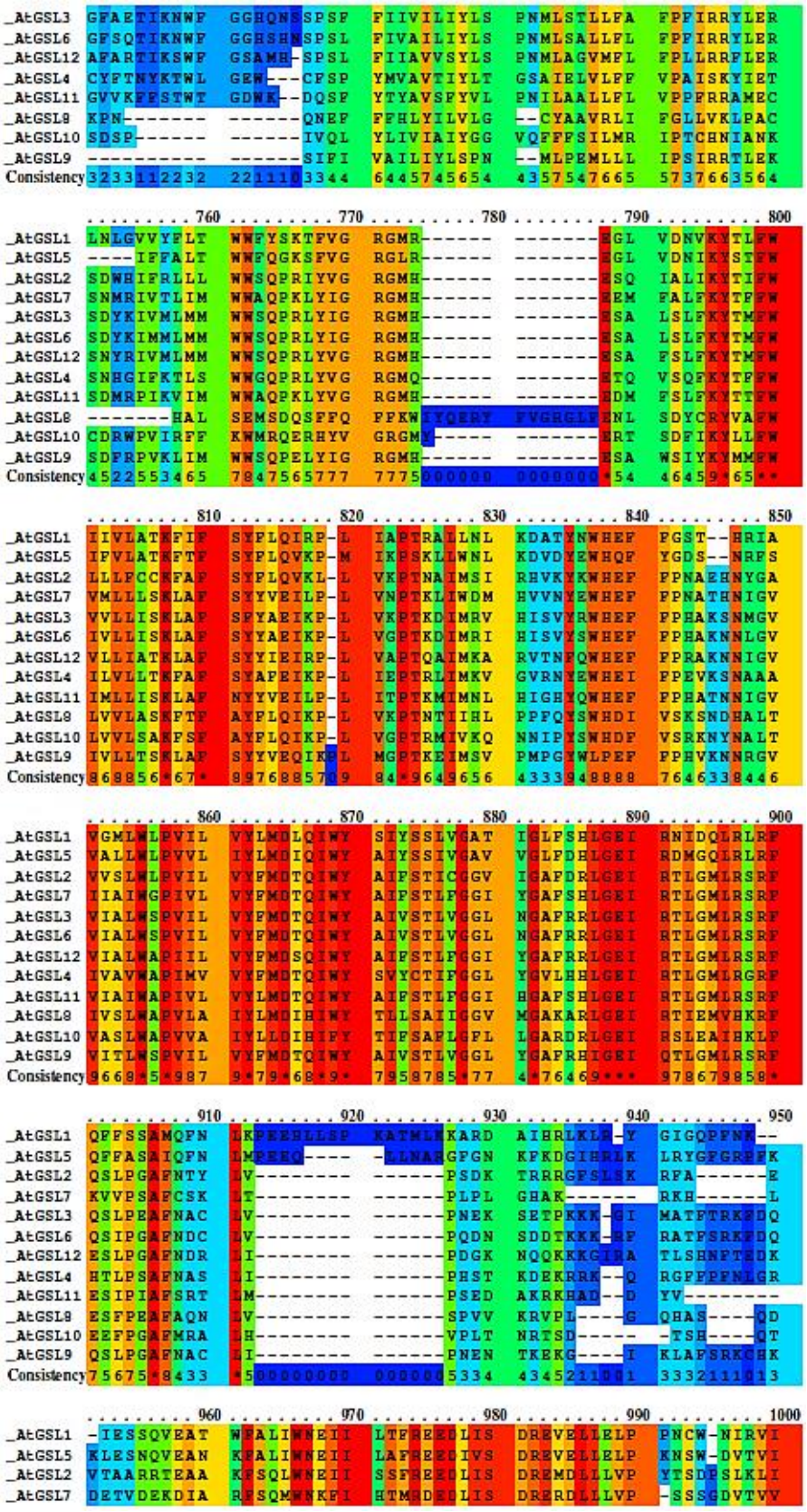

Appendix VII cont'd

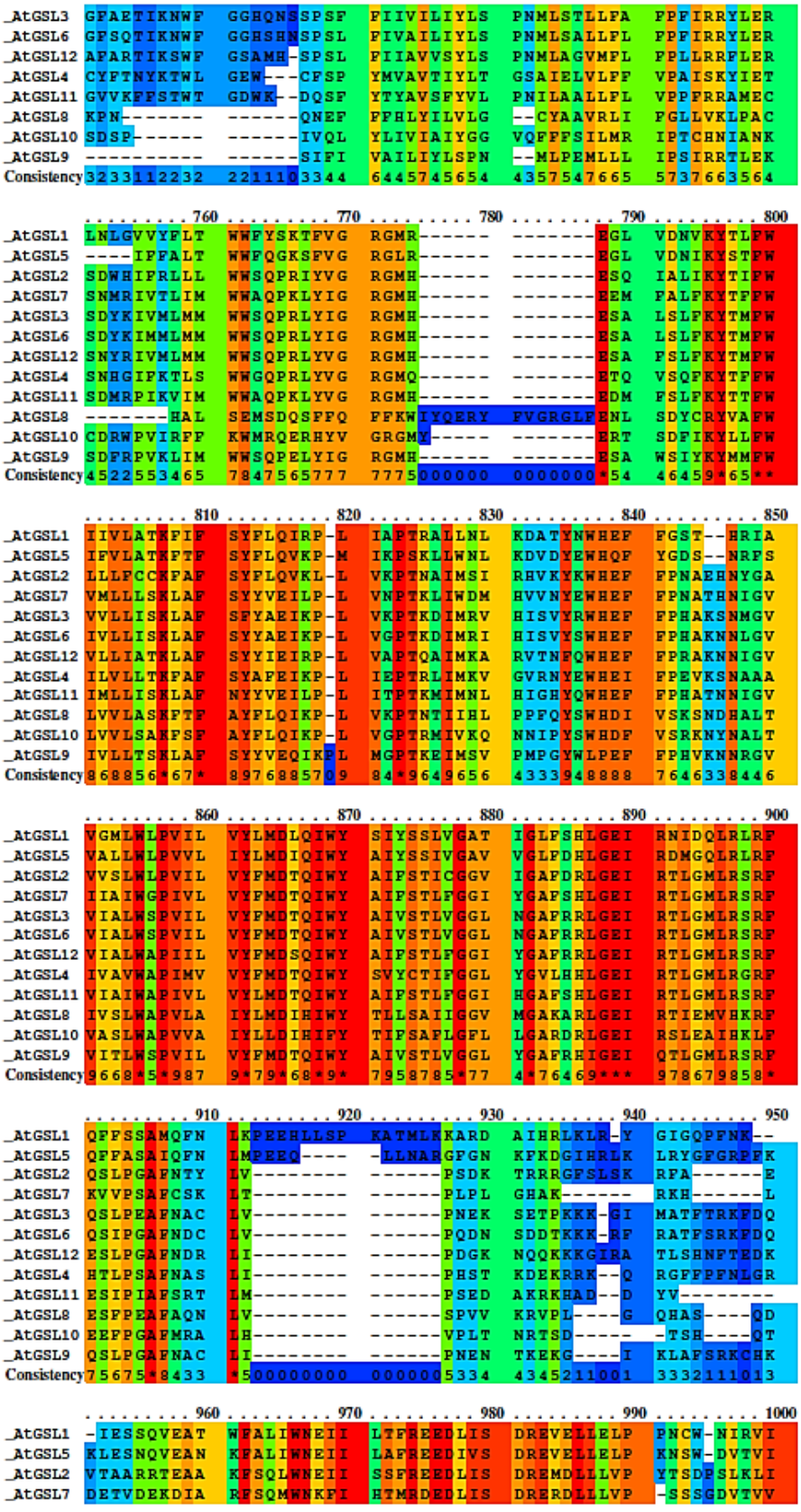

Appendix VII cont'd

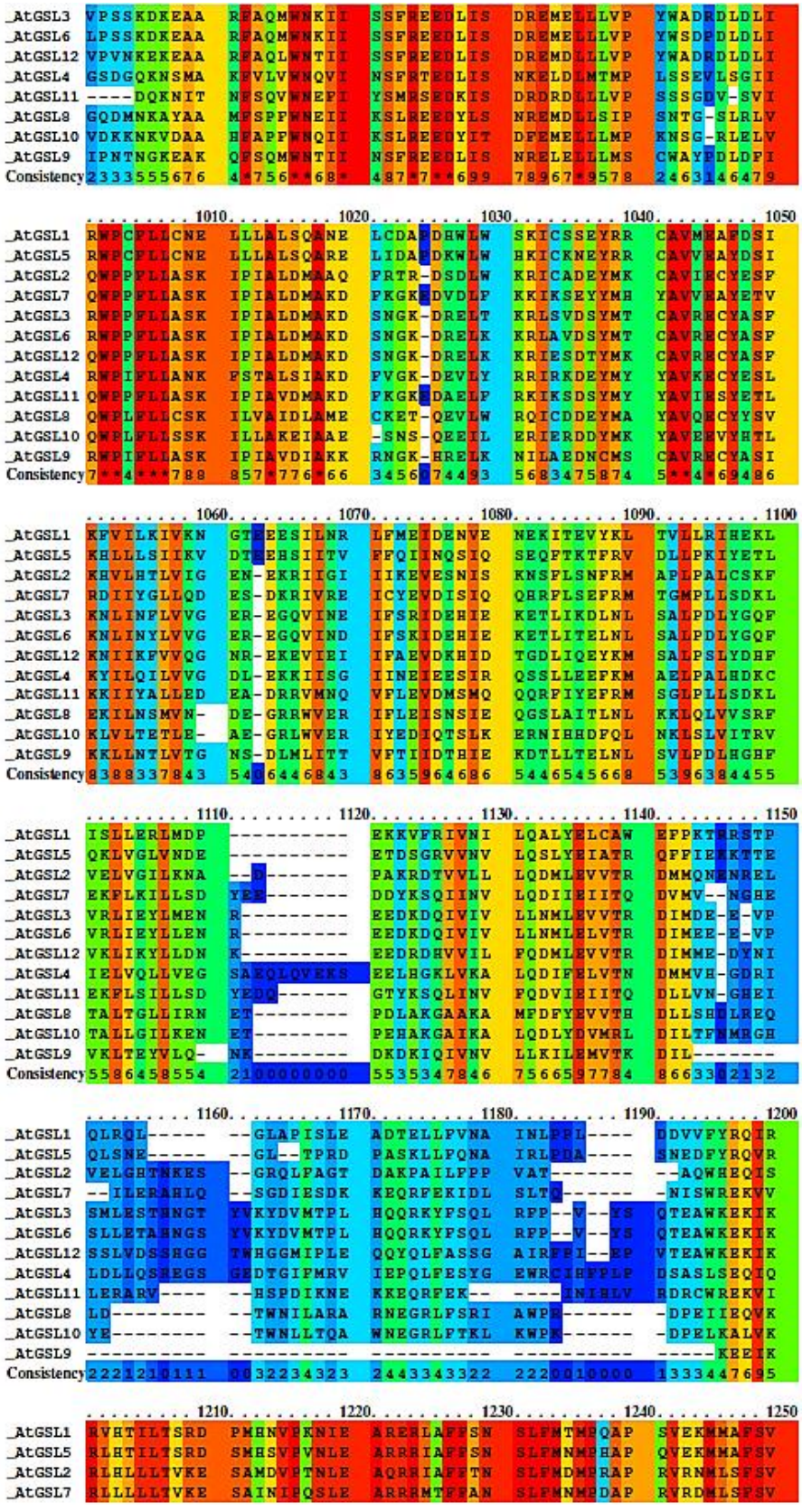

Appendix VII cont'd

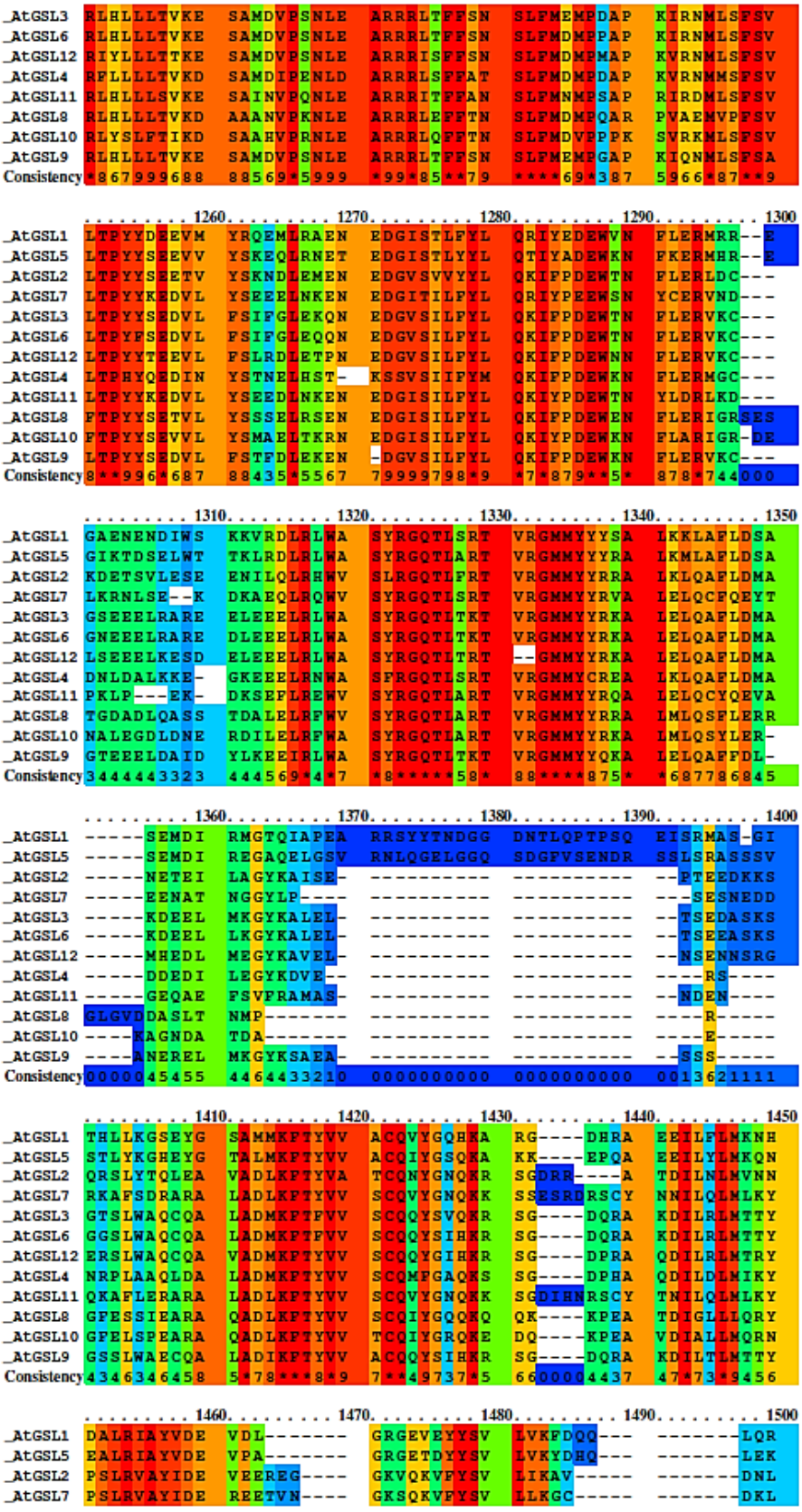

Appendix VII cont'd

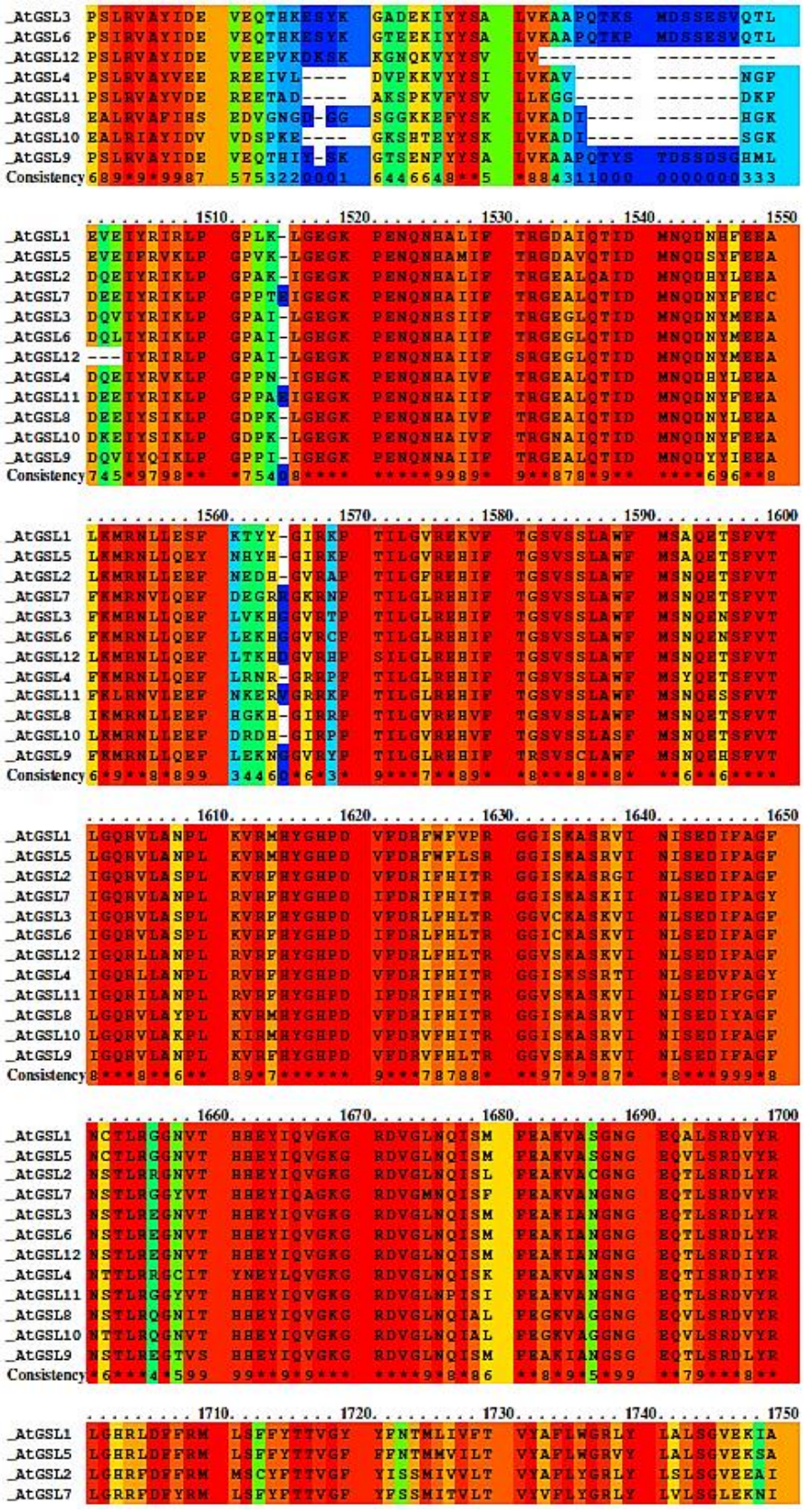

Appendix VII cont'd

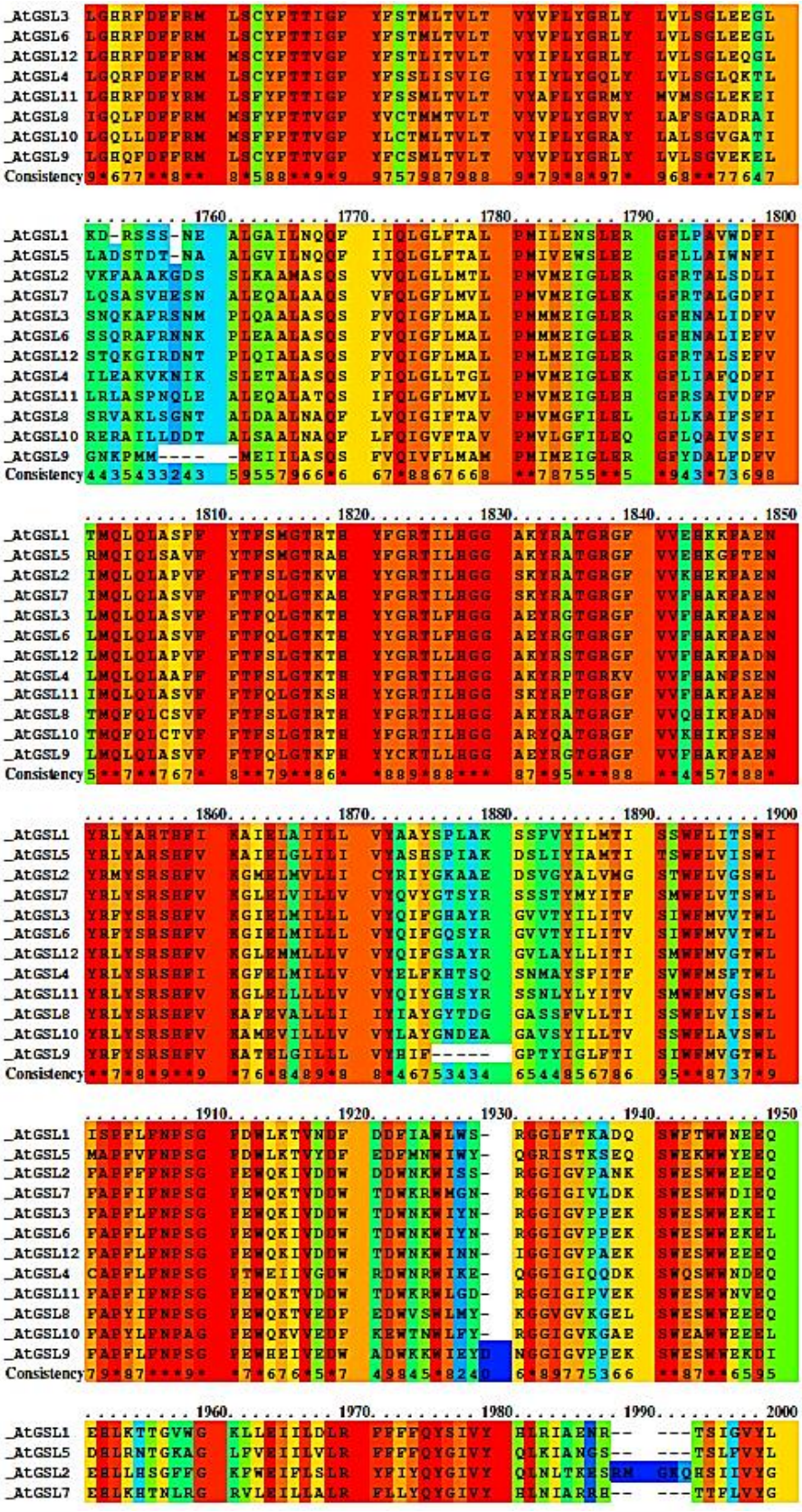

Appendix VII cont'd

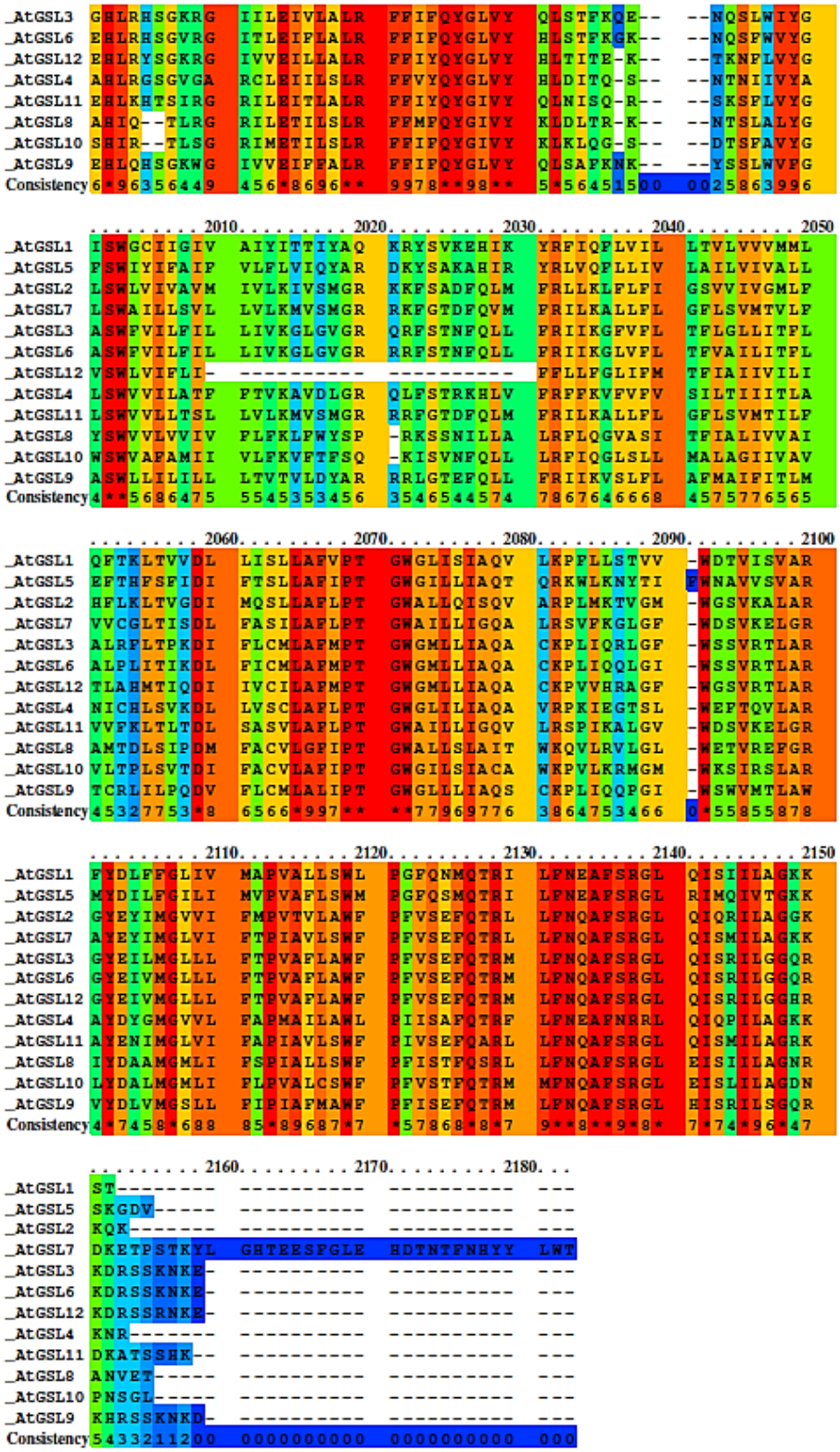

CURRICULUM VITAE

Behnaz Saatian

Education

Ph.D. **Western University, London, Ontario**
2010- present, Ph.D. Candidate

M.Sc. **University of Tehran, Tehran, Iran**
2002-2004

B.Sc. **Bu-Ali Sina University, Hamadan, Iran**
1997-2001

Honors and Scholarships

Western Graduate Research Scholarship (WGRS)
September 2010- August 2015
Western University

Graduate Student Travel Award
January 2014
Department of Biology, Western University

Ph.D. Comprehensive Exam, Passed with Distinction
June 2013
Department of Biology, Western University

Three Minutes Thesis (3MT) Competition, Finalist
April 2013
Western University

Best Oral Presentation
July 2005
4th National Conference of Biotechnology, Kerman, Iran

Experience

Teaching Assistant
September 2010-present
Western University

Research Assistant
September 2010-present
Agriculture and Agri-Food Canada

Teaching Assistant Training Program (TATP) Instructor
September 2013- Present
Teaching Support Center (TSC)
Western University

Faculty of Science Lead TA
September 2013- April 2014
TSC and School of Graduate and Postdoctoral Studies (SGPS)
Western University

Director of Quality Control Laboratory
March 2009- August 2010
Pharmaceutical Incubator, University of Tehran, Iran

Research Assistant
National Institute of Genetic Engineering and Biotechnology
March 2005- February 2009
Tehran, Iran

Selected Oral Presentations

Saatian, B., Austin, R. S., Kohalmi, S., Cui, Y. GLUCAN SYNTHASE-LIKE 8 regulates intercellular communication during early seedling development in Arabidopsis. CSPB/ SCBV Eastern Regional Meeting, University of Toronto, Canada, November 2015 (Ph.D. work).

Saatian, B., Austin, R. S., Kohalmi, S., Cui, Y. GLUCAN SYNTHASE-LIKE 8 is required for early seedling development in Arabidopsis. CSPB/ SCBV Eastern Regional Meeting, University of Guelph, Canada, November 2014 (Ph.D. work).

Saatian, B., Tian, G., Austin, R. S., Tsang, E. W. T., Kohalmi, S., Cui, Y. Next-generation mapping of seed storage protein gene repressors in Arabidopsis. CSPB/ SCBV Eastern Regional Meeting 2013, University of Toronto, Canada, December 2013 (Ph.D. work).

Saatian, B., Tian, G., Austin, R. S., Tsang, E. W. T., Kohalmi, S., Cui, Y. Next-generation mapping of Arabidopsis genes. Beyond the Genome Meeting, United States, October 2013 (Ph.D. work).

Saatian, B., Alizadeh, H., Naghavi, M. R., Omidi, M. *Agrobacterium*-mediated transformation of wheat (*Triticum aestivum* L.) using direct shoot regeneration. 4th Biotechnology National Conference, Iran, July 2005 (M.Sc. work).

Selected Poster Presentations

Saatian, B., Austin, R. S., Kohalmi, S., Cui, Y. GLUCAN SYNTHASE-LIKE 8 is required for early seedling development in Arabidopsis. 26th International Conference on Arabidopsis Research, France, July 2015 (Ph.D. work).

Saatian, B., Tian, G., Austin, R. S., Tsang, E. W. T., Kohalmi, S., Cui, Y. Create the scene and watch the show unfold: Identification of seed genes repressors in Arabidopsis Seedlings. 25th International Conference on Arabidopsis Research, Canada, July 2014 (Ph.D. work).

Saatian, B., Tian, G., Austin, R. S., Tsang, E. W. T., Kohalmi, S., Cui, Y. Identification of seed storage protein genes repressors in Arabidopsis seedlings using next-generation mapping. International Plant and Animal Genome XXII, United States, January 2014 (Ph.D. work).

Saatian, B., Tian, G., Austin, R. S., Tsang, E. W. T., Kohalmi, S., Cui, Y. Identification of seed gene repressors in Arabidopsis seedling using next-generation mapping. American Society of Plant Biologist (ASPB) Conference, United States, July 2012 (Ph.D. work).

Saatian, B., Mousavi, A. Detection of genetically modified seeds using PCR-based methods. 10th National Genetic Conference, Iran, May 2008 (M.Sc. work).

Saatian, B., Alizadeh, H., Naghavi, M. R., Omidi, M. Direct shoot regeneration of wheat (*Triticum aestivum* L.) using embryo explants and different plant growth regulators. ABIC 2004, Germany, September 2004 (M.Sc. work).

Saatian, B., Alizadeh, H., Naghavi, M. R., Omidi**,** M. Effect of plant growth regulators on direct shoot regeneration of wheat (*Triticum aestivum* L.) explants. 4th International Crop Science Conference, Australia, September 2004 (M.Sc. work).

Saatian, B., Alizadeh, H., Naghavi, M. R., Omidi, M. Study on synchronization of callus induction and regeneration from immature embryo apical meristem explants of wheat (*Triticum aestivum* L.). 2nd Conference on Applied Biology (International Approach), Iran, September 2004 (M.Sc. work).

Saatian, B., Alizadeh, H., Naghavi, M. R., Omidi, M. Optimization of direct shoot regeneration in wheat (*Triticum aestivum* L.) explants using different plant growth regulators. 8th Iranian Crop Production and Breeding Conference, Iran, August 2004 (M.Sc. work).